A SOLAR POWERED AQUA-AMMONIA
ABSORPTION REFRIGERATOR

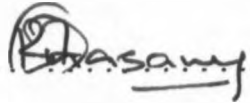BABAFEMI ADESOJI ONASANYA

B.Sc.(Hons.)(Lagos)

A thesis submitted in partial fulfilment for
the award of the degree of Master of Science
in Mechanical Engineering at the University of
Nairobi.

May 1989

This thesis is my original work and has not
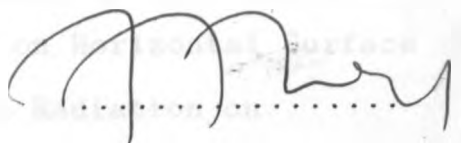been presented for a degree in any other
University.

.....Onasanya.....

Babafemi A. Onasanya

This thesis has been submitted for examination
with my knowledge as the University Supervisor.

.....

Dr. J.F. Kanyua

CONTENTS

DEDICATION

This work is dedicated to the glory
and honour of God, the Father,
without whose love, grace and mercy
this work would not have reached its
desired conclusion. Praise be to
God through our Lord and Saviour
Jesus Christ. Amen.

ACKNOWLEDGEMENT

I want to express my sincere gratitude to my supervisor, Dr. J.F. Kanyua for his invaluable suggestions, guidance and help during the course of this study. I would also like to thank Prof. C.I. Ezekwe for his suggestions and assistance.

I also want to thank my sponsor, ANSTI/UNESCO, for their financial asssistance during the whole period of this study and without whose generous financial support the work would not have been concluded.

My sincere appreciation, also, for the staff of the Mechanical Engineering Department's Workshop for their laboratory assistance and especially for Mr. Kimani and Mr. Mugo for their patience and relentless efforts during the fabrication and assembly of the test rig.

And, finally, I want to thank all those who have contributed to the success of this work one way or the other. God bless you all. Amen.

NOTATION

A_c Effective collector area, m^2

C   Number of components in a solution

C_p Specific heat capacity at constant pressure, kJ/kg.K

COP   Coefficient of performance of refrigeration system

D   Diameter of tube or pipe, m

F   Standard fin efficiency; number of degree of freedom

F'   Plate efficiency of a flat-plate collector

F''   Flow factor of a flat-plate collector

F_R Heat removal factor of a flat-plate collector

G_{sc} Sollar constant, 1353 W/m^2

G_o Apparent extraterrestrial solar irradiance, W/m^2

G_b Beam solar flux or irradiance of a horizontal surface, W/m^2

G_{bT} Beam solar flux or irradiance on tilted surface, W/m^2

h   Specific enthalpy, kJ/kg; heat transfer coefficient, $W/m^2 K$

H_o Daily extraterrestrial radiation on a horizontal surface, MJ/m^2

$\bar{H}_o$ Monthly mean daily extraterrestrial radiation on a horizontal surface, MJ/m^2

$\bar{H}, \bar{H}_T$ Monthly mean daily total global radiation on a horizontal or tilted surface with appropiate subscript to denote beam or diffuse, MJ/m^2

I   Insolation, defined as the instantaneous or hourly solar radiation on a surface, with appropiate subscripts to denote beam, diffuse, reflected, horizontal, tilted, etc., W/m^2

K   Extinction coefficient, m^{-1}; thermal conductuvity, $W/m.K$

$\bar{K}_T$ Ratio of monthly averaged, total horizontal radiation on a terrestrial surface to that on the corresponding extraterrestrial surface, i.e., the monthly clearness index

k_T Daily ratio of horizontal total radiation on terrestrial surface to that on the corresponding extraterrestrial surface, i.e., the daily clearness index

L   Lenght, m; thermal load or demand

m   Mass, kg

$\dot{m}$ Mass flow rate, kg/s

n   Index of refraction; number of daylight hours; number of tubes

N N^{th} day of the year; number of glass covers

NTU   Number of transfer units (dimensionless)

p   Pressure, bar

P   Number of phases

q   Rate of heat flow, W

Q	Quantity of energy or heat, kJ
r_t	Ratio of hourly total radiation to daily total radiation
R	Thermal resistance, m^2K/W
$\bar{R}$	Monthly elevation factor to transform total global radiation on a horizontal surface to that on a tilted surface
$\bar{R}_b$	Monthly elevation factor to transform total beam radiation on a horizontal surface to that on a tilted surface
S	Hourly absorbed radiation, MJ/m^2
T	Temperature, with appropiate subscripts to denote ambient, collector, storage, inlet, outlet or mean collector fluid temperature, K or $^\circ$C
u	Specific internal energy, kJ/kg
U	Overall heat transfer coefficient, W/m^2K
U_L	Overall heat transfer for heat loss from collector, W/m^2K
UA	Structure heat loss characteristic, with appropriate subscripts to denote storage or edge, MJ/K-day or W/K
W	Distance between tubes, m
X	Concentration, mass fraction of solute in a binary solution, kg/kg

Greek :

α Absorptance

δ Plate thickness, m

Δ Difference

ε Emittance

η Efficiency

ρ Ground reflectance

τ Transmittance of glazing

σ Stefan-Boltzmann's constant

$(\tau\alpha)$ Transmittance-absorptance product, optical
efficiency

Angular Measure

β Collector elevation or tilt angle, measured
upward from horizontal

γ Collector azimuth angle, measured ''-'' to the
east of south, ''+'' to the west of south

δ Declination angle

θ, θ_L Incident angle between the sun's radiation and
a line normal to the collector

θ_z Zenith angle between the line through the
centre of the earth and the sun's radiation

ϕ Local latitude

ω Hour angle of the sun

ω_s Hour angle of sunset/sunrise

ω'_s Hour angle of sunset/sunrise for the tilted
surface for the mean day of the month

Subscripts

a	Ambient, absorber, absorbed
b	Beam (direct) radiation
c	Collector
d	Diffuse, daily
e	Equivalent, effective, edge
f	Final, fluid
g	Ground
i	Inlet, inside, incident, insulation
l	Loss
m	Mean, monthly
n	Normal
o	Outlet, overall
p	Parallel, plate
r	Reflected
s	Storage, sunset or sunrise, shell-side
t	Top
T	Total, tilted
u	As used
v	Perpendicular
w	Wind
x	Cross-sectional
o	Intial, extraterrestrial

LIST OF FIGURES

LIST OF TABLES

ABSTRACT

An experimental intermittent solar refrigerator
using ammonia-water as the refrigerant-absorbent
combination and powered by two flat-plate collectors
has been designed, fabricated and tested under
outdoor conditions in Nairobi, Kenya. The research
was conducted in order to study the performance of
the system in the Kenyan climate and to determine the
prospects of the system in the climatic region. It
was also carried out with a view of investigating how
variations in the initial solution mass, the initial
ammonia concentration in the solution and the final
generator temperature affect the system performance.

The generator-absorber consisted of two copper
flat-plate collectors, each having eight 12.7 mm
diameter steel furniture tubes soldered onto it at
100 mm intervals and glazed by two glass covers. The
total effective collecting surface area of the two
collectors was 1.463 m^2. The condenser-evaporator
was a one shell pass, one tube pass, multi-tube
vertical heat exchanger, with condensation inside the
tubes and refrigerant storage in the condenser tubes.
The condenser was water cooled.

Tests were performed with different
concentrations in the range 0.35 to 0.58 kg NH_3/
kg solution with different solution masses. System
parameters during regeneration and refrigeration

processes were measured, and the cooling effect and the system coefficient of performance computed.

The maximum generator temperature attained was $100°C$ with an initial solution mass of 10.65 kg and an initial concentration of 0.37 kg NH_3/kg solution. Cooling ratios in the range of 0.24 to 0.49 were obtained and the overall coefficient of performance was found to be in the range of 0.07 to 0.17. The effective cooling per unit area of collector surface per day for the experimental refrigerator was in the range of 825.4 kJ/m^2, for an initial solution concentration of 0.37 kg NH_3/kg solution and initial solution mass of 10.65 kg, to 2463.4 kJ/m^2, for an initial solution concentration of 0.58 kg NH_3/kg solution and initial solution mass of 13.8 kg, for clear sunny days.

The results obtained herein compare favourably with those obtained by El-Shaarawi and Ramadan (1986) from their investigation carried out in Egypt, which is an example of a tropical climatic region. Hence the good performance of the system demonstrates the applicability of the system in the Nairobi climatic conditions. Although the performance is limited by the characteristics of the intermittent cycle as compared to the continuous cycles, the simplicity of the unit makes it adequate for use in small household and other food chillers in the rural areas where there is no electricity.

CHAPTER ONE

INTRODUCTION

Man has always benefited from the sun in the
form of food as a direct product of photosynthesis,
and fossil fuels as a by-product of plant
decomposition. However, over the past decades or so,
there has been a growing realisation that fossil
fuels, which are non renewable, are becoming more and
more expensive. Also, there is now a general
consensus that the growth in energy consumption which
has been experienced for many years cannot continue
indefinitely as there is a limit to our reserves of
fossil fuels. These problems have created an urgent
need into the research for alternative sources of
energy.

Thus, researches are going on in the
non-conventional sources of energy, such as, solar,
windpower, and ocean and wave power, to find ways in
which they can supplement the fossil fuels. However,
solar energy is by far the most attractive
alternative energy source for the future. Apart
from its non-polluting qualities, the amount of
energy which is available for conversion is several
orders of magnitude greater than all present world
requirements.

Refrigeration is available in the industrialized
nations through the use of electricity but is not

readily available in the majority of the world
especially in the third world. Solar energy,
however, is available in most areas, and the
conversion of solar energy into other forms which can
provide the refrigeration could be a tremendous
benefit to mankind. Since solar energy is the
cheapest and the most abundant source of energy known
to mankind, the use of solar energy in absorption
refrigeration is worth investigating. Much work has
been done in this area, and the extent of achievement
made is reviewed in the next chapter.

A great need exists in the developing countries
for a low-cost refrigeration system. An intermittent
absorption refrigeration cycle, requiring no
electrical power and utilizing solar energy as the
heat source for regeneration, offers the possibility
of providing such a system.

In Kenya, as in many parts of Africa, the
majority of the populace live in the rural areas
where there is no electricity. Hence, it is
proposed to study the performance of an intermittent
aqua-ammonia solar powered absorption refrigerator in
the Kenyan climate with the following objectives.

(i) To study the applicability of such a system
in the Nairobi climate. As mentioned above, this
study is by no means unique, however, the performance
of the system depends on the daily insolation level

and other environmental factors such as ambient air
temperature and wind speed.

(ii) To investigate the performance of such a
system in an equatorial climate like Kenya's and come
up with the proper design parameters to optimize the
system in view of the climatic conditions. In order
to optimize the system, the optimum ratio of the
ammonia to the water in the solution will have to be
established and the cooling ratio computed.

(iii) To investigate how variations in the
maximum solution temperature attainable in the solar
collector-generator and the minimum temperature
attainable in the evaporator affect the cooling ratio
and the overall performance of the system.

CHAPTER TWO

LITERATURE REVIEW

2.1   HISTORY OF REFRIGERATION

Jordan and Priester (1954) have given a
historical background of refrigeration beginning with
the Chinese who are said to have had ice cellars, as
early as 1000 BC. Later the Greeks and the Romans
kept snow cellars insulated with grass, earth and
manure.   Attempts into mechanical cooling began as
early as 1755 AD, [Jordan and Priester (1954)], using
air machines, but these proved to be ineffective.

With large scale transportation of ice around
1800 AD, there arose an urgent need to develop
machines to manufacture ice.   Thus the first patent
for a refrigeration machine using ether was issued in
Britain as early as 1834.   Other patents for other
machines, using different refrigerants followed.   It
is reported by Jordan and Priester (1954) that
machines of both the vapour compression and
absorption systems using ammonia were developed as
early as 1870, and those using carbon dioxide and
sulphur dioxide had been developed by 1891.
Steam-jet refrigeration was also in common use at
this period.

With the advent of industrialization, users of ice had progressively changed from natural to artificial ice by 1900 AD. Except for a few new designs, machines currently in commercial use, in both the conventional absorption and vapour compression systems, are improved modifications of these earlier machines.

2.2   REVIEW OF SOLAR ABSORPTION COOLING

2.2.1 Introduction

There are several methods of achieving cooling by solar energy [Freider and Kreith (1977) and ASHRAE (1985)]. The cooling effect can be produced directly by operating an absorption cycle, by a regenerative desiccant process or a steam jet system. It can alternatively be produced by a conventional vapour compression cycle in which the compressor is driven by a solar Rankine cycle or by an electric motor operated by photovoltaic cells. These means may be termed active. In addition there are passive means to cool the air in a building, all involving heat losses from water by nocturnal radiation, evaporation and convection, [Hay and Yellot (1970)]. Yanagimachi (1958,1964), Bliss (1964) and Hay (1973), describe systems that use nocturnal radiation to chill water for subsequent cooling. This review deals mainly with the absorption cycle which is the

only system among those mentioned above which is commercially available in a variety of cooling capacities.

Absorption cooling systems have long been employed. This cycle, requiring essentially only a heat source for its operation, has become one of the likely candidates for solar energy applications. There are two methods of operation of absorption coolers. The first is to use continuous coolers, similar in construction and operation to conventional gas or steam fired units, with energy supplied to the generator from the solar collector-storage-auxiliary system whenever conditions in the building dictate the need for cooling. The second approach is to use intermittent coolers similar in concept to that of commercially manufactured food coolers used many years ago in rural areas before electrification and mechanical refrigeration were widespread. Intermittent coolers have been considered for refrigeration but most work in solar air conditioning has been based on continuous cycles.

Recent works, [Gallo and de Souza (1982), Pailatowsky and Best (1982), Delgado et al.(1982) and Dupont et al.(1982)], testify to increasing interest in the intermittent refrigeration cycle as a result of its feasibility and despite its slightly lower cooling ratio, η, defined as the ratio of the heat absorbed by the refrigerant during refrigeration to the heat absorbed by the generator contents during

regeneration, as compared to the continuous cycle. Ammonia, NH_3, in combination with fluid absorbent such as water, H_2O, and sodium thiocyanate, NaSCN, [Agarwal and Agarwal (1983)], or solid absorbent such as calcium chloride, $CaCl_2$, and strontium chloride, $SrCl_2$, [Pilatowsky and Best (1982), Clausen and Worsoe-Schmidt (1982), Clausen and Worsoe-Schmidt (1983), and Iloeje (1986,1988)], is the most common refrigerant used to achieve temperatures below $0°C$. Methanol, CH_3OH, is also used in combination with active carbon and especially in the very promising binary and ternary combinations with lithium bromide, LiBr, and/or zinc bromide, $ZnBr_2$, [Iedema and Machielsen (1983), Grosman et al.(1983), and Alloush and Gosney (1983)]. In association with these bromides, CH_3OH has higher cooling ratio values than other working fluid combinations, and the same applies to the $CaCl_2-CH_3OH$ combination as compared to the $CaCl_2-NH_3$ system, [Grosman et al.(1983)].

The system performance of intermittent absorption refrigerators is highly dependent upon environmental factors such as cooling water temperature, air temperature and solar radiation. In consideration of the wide variation of these factors as well as of the cooling ratio values calculated under these conditions, the classic NH_3-H_2O system proves to be the most efficient combination of the above-mentioned ones. When the condenser is water-cooled this combination has cooling ratio

values higher than the NH_3-$CaCl_2$ system, [Pilawsky and
Best (1982)], and varies much less with changes in
the evaporation temperature than methanol-bromide
combinations, [Alloush and Gosney (1983)]. Moreover,
the risk of crystallisation, e.g., NaSCN-NH_3,
LiBr-CH_3OH, [Grosman et al.(1983)], is avoided, and
the system can work at temperatures below $90°C$,
requiring minor rectification only. The $CaCl_2$-$2CH_3OH$
combination has cooling ratio values 1.3 times higher
than those of $CaCl_2$-NH_3 system, therefore it is
comparable to the NH_3-H_2O system. However it
presents the disadvantage of desorption at high
temperatures and low absorbability of the absorbent,
[Grosman et al.(1983)]. For big cooling loads
intermittent cycles suffer from the problem that good
high temperature collectors such as evacuated tubes
containing selective surfaces cannot be good heat
rejectors. For such loads the continuous Rankine
cycle is preferable, [Sherwim (1983)].

Continuous absorption cycles can be adapted for
operation from flat-plate collectors. The principles
of operation of these cooling cycles are described in
ASHRAE (1975). The present temperature limitations
of flat-plate collectors restrict consideration among
commercial machines to lithium bromide-water systems.
Lithium bromide-water machines require cooling water
for the absorber and condenser, and their use will
probably require use of a cooling tower. Solar
operation of ammonia-water coolers, such as those

marketed for steam or gas operation, is difficult because of the high temperatures required to operate the machines. Coolers based on the other refrigerant-absorbent systems may be possible candidates for solar operation, but are not yet developed to the point where they can be evaluated.

Intermittent absorption cooling, on the other hand, may be an alternative to continuous systems. Most work to date on these cycles has been directed at food preservation rather than comfort cooling. These cycles may be of interest in air conditioning because they offer potential solutions to the energy storage problem. In these cycles, distillation of the refrigerant from the absorbent occurs during the regeneration stage of operation, and the refrigerant is condensed and stored. During the cooling stage of the cycle, the refrigerant is evaporated and reabsorbed. Thus, "storage" is in the form of separated refrigerant and absorbent. Modifications of this basically simple cycle, using pairs of evaporators, condensers, or other arrangements, may result in an essentially continuous cooling capacity and improved performance.

2.2.2 Solar Absorption Refrigeration System

Swartman et al.(1973) mention the work done by Hainsworth and by Buffington on 180 possible refrigerant-absorbent combinations and their

qualitative considerations. Their objective was to find a working fluid combination with desirable characteristics of: availability, low cost, low vapour pressure, low viscosity, high thermal conductivity, low volatility, high latent heat of vapourization for the refrigerant, low heat capacity of absorbent, non-toxicity, non-corrosive, stable and high solubility of refrigerant in absorbent at room temperature. All the desirable characteristics mentioned above could not be satisfied by any of the refrigerant-absorbent combination investigated. In solar applications, low generator temperatures have put a limit to the possible combinations that can be of practical use. Today, only ammonia-water and water-lithium bromide combinations in the liquid absorbent category have been accepted and applied, [Swartman et al.(1973)].

An analysis of intermittent adsorption and absorption refrigeration cycles, for the systems ammonia-calcium chloride and ammonia-water was made by Linge (1929). By establishing an arbitrary ideal cycle in which the final absorber temperature was equal to the temperature of condensation, he calculated the cooling effects per unit mass of absorbent as functions of condensation temperature, evaporation temperature, and final generator tempera-ture. Then, the cooling ratio was correlated with these variables. On the basis of this analysis, he concluded that the ammonia-calcium chloride system is

superior to the ammonia-water system because of the
higher cooling ratios, especially at higher
condensation and absorption temperatures.

The first recorded major project on an all solar
absorption refrigeration system was undertaken at the
Montlovis Laboratory in France in 1957 by Trombe and
Foex (1957). Their devise used an ammonia-water
absorption system with intermittent operation. A
cylindro-parabolic mirror with an area of $1.5m^2$ was
used as the collector. Generation occurred during the
four hours of maximum sunshine, with evaporation the
remainder of the time. This unit produced 6 kg of
ice per day.

Williams et al.[(1957),(1958)] described a
comprehensive investigation which included a
theoretical estimate of the performance of four
different binary systems (methanol-silica gel,
acetone-silica gel, ammonia-water and freon
21-tetraethylene glycol dimethyl ether), and an
experimental study of two of these systems
(ammonia-water and freon 21-tetraethylene dimethyl
ether). In both investigations the heat source was
solar radiation focussed onto the generator by means
of a reflector. The freon-glycol ether system gave
maximum cooling ratios in the range of 0.13 to 0.26,
whereas ammonia-water cooling ratios ranged from 0.38
to 0.41. The performance in the freon system was
attributed to low latent heat of the refrigerant and
its requirement for relatively large amounts of

absorbent.   Maximum solar heating ratios of 0.33 for
the freon unit and 0.41 for the ammonia unit were
recorded.

Experimental over-all performance ratios,
$(COP)_{overall}$, defined as the ratio of the
refrigeration effect to the incident daily insolation
for the period regeneration was on, for the
ammonia-water and freon-glycol ether units, showed
maximum values in the range of 0.14 to 0.16 for the
former and the latter 0.03 to 0.08. These studies
demonstrated that useful refrigeration can be
obtained by the use of intermittent absorption
refrigeration cycles with solar regeneration.

Chinnappa (1961) made a systematic experimental
study of the intermittent vapour absorption
refrigeration cycle employing two binary mixtures
(ammonia-water and ammonia-lithium nitrate) with
maximum solution temperatures up to about 405 K.
Using a solution with an initial concentration of
about 0.48 kg/kg solution, the effective cooling
below 273.1 K per kg of solution, and the actual
cooling ratio were calculated, and compared with
theoretical values.   For both systems, it was found
that while the values of the actual cooling ratio
were quite close to the values of the theoretical
cooling ratio, the actual cooling per kg of solution
was 5 to 15 percent less than the theoretical value.
This difference was attributed to the area of the
condensing surface provided for a particular rate of

heat supply during regeneration. cooling ratio for the ammonia-lithium nitrate system was higher than for ammonia-water but more refrigeration per kg of solution was possible with ammonia-water combination.

Chinnappa (1962) experimentally studied the operation of intermittent ammonia-water refrigeration systems in which flat-plate collectors served as the energy supply. The collector plate was a copper sheet of dimensions 1524mm by 1067mm and 0.762mm thick, onto which were soldered six 6.35mm diameter steel pipes at 152.4mm intervals. Three glass covers were used. The absorber and generator were separate vessels. The generator was an integral part of the flat plate collector, with refrigerant-absorbent solution in the tubes of the collector circulated by a combination of thermosyphon and a vapour lift pump. Using approximately equal cycle times for the regeneration and refrigeration steps (5 to 6 hours each), the overall coefficient of performance $(COP)_{overall}$ was found to be approximately 0.06 at generation temperatures rising from ambient to approximately 372 K. With cooling water at approximately 303 K, the effective cooling per day for the experimental machine was in the range of 50 to 85 kJ/m^2 for clear days.

A small and simple refrigerating apparatus using an ammonia-water solution was designed in Pakistan by de Sa (1964). The focus of 1.37m^2 parabolic reflector was used to generate ammonia vapour. Tests

showed that 0.25 kg of ammonia could be generated from 2 kg of working solution having a concentration of 58%.

Sargent and Beckman (1968) made a theoretical study of the performance of the refrigerant-absorbent combination of ammonia-sodium thiocyanate, NH_3-NaSCN, intermittent absorption refrigeration cycle and compared it with an ammonia-water cycle. An experimental investigation was made to determine the heat capacity of solutions of sodium thiocyanate in liquid ammonia at varying concentrations and temperatures. The results, together with already existing heat of solution data, were used to generate a temperature-enthalpy diagram for the combination. An idealised intermittent cooling cycle, in which the generator containing the NH_3-NaSCN solution is heated by solar energy, was chosen and ideal cooling ratios evaluated as function of initial and final generator temperatures and condenser temperatures. The cooling ratios were found to be nearly equal to those of the ammonia-water combination for the same ideal cycle. The NH_3-NaSCN combination possesses the advantage of not requiring a rectifier to prevent transfer of the absorbent to the condenser because of the low volatility of the NaSCN absorbent.

As a follow-up on the work of Chinnappa (1961) and Sargent and Beckman (1968), Swartman et al.(1975) made an experimental study to compare the ammonia-water and ammonia-sodium thiocyanate systems. Once

more they demonstrated the feasibility of using a
flat-plate collector incorporating the generator-
absorber in a working intermittent absorption
refrigerator. Extensive tests were carried out to
determine performance of the NH_3-H_2O and $NH_3-NaSCN$
refrigerant-absorbent combinations. The experimental
results showed that the $NH_3-NaSCN$ combination has a
better performance than NH_3-H_2O. In addition, the
$NH_3-NaSCN$ offers lower equipment costs as it does not
require a rectifier to prevent carry over of the
absorbent to the condenser.

Working on the same principle as Chinnappa
(1962) but using different collector material,
Farber (1970) designed and tested an ammonia-water
system using a flat-plate collector. The unit gave
an overall performance coefficient of 0.1 and
produced 5.5 kgs of ice per $0.1m^2$ of collector area
per day. The system was however not all solar, as
auxiliary equipment such as electric pumps were used.

A simple intermittent refrigeration system
incorporating the generator-absorber with a $1.4m^2$
flat-plate collector was designed and constructed at
the University of Western Ontario by Swartman and
Swaminathan (1970). Ammonia-water solution of
concentration varying from 58 to 70% were tested.

Another study at the University of Western
Ontario was made in 1972 by Swartman and Va (1972).
This study investigated an ammonia-sodium thiocyanate
solution in the same system described above. The

system was unable to make any considerable amount of ice.

Perry (1975) theoretically investigated the performance of the water-lithium bromide intermittent absorption refrigeration cycle. For low generator temperatures, the system performed in conformity with the conventional solar absorption system. However, at higher generator temperatures, the LiBr crystallises out of solution, thus putting an upper bound to the generator temperatures that could be applied to such a system.

A 56-litre capacity solar energy stimulated ammonia-water absorption-cycle refrigerator has been developed to store vaccine in remote locations, [Norton et al.(1986)]. The system employs a commercially manufactured (but modified) refrigerator operating on the Platens-Munz absorption cycle which requires a heat input of 95W and has an evaporator capacity of 21W. It was powered by 30 evacuated-tube heat-pipe solar-energy collectors, each collector having an absorber area of $0.1m^2$.

An experimental intermittent solar absorption refrigerator using aqua-ammonia was manufactured and tested in the Egyptian climate by El-Shaarawi and Ramadan (1986). Tests performed on this experimental intermittent refrigerator proved that cooling by solar energy using NH_3-H_2O systems is technically feasible in the Egyptian climate without the need of any help from other external sources of energy.

An average cooling ratio of 0.52 was obtained
and the measured minimum evaporator temperature was
271.0 K.   It was concluded that ammonia-water
combination gives the best performance under the
assumption that no water is transferred to the
condenser.   However, in practice, it is very
difficult to prevent water from being carried over to
the condenser during regeneration.   This transfer
reduces the cooling ratio.

Staicovici (1986) has designed and operated an
intermittent single-stage ammonia-water absorption
refrigeration system for short-term preservation of
fish in the Danube delta, where ice is needed from
early in the morning.   The designed cooling load was
46 MJ/cycle.   The system's overall coefficient of
performance $(COP)_{overall}$, varies between 0.152 and
0.09 in the period of May to September. Solar
radiation availability and the theoretical cooling
ratio, also applicable to the Trombe-Foex system,
were also assessed.

At usual condensation temperatures, maximum
theoretical values of $(COP)_{overall}$ were achieved for
generator outlet temperatures below $100°C$, the actual
maximum values being expected in the range of
0.25-0.30 at generation and condensation temperatures
of $80°C$ and $24.3°C$ respectively.   Subject to a total
insolation of 750 W/m^2 being available 7 hours a day
and assuming that an amount of 450 kJ/kg ice is
required at $(COP)_{overall}$ of 0.25, the resulting solar

cooling capacity amounts to 10.5 kg ice/m^2 collector. For bigger capacities of 450-675 MJ/day, the pay-off period is estimated to be 4-6 years respectively and the life-time to be 15-18 years.

Kouremenos et al.(1987) have given prediction along a typical year in Athens area of the performance of solar driven NH_3-H_2O absorption units, operating in conjunction with high and intermediate temperature solar collectors, in the cases (a) of absorption refrigeration units working as refrigerators, (b) of absorption refrigeration units working as heat pumps and (c) of reversed absorption units working as heat transformers.

In all cases, the operation of the units and the related thermodynamics were simulated by suitable computer codes, and the required local climatological data (i.e. the incident solar radiation and the ambient temperature) were determined by statistical processing of related hourly measurements over a considerable number of years. It was found that in the case of the refrigerator, for operation over the whole year, the theoretical cooling ratio varies in the range from 0.72 to 0.75 and a maximum theoretical specific cooling power of 223 W/m^2 was observed in July at 13 hrs local time. In the case of the heat pump, for operation from November to April, a maximum theoretical heat gain factor of about 1.7 was obtained in December with corresponding specific heat gain power amounting to 213 W/m^2 at 14 hrs while a

maximum theoretical specific heat gain factor of about 1.655. Lastly, in the case of the heat transformer, for operation over the whole year, a maximum theoretical heat gain factor of about 0.483 was observed during winter at about 13 hrs but with very small specific heat gain power, while a maximum specific heat gain power of 175 W/m^2 was obtained in July at noon with a corresponding heat gain factor of 0.445.

Gutieirrez (1988) has successfully developed from a commercial absorption-diffusion type generator, a solar refrigerator by substituting the burner for generation by a flat-plate collector. An ammonia-water solution and hydrogen was used in the system. There was no hot thermal storage to operate the system continuously, hence cooling occurred during daytime only. The heat rejection was by natural air convection. A series of experiments were performed in which the system was solar powered and also operated in a solar simulator, in order to know the effects of the ambient temperature on the behaviour of the apparatus. It was observed that under good insolation conditions, the refrigerator maintains freezing temperatures five hours a day, provided that the ambient temperature does not exceed $28°C$.

A $(COP)_{overall}$ value of 0.11 was obtained with the collector operation at constant radiation (850 W/m^2) in the simulator with an exit temperature of

$105°C$. This value is a third of what was reached when the refrigerator was operated with a gas burner and a generator temperature of $160°C$. Also the system had a collection efficiency of 23% and the system thermal ratio (STR) indicates that for every watt of solar incident radiation on the collector, the evaporator takes out 1/40 W.

2.2.3 Application of Solar Cooling to Air-Conditioning

Air conditioning is a welcomed application of solar energy since the sun is used to overcome its own discomforting effect. The near coincidence of maximum cooling load with the period of greatest insolation is an advantage since the greatest cooling effect is available when needed most. Absorption air conditioners appear promising in this application because of their state of development, their high performance at available temperatures and their mechanical simplicity compared to other air conditioning system alternatives.

Figure 2.1 shows the energy flow pattern of a generalised absorption air conditioning system. Solar energy received by collector is transferred through a high temperature storage reservoir to the absorption unit. This unit draws heat from a low temperature reservoir and rejects it together with high temperature energy to the outside ambient air. The

low temperature reservoir can then be used to remove heat from the space to be cooled. In the event that there is insufficient stored cooling capacity available to meet the cooling load, auxiliary energy is supplied.

Eisenstadt et al. (1959) carried out tests on an experimental intermittent absorption refrigeration system utilizing hot water from a flat-plate solar collector for regeneration using the ammonia-water system with solution concentration varying from 0.4 to 0.7. The temperatures of the hot water used for generation varies from 333 K to 355 K. These tests demonstrated the feasibility of the use of solar energy for comfort cooling in air conditioning.

A commercial water-lithium bromide air conditioner, slightly modified to allow supplying the generator with hot water rather than steam, was operated from a flat-plate water heater by Chung et al. (1963). An analytical study of solar operation of a water-lithium bromide cooler and flat-plate collector combination by Duffie and Sheridan (1965) identified critical design parameters and assessed the effects of operating conditions on integrated solar operation.

Under the assumptions made in this study, design of the sensible heat exchanger between the absorber and generator, cooling water temperature, and generator design are important, the latter is more critical here than in fuel-fired coolers because of

the coupled performance of the collector and cooler.
An experimental program was also developed at the
University of Queensland, Australia, in a specially
designed laboratory house, [Sheridan (1970)].   It was
concluded that the equipment performance should be
adequate for the air conditioning of houses in the
Australian tropics where reliable summer insolation
is available.

Ward and Lof (1975) installed a lithium
bromide-water absorption cooling unit to a Colorado
State University house and tested the different
operating modes for both heating and cooling.   A
60-40 percent ethylene glycol-water mixture was used
in the solar flat-plate collectors which supplied
heat to the air in the building and to the lithium
bromide absorption air conditioner.   Approximately
two-thirds of the heating and cooling loads were
expected to be met by solar energy and the balance by
natural gas.   A thermal simulation of the Colorado
State University (CSU) solar house was also carried
out by Duffie et al.(1975).   A computer model of the
solar energy system was developed and used to
determine the important design features and to show
the effect on the system performance of the collector
tilt, collector area and number of covers.

Other investigators of solar powered air
conditioning include Chinnappa (1974), who gave an
assessment of the performance of the less
conventional types of ammonia-water cycle (including

two with multistaging) when supplied with solar
energy. Also the performances of the three cycles
were compared to the conventional cycle. It was
concluded that though the less conventional cycle
require smaller solar collectors to produce the same
cooling effect, this improvement is realised at the
cost of greater complexity of plant, and therefore,
greater initial capital cost.

Wilbur and Mitchell (1975) in their paper on air
conditioning alternatives showed the relative
advantages of a single stage, lithium bromide-water
absorption air conditioner heated from a flat-plate
solar collector over those of ammonia-water system in
a theoretical comparative study. They also showed
that systems utilizing refrigerant storage and heat
rejection buffer between a cooling tower and the
absorber and condenser require smaller cooling towers
than the conventional units, and that the operation
with an air heat exchanger rather than the cooling
tower in such a system yields acceptable system
performance with a small reduction in the fraction of
the cooling load which can be met with solar energy.

In another study on air conditioning systems by
Wilbur and Mancini (1976), the performance of the
lithium bromide-water working fluid was also shown to
be superior to that of aqua-ammonia systems.

A hybrid solar air conditioning system has been
designed and built by Costello (1976). It is partly
an absorption system and partly a vapour compression

system. Hence, it combines the two most popular types of solar refrigeration systems. The refrigerant-absorbent combination used was water-lithium bromide and the heat source in the generator was hot water supplied by a solar collector. The system offers the advantages of a lower initial cost than the absorption system, and a lower operating cost and power consumption than the vapour-compression system. It permits designing with an optimal mix of solar and electrical energy for driving the system.

A solar-powered air-conditioning system has been designed, installed and operated in Singapore by Bong et al.(1987). The system made use of $32m^2$ of heat-pipe collectors and a lithium bromide-water absorption chiller of 7 kW cooling capacity. The operation of the system was fully automated. The chiller operation was described by the relationship between its solar and auxiliary heater contributions. The performance of the system over a representative local insolation condition was compared with that of the reported performance of two systems operating in the USA.

It provided an average cooling capacity of 4 kW with a cooling ratio of 0.58 at a solar fraction of 0.388. The average electrical power consumed to provide solar cooling was 16.7 MJ over a 9-hour daily operation. 9.9% of the incident solar energy was converted into cooling effect and the net savings of

converted into cooling effect and the net savings of
non-renewable energy per day was 13.9 MJ.

2.2.4 Solar Vapour Compression Systems

Another type of solar cooling system that has
received attention in recent years couples a
solar-powered Rankine cycle engine with more or less
conventional air conditioning system. Solar
collectors are used to heat a fluid usually water, in
a storage tank. Energy from the storage tank is
transferred through a heat exchanger to a heat
engine. The heat engine exchanges energy with
surroundings and produces work which is used to drive
the compressor of the vapor compression system.

In 1954, Kirpichev and Baum of Russia, [as
reported by Swartman et al.(1973)] successfully
produced 150 kg of ice per day on this type of
system. Their refrigerators were of the conventional
vapour compression type, driven by a heat engine
operating on steam, produced by a boiler placed at
the focus of a large parabolic mirror. Low
efficiency of solar collection, coupled with the
complexity and cost of this system, has made the
system more viable for power generation, than for
solar refrigeration.

Studies on Rankine-cycle solar air conditioning
systems to date have concentrated on theoretical
analysis [Prigmore and Barber (1974), Beekman (1975)

and Olson (1977)]. An experimental system in a
mobile laboratory is described by Prigmore and Barber
(1974). Hot water from flat plate collectors was
passed through a heat exchanger and pumped back to
the collectors. The heat exchanger was also the
generator of a subsystem operating on a Rankine
cycle. The fluid in the generator (the refrigerant)
was fed to an expander which provided the shaft power
for the vapour compression system. From the
expander, the refrigerant was condensed and pumped
back to the generator-cum-heat exchanger.

The application of this type of system to
refrigeration posed a few substantial problems,
[Barber (1977)], due to the low efficiencies of both
the flat plate collectors and the Rankine cycle.
Generation of mechanical power from solar radiation
has not yet been shown to be economical in
large-scale systems, and it is difficult to envision
a household scale system that will convert solar to
mechanical energy at less expense than a large-scale
solar system.

The design and control of Rankine engine-vapour
compression cooling has been studied by Olson (1977),
who found that for a given location and collector
size, there are optimum sizes of both the engine and
the storage tank which maximize annual solar
contribution to meeting the cooling load.

As with all solar processes, steady-state
conditions cannot be used to find optimum designs.

It is necessary to evaluate design options based on estimates of integrated yearly performance, since the effects of design variables are not intuitively obvious.

2.2.5 Solar Thermoelectric Refrigerator

A thermoelectric generator consisting of a small number of thermocouples generally produces a small e.m.f. but can easily be made to yield a large current. It has the advantage that it can operate from a low-grade heat source and is, therefore, attractive as a means of converting solar energy into electricity. This is especially so if the electrical load is a thermoelectric refrigerator also consisting of a small number of thermocouples since such a device requires a large current and only a small e.m.f.. In other words, a thermoelectric generator and a thermoelectric refrigerator make a highly compatible combination. Although the combination does not have a very high efficiency, its simplicity of construction may enable it to overcome this disadvantage.

Vella et al.(1976) demonstrated the feasibility of a thermoelectric generator, which draws its heat from the sun, as a source of electrical power for the operation of a thermoelectric refrigerator. The theory of the combined thermoelectric generator and refrigerator was derived and the ratio of the number

of thermocouples needed for the two devices was
determined. It was found that this ratio can, in
principle, be as low as unity, even for
unconcentrated solar radiation, though practical
considerations indicate that a ratio of 4 t0 1 is
preferred in this case. A 4-couple thermoelectric
generator was used to power a single-couple
refrigerator, [Vella et al.(1976)]. Temperatures
below 273 K were achieved for a temperature
difference across the generator of about 40 K.
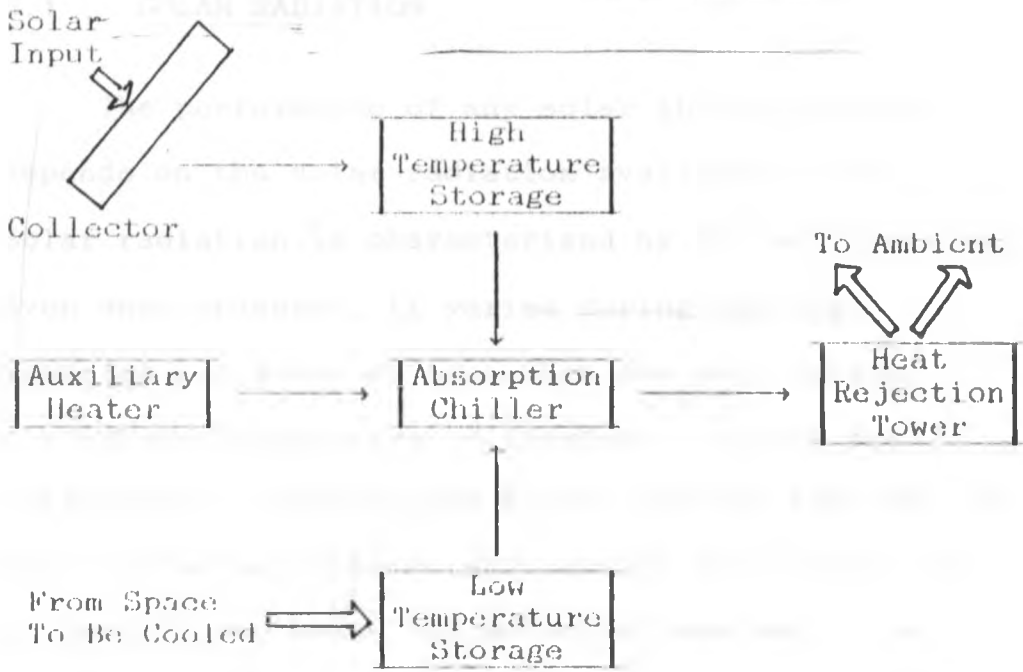
Figure 2.1: Absorption cooling system
energy flow diagram.

CHAPTER THREE

THEORY OF THE SOLAR SUBSYSTEM

3.1   SOLAR RADIATION

The performance of any solar thermal system
depends on the solar radiation available to it.
Solar radiation is characterized by its availability.
Even when abundant, it varies during the day,
reaching a maximum at noon when the path length
through the atmosphere is shortest. Unless the
collector is continuously turned to face the sun, the
sun's changing altitude and azimuth will reduce the
collected heat below the potential maximum. The
hours of day-light also vary seasonally, being the
shortest in winter when the need for heat is the
greatest. Therefore, unlike most other power
production equipment, solar collectors remain dormant
for one-third to two-thirds of the day, increasing
system cost considerably.

The local atmosphere, of course, appreciably
affects the available sunlight. Ordinary pollution
may reduce it by 10%. Clouds are also a part of the
climate in most localities, and the solar efficiency
suffers accordingly.

The utilization of solar energy involves
collecting surfaces at various orientations to the
horizontal. While radiation measurements on the

horizontal surfaces are available for many locations, the insolation on inclined surfaces must be calculated. It is the objective of this chapter to give a method for calculating the radiation on inclined surfaces from measured data on horizontal surfaces.

In this chapter, the value of the solar constant is given followed by the expression for the position of the sun used in determining the direct component of the radiation on an inclined surface. Calculation of the diffuse and reflected radiation components then allows the total radiation on such a surface to be determined. Also methods are described to obtain monthly values of total radiation on inclined surfaces from the monthly total horizontal radiation. This monthly measurement, generally expressed as the daily average of the monthly total radiation, is the only available solar radiation data for a great many locations.

When hourly radiation values are available from measurement or from cloud cover information, these data can be used more accurately for system design than average monthly information if they are pre-processed into detailed tables of radiation and weather data.

3.1.1 The Solar Constant

The Solar constant, G_{sc}, is the energy from the sun, per unit time, received on a unit area of surface perpendicular to the direction of propagation of the radiation, at the earth's mean distance from the sun, outside of the atmosphere. The value of G_{sc} has been determined within an estimated accuracy of $\pm 1.5\%$ as 1373 Wm^{-2}, [ASHRAE (1985)].

3.1.2 Variation of Extraterrestrial Radiation

The apparent extraterrestrial solar irradiance G_o varies over the year as the earth-sun distance changes seasonally, being about 3.5% higher than G_{sc} in January and 3.5% lower in June.

The dependence of extraterrestrial radiation on time of the year can be closely approximated by the empirical formula given by Klein (1977) as:

$$G_o = G_{sc}\left[1 + 0.033\cos\left(\frac{360N}{365}\right)\right] \qquad (3.1)$$

where

G_o is the extraterrestrial radiation, measured on the plane normal to the radiation and N is the Nth day of the year.

3.1.3 Direction of the Beam Radiation

The geometric relationships between a plane of any particular orientation relative to the earth at any time (whether that plane is fixed or moving relative to the earth) and the incoming beam solar radiation, that is, the position of the sun relative to that plane, can be described in terms of several angles, [Benford and Bock (1939)]. These angles and the relationships between them are as follows (see Figures 3.1 and 3.2):

ϕ Latitude, that is, the angular location north or south of the equator, north positive, $-90° \leq \phi \leq 90°$.

δ Declination, that is, the angular position of the sun at solar noon with respect to the plane of the equator, north positive $-23.45° \leq \delta \leq 23.45°$.

β Slope, that is, the angle between the plane surface in question and the horizontal, $0° \leq \beta \leq 180°$. ($\beta > 90°$ means that the surface has a downward facing component).

γ Surface azimuth angle, that is, the deviation of the projection on a horizontal plane of the normal to the surface from the local meridian, with zero due south, east negative, west positive, $-180° \leq \gamma \leq 180°$.

ω Hour angle, that is, the angular displacement of the sun east or west of the local meridian

due to rotation of the earth on its axis at 15° per hour, morning negative, afternoon positive.

θ Angle of incidence, that is, the angle between the beam radiation on a surface and the normal to that surface.

The following empirical equation of Cooper (1969) can be used to calculate the declination, δ.

$$\delta = 23.45° Sin \left[360 \times (\frac{284+N}{365}) \right] \tag{3.2}$$

where

N is the day number in the year.

The equation relating the angle of incidence of beam radiation θ, and the other angles is:

$$
\begin{aligned}
Cos\theta = \ & Sin\delta Sin\phi Cos\beta \\
& - Sin\delta Cos\phi Sin\beta Cos\gamma \\
& + Cos\delta Cos\phi Cos\beta Cos\omega \\
& + Cos\delta Sin\phi Cos\gamma Cos\omega \\
& + Cos\delta Sin\beta Sin\gamma Sin\omega
\end{aligned} \tag{3.3}
$$

There are several commonly occurring cases for which Equation 3.3 is simplified. For fixed north, that is, with a surface azimuth angle, γ, of 0° or 180° (a very common situation for fixed flat-plate collectors), the last term drops out.

For horizontal surfaces, $\beta=0°$, and the angle of incidence is the zenith angle of the sun, θ_z. Equation 3.3 becomes

$$Cos\theta_z = Cos\delta Cos\phi Cos\omega + Sin\delta Sin\phi \tag{3.4}$$

Equation 3.4 can be solved for the sunset hour angle, ω_s, when $\theta_z = 90°$.

$$Cos\omega_s = -\frac{Sin\phi Sin\delta}{Cos\phi Cos\delta} \qquad (3.5a)$$

$$Cos\omega_s = -Tan\phi Tan\delta \qquad (3.5b)$$

It follows that the number of daylight hours is given by

$$n = \frac{2}{15}Cos^{-1}(-Tan\phi Tan\delta) \qquad (3.6)$$

3.1.4 Ratio of Beam Radiation on Tilted Surface to that on Horizontal Surface

For purposes of solar process design and performance calculations, it is often necessary to calculate the hourly radiation on a tilted surface of a collector from measurements or estimates of solar radiation on a horizontal surface. The most commonly available data are total radiation for hours or days on the horizontal surface, whereas the need is for information on the plane of a collector, either total or beam and diffuse.

The geometric factor, R_b, the ratio of beam radiation on the tilted surface to that on a horizontal surface at any time, can be calculated by appropriate use of Equation 3.3. The ratio G_{bT}/G_b is given by

$$R_b = \frac{G_{bT}}{G_b} = \frac{G_{bn}Cos\theta}{G_{bn}Cos\theta_z} = \frac{Cos\theta}{Cos\theta_z} \qquad (3.7)$$

and $Cos\theta$ and $Cos\theta_z$ are both determined from Equation 3.3.

The optimum azimuth angle for flat plate collectors is usually $0°$ in the northern hemisphere (or $180°$ in the southern hemisphere). Thus it is a common situation that $\gamma = 0°$ (or $180°$). In this case, Equation 3.3 can be used to determine $Cos\theta_z$ and $Cos\theta$, which in the northern hemisphere for $\gamma = 0°$, gives

$$R_b = \frac{Cos(\phi-\beta)Cos\delta Cos\omega + Sin(\phi-\beta)Sin\delta}{Cos\phi Cos\delta Cos\omega + Sin\phi Sin\delta} \qquad (3.8)$$

In the southern hemisphere, $\gamma = 180°$ and the equation is

$$R_b = \frac{Cos(\phi+\beta)Cos\delta Cos\omega + Sin(\phi+\beta)Sin\delta}{Cos\phi Cos\delta Cos\omega + Sin\phi Sin\delta} \qquad (3.9)$$

3.1.5 Extraterrestrial Radiation on Horizontal Surface

At any point in time, the solar radiation outside the atmosphere incident on a horizontal plane is:

$$G_o = G_{sc}\left[1 + 0.033Cos(\frac{360N}{365})\right]Cos\theta_z \qquad (3.10)$$

where G_{sc} is the solar constant, and N is the day of the year. Equation 3.4 gives $Cos\theta_z$. Combining with

Equation 3.10, G_o for a horizontal surface at any time between sunrise and sunset is given by :

$$G_o = G_{sc}\left[1 + 0.033\text{Cos}(\frac{360N}{365})\right]$$

$$\times (\text{Sin}\phi\text{Sin}\delta + \text{Cos}\phi\text{Cos}\delta\text{Cos}\omega) \qquad (3.11)$$

It is often necessary for calculation of daily solar radiation to have the integrated daily extraterrestrial radiation on a horizontal surface, H_o. This is obtained by integrating Equation 3.11 over the period from sunrise to sunset. If G_{sc} is in watts per square meter, H_o in Joules per square meter is:

$$H_o = \frac{24\times3600G_{sc}}{\pi}\left[1 + 0.033\text{Cos}(\frac{360N}{365})\right] \times$$

$$\times \text{Cos}\phi\text{Cos}\delta\text{Cos}\omega_s + \frac{2\pi\omega_s}{360}\text{Sin}\phi\text{Sin}\delta \qquad (3.12)$$

where ω_s is the sunset angle, in degrees, from Equation 3.5.

The monthly mean daily extraterrestrial radiation, $\overline{H}_o$ is a useful quantity. It can be calculated with Equation 3.12 using N and δ for the mean day of the month from Table 3.1.

3.2   AVAILABLE SOLAR RADIATION ON TILTED SURFACES

Practical use of monthly horizontal surface data requires the estimation of the corresponding radiation on the tilted surface of the solar

collector. This is not a simple process because
elevation of the direct and diffuse components
involves a different procedure, and generally global
radiation data are all that are available. The
procedure, [Klein (1977)], requires calculation of
the proportion of the potential extraterrestrial
radiation available daily at the site, from which an
empirical correlation then permits estimation of the
diffuse component. To find the daily total
extraterrestrial radiation, Equation 3.11 must be
integrated over the daylight hours as the incident
angle θ changes. The ratio of the extraterrestrial
radiation on the tilted and horizontal surfaces is
used to "elevate" the direct component, as described
below. Then the diffuse component is elevated, and
the two summed up to give the global radiation on the
tilted surface.

3.2.1 Diffuse Radiation

Since most radiation data are global, it is
necessary to determine the proportion of the
radiation that is diffuse before the radiation on a
tilted surface can be found. Obviously, the cloudier
the climate, the higher the proportion of diffuse
radiation. Liu and Jordan (1960) and Page (1961)
found that the proportions of diffuse radiation in
horizontally collected monthly radiation data is a

function of the clearness index $\overline{K}_T$, the proportion of the horizontal extraterrestrial radiation reaching the site.

$\overline{K}_T$, the monthly average clearness index, is the ratio of monthly average radiation on a horizontal surface to the monthly average daily extraterrestrial radiation. In equation form,

$$\overline{K}_o = \frac{\overline{H}}{\overline{H}_o} \tag{3.13}$$

Collares-Pereira and Rabl (1979) found a seasonal dependence of the monthly fraction that is diffuse, $\overline{H}_d/\overline{H}$, on the monthly average clearness index, $\overline{K}_T$, which they expressed in terms of the sunset hour angle of the mean day of the month, as a function of latitude and declination given by Equation 3.5. The equation for $\overline{H}_d/\overline{H}$ (ω_s in degrees) is:

$$\frac{\overline{H}_d}{\overline{H}} = 0.775 + 0.00653(\omega_s - 90)$$
$$-[0.505 + 0.00455(\omega_s - 90)]Cos(115\overline{K}_T - 103) \tag{3.14}$$

Duffie and Beckman (1980) recommended that the Collares-Pereira and Rabl correlation of Equation 3.14 be used until a better data base or better methods of correlation indicate otherwise.

3.2.2 Diffuse Component of Daily Radiation

Studies of available daily radiation data have shown that the average fraction which is diffuse, H_d/H, is a function of K_T, where K_T is the day's clearness index, defined as the ratio of a particular day's radiation to the extraterrestrial radiation for that day.   In equation form

$$K_T = \frac{H}{H_o} \tag{3.15}$$

Duffie and Beckman (1980) recommends that pending further work, the correlation of Collares-Pereira and Rabl (1979) be used.   An equation representing the correlation is :

$$\frac{H_d}{H}\begin{cases} =0.99 & \text{for } K_T \leq 0.17 \\ =1.188-2.272K_T+9.473K_T^2 \\ \quad -21.865K_T^3+14.648K_T^4 & \text{for } 0.17<K_T<0.75 \\ =-0.54K_T+0.632 & \text{for } 0.75<K_T<0.80 \\ =0.2 & \text{for } K \geq 0.80 \end{cases} \tag{3.16}$$

3.2.3 Total Radiation on Fixed Slopes Surfaces

Flat-plate solar collectors absorb both beam and diffuse components of solar radiation.   To use horizontal total radiation data to estimate radiation on the tilted surface of a collector of fixed orientation, it is necessary to know R, the ratio of total radiation on a tilted surface to that on the horizontal surface.

R is by definition :

$$R = \frac{\text{Total radiation on a tilted surface}}{\text{Total radiation on a horizontal surface}}$$

$$= \frac{I_T}{I} \qquad\qquad (3.17)$$

It can expressed in terms of the contributions of the beam and diffuse radiation :

$$R_b = \frac{\text{Beam radiation on a tilted surface}}{\text{Beam radiation on a horizontal surface}}$$

$$= \frac{I_{bt}}{I_b} \qquad\qquad (3.18)$$

and

$$R_d = \frac{\text{Diffuse radiation on a tilted surface}}{\text{Diffuse radiation on a horizontal surface}}$$

$$= \frac{I_{dT}}{I} \qquad\qquad (3.19)$$

Then

$$R = \frac{I_b}{I}R_b + \frac{I_d}{I}R_d \qquad\qquad (3.20)$$

The angular correction for the beam component is straightforward and can be calculated by methods of Section 3.1.4. The correction for the diffuse component depends on the distribution of diffuse radiation over the sky, which generally is not well known; this distribution depends on the type, extent, and locations of clouds and also on the amounts and spacial distribution of other atmospheric components that scatter solar radiation. Also, some solar

radiation may be reflected from the ground to the surface.

Liu and Jordan (1963) considered the radiation on the tilted surface to be made up of three components: beam radiation, diffuse solar radiation, and solar radiation diffusely reflected from the ground. A surface tilted at slope β from the horizontal has a view factor to the sky given by $(1+\text{Cos}\beta)/2$. If the diffuse solar radiation is isotropic, this is also R_d. The surface has a view factor to the ground of $(1-\text{Cos}\beta)/2$, and if those surroundings have a reflectance of ρ for the total solar radiation, the reflected radiation from the surroundings on the surface from the solar radiation is $(I_b+I_d)\rho(1+\text{Cos}\beta)/2$. The total solar radiation on the tilted surface for an hour is then the sum of the three terms :

$$I_T^{'} = I_b R_b + I_d \left(\frac{1+\text{Cos}\beta}{2}\right)$$
$$+ (I_b + I_d)\rho\left(\frac{1-\text{Cos}\beta}{2}\right) \qquad (3.21)$$

and by definition of R

$$R = \frac{I_b}{I}R_b + \frac{I_d}{I}\left(\frac{1+\text{Cos}\beta}{2}\right)$$
$$+ \left(\frac{1-\text{Cos}\beta}{2}\right) \qquad (3.22)$$

Liu and Jordan suggest values of diffuse ground reflectance of 0.2 for ordinary ground or vegetation, and the relation

$$\rho = 0.2(1 - c) + 0.7c \qquad\qquad (3.23)$$

for ground covered in snow, where c is the fractional time of a month when the ground is covered in more than one inch of snow. The maximum value is therefore 0.7. Lunde (1980) suggests a value of 0.15 for a gravel roof. The last two terms of Equation 3.21 are sometimes considered together as the diffuse radiation incident on the surface.

3.2.4 Average Radiation on Fixed Sloped Surfaces

The ratio of the monthly average daily radiation on the tilted surface to that on a horizontal surface, $\bar{R}$ is calculated in exactly the same manner as that for R, that is, by adding the contributions of the beam radiation, the diffuse radiation and the reflected solar radiation from the ground. The method outlined here is that by Liu and Jordan (1962) and extended by Klein (1977). If the diffuse and reflected radiation are each assumed to be isotropic, then, in a manner analogous to Equation 3.22, the monthly mean ratio $\bar{R}$ can be expressed as :

$$\bar{R} = \frac{\bar{H}_T}{\bar{H}}$$

$$= \left(1 - \frac{\bar{H}_d}{\bar{H}}\right)\bar{R}_b + \frac{\bar{H}_d}{\bar{H}}\left(\frac{1+\cos\beta}{2}\right) + \rho\left(\frac{1-\cos\beta}{2}\right) \qquad (3.24)$$

and

$$\overline{H}_T = \overline{H}\left(1 - \frac{\overline{H}_d}{\overline{H}}\right)\overline{R}_b + \overline{H}_d\left(\frac{1+Cos\beta}{2}\right) + \overline{H}\rho\left(\frac{1-Cos\beta}{2}\right) \quad (3.25)$$

$\overline{H}_d/\overline{H}$ is the ratio of monthly average daily diffuse radiation to monthly average daily total radiation on a horizontal surface, a function of $\overline{K}_T$ as given by Equation 3.13. $\overline{R}_b$ is the ratio of the average daily beam radiation on the tilted surface to that on a horizontal surface for the month, $\overline{H}_{bT}/\overline{H}_b$. It is a function of transmittance of the atmosphere, but Liu and Jordan suggest that it can be estimated by assuming that it has the value which would be obtained if there were no atmosphere.

For surfaces sloped toward the equator in the northern hemisphere, that is, for surfaces with $\gamma = 0°$,

$$\overline{R}_b = \frac{Cos(\phi-\beta)Cos\delta Cos\omega'_s + \frac{\pi}{180}\omega'_s Sin(\phi-\beta)Sin\delta}{Cos\phi Cos\delta Sin\omega_s + \frac{\pi}{180}\omega_s Sin\phi Sin\delta} \quad (3.26)$$

where ω'_s is the sunset hour angle for the tilted surface for the mean day of the month, which is given by

$$\omega'_s = min\begin{bmatrix} Cos^{-1}(-Tan\phi Tan\delta) \\ Cos^{-1}(-Tan(\phi-\beta)Tan\delta) \end{bmatrix} \quad (3.27)$$

where "min" means the smaller of the two items in the bracket.

For surfaces in the southern hemisphere sloped toward the equator, with $\gamma = 180°$, the equations are

$$\bar{R}_b = \frac{Cos(\phi+\beta)Cos\delta Sin\omega_s' + \frac{\pi}{180} \omega_s' Sin(\phi-\beta)Sin\delta}{Cos\phi Cos\delta Sin\omega_s + \frac{\pi}{180} \omega_s Sin\phi Sin\delta} \qquad (3.28)$$

and

$$\omega_s' = min\begin{bmatrix} Cos^{-1}(-Tan\phi Tan\delta) \\ Cos^{-1}(-Tan(\phi+\beta)Tan\delta) \end{bmatrix} \qquad (3.29)$$

The numerator of Equation 3.26 or Equation 3.28 is the extraterrestrial radiation on the tilted surface, and the denominator is that the horizontal surface. Each of these is obtained by integration of Equation 3.11 over the appropriate time period, from true sunrise to sunset for the horizontal surface and from apparent sunrise to sunset on the tilted surface.

3.2.5 Estimation of Hourly Radiation from Daily Data

When hourly (or other short time base) performance calculations for a system are to be done in the absence of measured hourly irradiation data, it may be necessary to start with daily data and estimate hourly values from daily values. As with the estimation of diffuse from total radiation, this is not an exact process. For example, a daily total radiation may result from conditions of varying cloud cover throughout the day, and in predicting hourly radiation from that total there is no means of predicting which hour is cloudy and which is clear.

However, the methods presented here work best for clear days, and those are the days that produce most of the output of solar processes (particularly those processes that operate at temperatures significantly above ambient). And, they tend to produce conservative estimates of long-time process performance.

The work of Whillier (1959,1965) and Liu and Jordan (1979) has led to generalised charts on the ratio of hourly total to daily total radiation as a function of the hour relative to solar noon and the day length. Days are assumed to be symmetrical about solar noon and the hours are indicated by their mid-point. Knowing the day length (calculated from Equation 3.6) and the daily total radiation, the hourly total radiation may be estimated. In a further investigation by Collares- Pereira and Rahl (1979), new data were combined with the earlier results to give the following empirical equation:

$$r_t = \frac{\pi}{24}(a + b\text{Cos}\omega)\frac{\text{Cos}\omega - \text{Cos}\omega_s}{\text{Sin}\omega_s - (2\pi\omega_s/360)\text{Cos}\omega_s} \qquad (3.30)$$

$$= \frac{\text{Hourly total radiation}}{\text{Daily total radiation}}$$

The coefficients a and b are given by :

$$\left.\begin{array}{l} a = 0.4090 + 0.5016\text{Sin}(\omega_s - 60°) \\ b = 0.6609 - 0.4767\text{Sin}(\omega_s - 60°) \end{array}\right\} \qquad (3.31)$$

In these equations ω is the hour angle in degrees for the time in question (e.g., the mid-point

of the hour for which the calculation is made), and
ω_s is the sunset hour angle.

Similarly, the ratio of the hourly diffuse to
the daily diffuse radiation, r_d can be estimated
using the following equation from Liu and Jordan
(1960):

$$r_d = \frac{\pi}{24} \frac{Cos\omega - Cos\omega_s}{Sin\omega_s - (2\pi\omega_s/360)Cos\omega_s} \qquad (3.32)$$

3.3   RADIATION TRANSMISSION THROUGH COVERS AND ABSORPTION BY COVERS

The transmission, reflection, and absorption of
solar radiation by the various parts of a solar
collector are important in determining collector
performance. The transmittance, reflectance, and
absorptance are functions of the incoming radiation,
and the thickness, refractive index, and extinction
coefficient of the material. Generally, the
refractive index, n, and the extinction coefficient,
k, are functions of the wavelength of the radiation.
However, all properties will be assumed to be
independent of wavelength. This is an excellent
assumption for glass, the most common solar collector
cover material. Incident solar radiation is assumed
unpolarized (or only slightly polarized). However,
polarization consideration are important as radiation

becomes partially polarized as it passes through collector covers.

3.3.1 Reflection of Radiation

For smooth surfaces Fresnel has derived expressions for the reflection of unpolarized radiation on passing from a medium 1 with a refractive index, n_1, to medium 2 with refractive index, n_2.

$$r_v = \frac{Sin^2(\theta_2 - \theta_1)}{Sin^2(\theta_2 + \theta_1)} \tag{3.33}$$

$$r_p = \frac{Tan^2(\theta_2 - \theta_1)}{Tan^2(\theta_2 + \theta_1)} \tag{3.34}$$

$$r = \frac{I_r}{I_i} = \frac{1}{2}(r_v + r_p) \tag{3.35}$$

where θ_1 and θ_2 are the angles of incidence and refraction, as shown in Figure 3.3. Equation 3.33 represents the perpendicular component of unpolarized radiation, r_v, and Equation 3.34 represents the parallel component of unpolarized radiation, r_p. (Parallel and perpendicular refer to the plane defined by the incident beam and the surface normal). Equation 3.35, then, gives the reflection of unpolarized radiation as the average of the two

components. The angles θ_1 and θ_2 are related by Snell's Law to the indices of refraction,

$$\frac{\sin \theta_2}{\sin \theta_1} = \frac{n_1}{n_2} = n_r \tag{3.36}$$

Thus, if the angle of incidence and refractive indices are known, Equations 3.33 through 3.36 are sufficient to calculate the reflectance of the single interface.

For radiation at normal incidence, both θ_1 and θ_2 are 0, and Equations 3.35 and 3.36 can be combined to yield

$$r(0) = \frac{I_r}{I_i} = \left[\frac{(n_1 - n_2)}{(n_1 + n_2)}\right]^2 \tag{3.37}$$

If one medium is air (i.e., a refractive index of nearly unity), Equation 3.37 becomes

$$r(0) = \frac{I_r}{I_i} = \left[\frac{(n - 1)}{(n + 1)}\right]^2 \tag{3.38}$$

In solar energy applications, the transmission of radiation is through a slab or film of material so that there two interfaces per cover to cause reflection losses. At off-normal incidence, the radiation reflected at an interface is different for each component of polarization, so the transmitted and reflected radiation becomes partially polarized. Consequently, it is necessary to treat each component of polarization separately.

Neglecting absorption in the slab shown in Figure 3.4, and considering for the moment only the perpendicular component of polarization of the incoming radiation, $(1-r_v)$ of the incident beam reaches the second interface. Of this, $(1-r_v)^2$ passes through the interface and $r_p(1-r_v)$ is reflected back to the first, and so on. Summing up the transmitted terms, the transmittance for the perpendicular component of polarization is

$$\tau_v = (1-r_v)^2 \sum_{n=0}^{\infty} r_v^{2n} = \frac{(1-r_v)}{(1-r_v^2)} = \frac{(1-r_v)}{(1+r_v)} \qquad (3.39)$$

Exactly the same expansion results when the parallel component of polarization is considered. r_v and r_p are not equal (except at normal incidence) and the transmittance of initially unpolarized radiation is the average transmittance of the two components.

$$\tau_r = \frac{1}{2}\left[\frac{1-r_p}{1+r_p} + \frac{1-r_v}{1+r_v}\right] \qquad (3.40)$$

where the subscript r is a reminder that only reflection losses have been considered.

For a system of N covers, all of the same materials, a similar analysis yields

$$\tau_{rN} = \frac{1}{2}\left[\frac{1+r_v}{1+(2N-1)r_v} + \frac{1-r_p}{1+(2N-1)r_p}\right] \qquad (3.41)$$

3.3.2 Absorption of Radiation

The absorption of radiation in a partially transparent medium is described by Bouguer's Law, which is based on the assumption that the absorbed radiation is proportional to the local intensity in the medium and the distance the radiation travels in the medium, x :

$$dI = IK \, dx \qquad\qquad (3.42)$$

where K is the proportionality constant, called the extinction coefficient, and is assumed to be constant in the solar spectrum. Integrating along the actual path length in the medium (i.e., from 0 to $L/\cos\theta_2$) gives

$$\tau_a = \frac{I_\tau}{I_o} = e^{-(KL/\cos\theta_2)} \qquad\qquad (3.43)$$

where the subscript, a, is a reminder that only absorption losses have been considered. For glass, the value of K varies from approximately 4 m^{-1} for "water white" glass (which appears white when viewed on the edge) to approximately 32 m^{-1} for poor (greenish cast of edge) glass.

3.3.3 Optical Properties of Cover Systems

The transmittance, reflectance and absorptance of a single cover, allowing for both reflection and absorption losses, can be determined by ray-tracing techniques similar to that used to derive Equation 3.39. For the parallel component of polarization, the transmittance, τ_p, reflectance, ρ_p, and absorptance, α_p, of the cover are:

$$\tau_p = \frac{\tau_a (1-r_p)^2}{1-(r_p \tau_a)^2} = \tau_a \left(\frac{1-r_p}{1-r_p}\right)\left(\frac{1-r_p^2}{1-(r_p\tau_a)^2}\right) \tag{3.44}$$

$$\rho_p = r_p + \frac{(1-r_p)^2 \tau_a^2 r_p}{1-(r_p\tau_a)^2} = r_p(1+\tau_a r_p) \tag{3.45}$$

$$\alpha_p = (1-\tau_a)\left(\frac{1-r_p}{1-r_p\tau_a}\right) \tag{3.46}$$

Similar results are found for the perpendicular component of polarization. For incident unpolarized radiation, the optical properties are found by averaging the two components.

The equation for the transmittance of a collector can be simplified by noting that the last term in Equation 3.44 (and it's equivalent for the perpendicular component of polarization) is nearly unity, since τ_a is seldom less than 0.9 and r is of the order of 0.1 for practical collector covers.

With this simplification, and with Equation 3.40, the transmittance of a single cover becomes:

$$\tau \cong \tau_a \tau_r \tag{3.47}$$

This is a satisfactory relationship for solar collectors with cover materials and angles of practical interest.

The absorptance of a solar collector cover can be approximated by letting the last term in Equation 3.46 be unity so that:

$$\alpha \cong 1 - \tau_a \tag{3.48}$$

Although the neglected term in Equation 3.46 is larger than the neglected term in Equation 3.44 , the absorptance is much smaller than the transmittances so that the overall accuracy of the two approximations is essentially the same.

The reflectance of single cover is then found from:

$$\rho = 1 - \alpha - \tau \tag{3.49}$$

so that:

$$\rho \cong \tau_a (1 - \tau_r) = \tau_a - \tau \tag{3.50}$$

The advantage of Equations 3.47 through 3.50 over Equations 3.44 through 3.46 is that polarization is accounted for in the approximate equations through the single term, τ_r, rather than by the more complicated expressions for each individual optical property.

Although Equations 3.47 through 3.50 were derived for a single cover, they apply equally well

to identical multiple covers. The quantity τ_r should
be evaluated from Equation 3.41 and the quantity τ_a
from Equation 3.43 with L equal to the total cover
system thickness.

3.3.4   Transmittance for Diffuse Radiation

The preceding analysis only applied to the beam
component of solar radiation. Radiation incident on
a collector also consists of scattered solar
radiation from the sky and possibly reflected solar
radiation from the ground. In principle, the amount
of this radiation that passes through a cover system
can be calculated by integrating the transmitted
radiation over all angles. However, the angular
distribution of this radiation is generally unknown.

If the incident radiation is isotropic (i.e.,
independent of angle), then the integration can be
performed. The presentation of the results can be
simplified by defining an equivalent angle for beam
radiation that gives the same transmittance as for
diffuse radiation. For a wide range of conditions
encountered in solar collector application, this
equivalent angle is essentially $60°$. In other words,
beam radiation incident at an angle of $60°$ has the
same transmittance as isotopic diffuse radiation.

Solar collectors are usually oriented so that
they "see" both the sky and the ground if the diffuse

radiation from the sky and ground are both isotopic,
then the transmittance of the glazing systems can be
found by integrating the beam transmittance over the
appropriate incidence angles. This integration has
been done by Brandemuehl and Beckman (1980) and the
results are presented in terms of the effective beam
radiation incidence angle. Using least-squares curve
fits, their results can be presented by the following
equations:

For diffuse radiation from the sky the effective
beam incident angle is given by:

$$\theta_e = 59.68° - 0.1388\beta + 0.001497\beta^2 \tag{3.51}$$

and for diffuse ground radiation

$$\theta_e = 90° - 0.5788\beta + 0.002693\beta^2 \tag{3.52}$$

3.3.5 Transmittance-Absorptance Product

For the analysis of flat plate solar collectors,
it is necessary to evaluate the
transmittance-absorptance product, $(\tau\alpha)$. Of the
radiation passing through the cover system and
striking the plate, some is reflected back to the
cover system. However, all this radiation is not
lost since some of it is, in turn, reflected back to
the plate.

The situation is illustrated in Figure 3.5,
where τ is the transmittance of the cover system at
the desired angle and α is the angular absorptance of

the absorber plate. Of the incident energy, $\tau\alpha$ is absorbed by the absorber plate and $(1-\alpha)\tau$ is reflected back to the cover system. The reflection from the absorber plate is assumed to be diffuse (and unpolarized) so that the fraction $(1-\alpha)\tau$ that strikes the cover plate is diffuse radiation and $(1-\alpha)\tau\rho_d$ is reflected back to the absorber plate. The quantity ρ_d refers to the reflectance of the cover system for diffuse radiation incident from the bottom side and can be estimated from Equation 3.49 at an angle of $60°$. The multiple reflection of diffuse radiation continues so that the energy ultimately absorbed is

$$(\tau\alpha) = \tau\alpha \sum_{n=0}^{\infty} \left[(1-\alpha)\rho_d\right]^n = \frac{\tau\alpha}{1 - (1-\alpha)\rho_d} \tag{3.53}$$

3.3.6 Absorbed Solar Radiation

The prediction of collector performance requires information on the solar energy absorbed by the collector absorber plate. The solar energy incident on a tilted collector can be found by the methods of Section 3.1. This incident radiation has three different spatial distributions: beam radiation, diffuse sky radiation and diffuse ground-reflected radiation, and each must be treated separately. On an hourly basis the absorbed radiation, S, is

$$S = I_b R_b \ (\tau\alpha)_b + I_d (\tau\alpha)_d \frac{(1+\text{Cos}\beta)}{2}$$

$$+ \rho_g (I_b + I_d)(\tau\alpha)_g \frac{(1-\text{Cos}\beta)}{2} \qquad (3.54)$$

where $(1+\text{Cos}\beta)/2$ and $(1-\text{Cos}\beta)/2$ are the view factors
from the collector to the sky and from the collector
to the ground, respectively. The subscripts b,d and
g represent beam, diffuse, and ground. For a given
collector tilt, the effective beam incidence angles
of Equations 3.51 and 3.52 can be used to find the
proper transmittance values for diffuse sky and
ground radiation. Equation 3.53 can then be used to
find $(\tau\alpha)_d$ and $(\tau\alpha)_g$. The angle θ, which is needed
in evaluating R_b, is used to find $(\tau\alpha)_b$.

Table 3.1 Recommended Average Day for Each Month
[from Klein (1977)] and Values of N by Months.

Month	N for i^{th} Day of Month	For the Average Day of the Month		
		Date	Day of Year	δ, Declination
Jan.	i	17	17	-20.9
Feb.	31+i	16	47	-13.0
March	59+i	16	75	- 2.4
April	90+i	15	105	9.4
May	120+i	15	135	18.8
June	151+i	11	162	23.1
July	181+i	17	198	21.2
Aug.	212+i	16	228	13.5
Sep.	243+i	15	258	. 2.2
Oct.	273+i	15	288	- 9.6
Nov.	304+i	14	318	-18.9
Dec.	334+i	10	334	-23.0
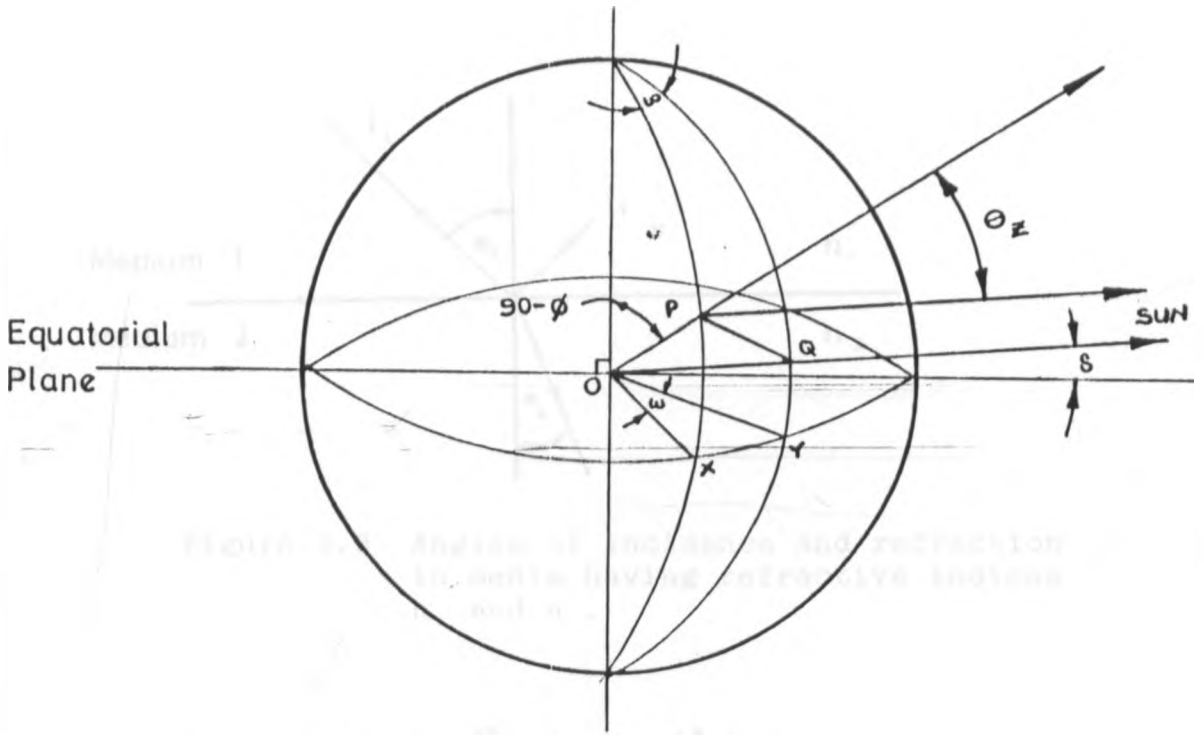
Figure 3.1   Position of the sun.
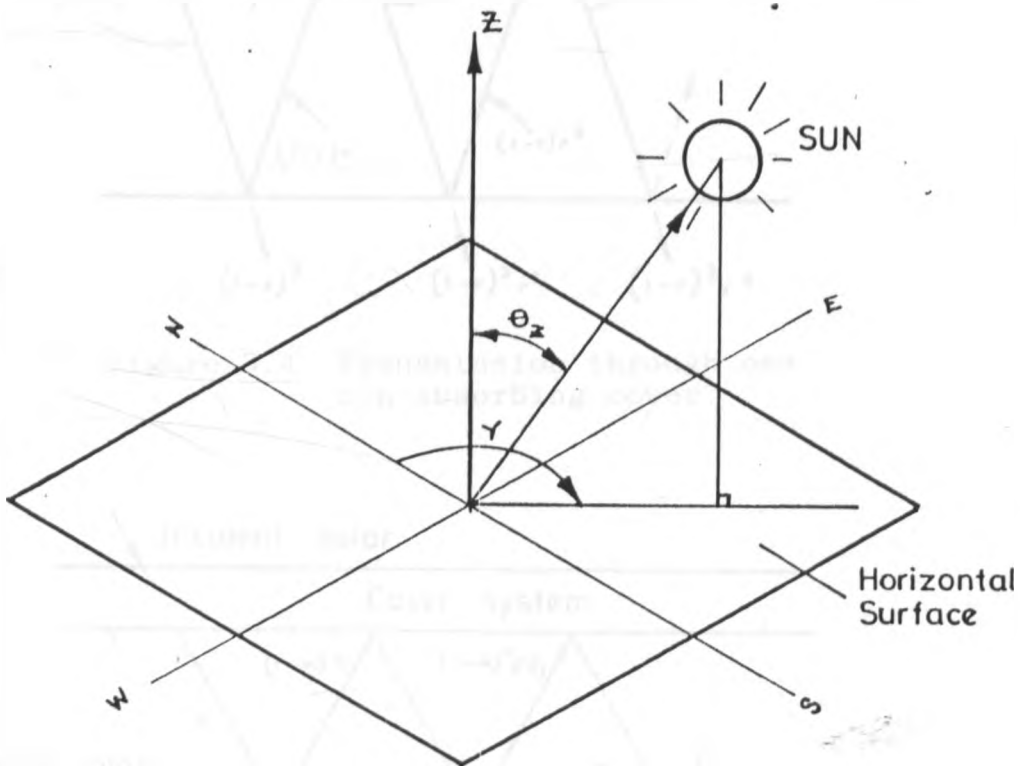
Figure 3.2   Solar zenith angle, Θ_z and azimuth, Υ, shown in their relationship to a horizontal surface on the earth's surface.
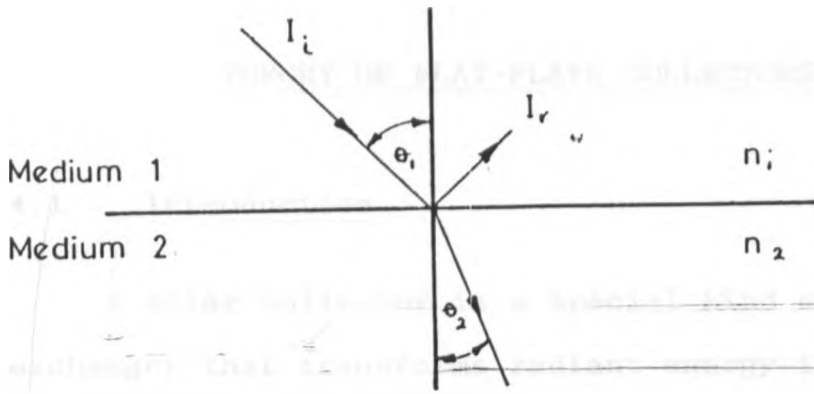
Figure 3.3 Angles of incidence and refraction in media having refractive indices n and n .
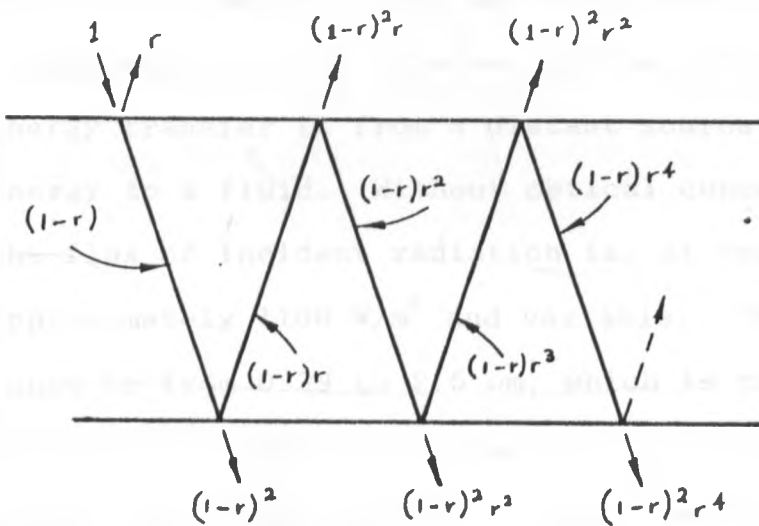
Figure 3.4 Transmission through one non-absorbing cover.
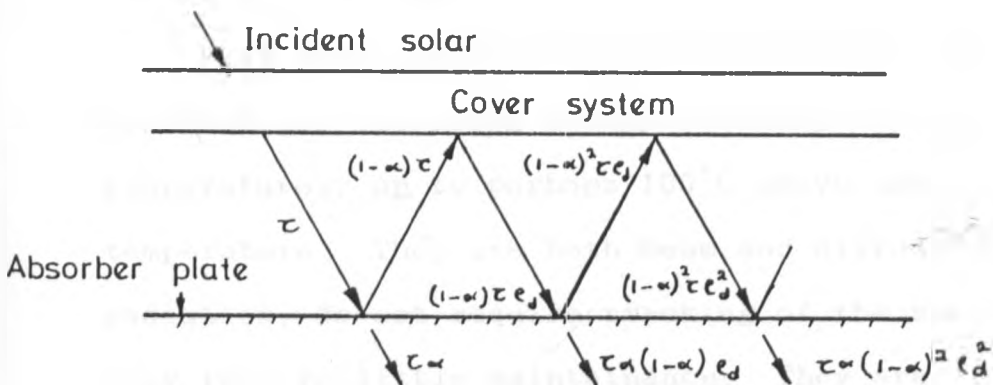
Figure 3.5 Adsorption of solar radiation by absorber plate.

CHAPTER FOUR

THEORY OF FLAT-PLATE COLLECTORS

4.1   Introduction

A solar collector is a special kind of heat exchanger that transforms radiant energy into heat. A solar collector differs in several aspects from the more conventional heat exchangers in that the latter usually accomplish a fluid-to-fluid exchange with high heat transfer rates and with radiation as an unimportant factor. Whereas in the solar collector, energy transfer is from a distant source of radiant energy to a fluid. Without optical concentration, the flux of incident radiation is, at best, approximately 1100 W/m^2 and variable. The wavelength range is from 0.39 to 2.5 μm, which is considerably shorter than that of the emitted radiation from most energy-absorbing surfaces. Thus, the analysis of solar collectors presents unique problems of low and variable energy fluxes and the relatively large importance of radiation.

Flat-plate collectors can be designed for applications requiring energy delivery at moderate temperatures, up to perhaps 100°C above ambient temperature. They use both beam and diffuse solar radiation, do not require tracking of the sun, and they require little maintainance. They are

mechanically simpler than concentrating collectors.
The major applications of these units currently are
in solar water heating, building air conditioning and
industrial process heat.

4.2   General Description of Flat-Plate Collectors

The important parts of a typical liquid heating
flat-plate solar collector are, as shown in Figure
4.1, the "black" solar energy-absorbing surface, with
means for transferring the absorbed energy to a fluid;
envelopes transparent to solar radiation over the
solar absorber surface that reduces convection and
radiation losses to the atmosphere; and back
insulation to reduce conduction losses as the
geometry of the system permits.

Flat-plate collectors are almost always mounted
in a stationary position (e.g., as an integral part
of a wall or roof structure) with an orientation
optimised for the time of the year in which the solar
device is intended to operate.   In their most common
forms, they are air or liquid heaters or low-pressure
vapour generators.

4.3   The Basic Flat-Plate Energy Balance Equation

In steady state, the performance of a solar
collector is described by an energy balance that

indicates the distribution of incident solar energy
into useful energy gain, thermal losses, and optical
losses. The solar radiation absorbed by a collector
S, is equal to the difference between the incident
solar radiation and the optical losses and is defined
by Equation 3.54. The thermal energy lost from the
collector to the surroundings by conduction,
convection and infrared radiation can be represented
by a heat transfer coefficient, U_L, times the
difference between the mean absorber plate
temperature, $T_{p,m}$ and the ambient temperature, T_a.
In steady state the useful energy output of a
collector is then the difference between the absorbed
solar radiation and the thermal loss:

$$Q_u = A_c \left[S - U_L (T_{p,m} - T_a) \right] \tag{4.1}$$

The problem with this equation is that the mean
absorber plate temperature is difficult to calculate
since it is a function of the collector design, the
incident solar radiation, and the entering fluid
conditions. Hence, it has to be reformulated so that
the useful energy can be expressed in terms of the
inlet fluid temperature and a parameter, called the
collector heat removal factor, which can be evaluated
analytically from basic principles or measured
experimentally.

A measure of collector performance is the
collection efficiency, defined as the ratio of the

useful gain over some specified time period to the
incident solar energy over the same time period.

$$\eta = \frac{\int Q_u \, d\tau}{A_c \int G_r \, d\tau} \tag{4.2}$$

4.4 Temperature Distribution in Flat-Plate Solar Collectors

A detailed and precise analysis of the
efficiency of a solar collector is complicated by the
nonlinear behaviour of radiation heat transfer.
However, a simple linearized analysis is normally
sufficiently accurate in practice. In addition, the
simplified analytical procedure is very important,
because it illustrates the parameters of significance
for a solar collector and how these parameters
interact. For a proper analysis and interpretation
of these test results an understanding of the thermal
analysis is imperative, although for design and
economic evaluation the results of standardized
performance tests are generally used.

To illustrate these basic principles, a liquid
heating collector, as shown in Figure 4.2 will be
examined first. The analysis presented follows the
basic derivation of Hottel and Whillier (1958) and
Whillier (1977).

To appreciate the development that follows, it
is desirable to have an understanding of the

temperature distribution that exists in a solar collector constructed as shown in Figure 4.2. Figure 4.3 shows the qualitative temperature distributions in a flat-plate collector region between two tubes. Radiation impinges on top of the plate connecting any two adjacent tubes, and is absorbed uniformly by the plate and conducted along the plate to the region of the tubes, where it is then transferred by convection to the working fluid flowing in the tubes. It is apparent that at any cross section perpendicular to the direction of flow, the temperature is a maximum at the mid-point between two adjacent tubes and decreases along the plate towards the tubes. The temperature above the tubes will be nearly uniform because of the presence of the tube and weld metal.

The energy transferred to the fluid then heats up the fluid causing a temperature gradient to exist in the direction of flow. Since in any region of the collector the general temperature level is governed by the local temperature level of the fluid, a situation as shown in Figure 4.3b is expected. At any location y, the general temperature distribution in the x direction is as shown in Figure 4.3c, and at any location x, the temperature distribution in the y direction will look like Figure 4.3d.

To model the situation shown in Figure 4.3 a number of simplifying assumptions can be made to lay the foundations without obscuring the basic physical

situation.   These important assumptions are as
follows:

1.   Performance is steady-state.

2.   Construction is of sheet and parallel tube type.

3.   The headers cover a small area of collector and
     can be neglected.

4.   The headers provide uniform flow to tubes.

5.   There is no absorption of solar energy by covers
     in so far as it affects losses from the
     collectors.

6.   There is one-dimensional heat flow through
     covers.

7.   There is negligible temperature drop through a
     cover.

8.   The covers are opaque to infrared radiation.

9.   There is one-dimensional heat flow through
     back-insulation.

10. The sky can be considered as a blackbody for
     long-wavelength radiation at an equivalent sky
     temperature.

11. Temperature gradients around tubes can be
     neglected.

12. The temperature gradient in the direction of flow
     between the tubes can be treated independently.

13. Properties are independent of temperature.

14. Loss through front and back are to the same
     ambient temperature.

15.   Dust and dirt on the collector are negligible.

16. Shading of the collector absorber plate is negligible.

4.5 Collector Overall Heat Transfer Coefficient

In order to obtain an understanding of the parameters determining the thermal efficiency of a solar collector, it is important to develop the concept of collector overall heat coefficient. Consider the thermal network for a two-cover system shown in Figure 4.4. At some typical location on the plate where the temperature is T_p, solar energy of amount S is absorbed by the plate; S is equal to the incident solar radiation, less the optical losses. This absorbed energy S is distributed to thermal losses through the top and bottom, and to useful energy gain. The heat loss through the bottom of the collector can be represented by two series resistors, R_4 and R_5 in Figure 4.4b. R_4 represents the resistance to heat flow through the insulation and R_5 represents the convection and radiation resistance to the environment. The magnitudes of R_4 and R_5 are such that it is usually possible to assume R_5 is zero and all resistance to heat flow is due to the insulation. Thus, the back loss coefficient, U_b is approximately.

$$U_b = \frac{1}{R_4} = \frac{K_i}{L_i} \tag{4.3}$$

For most collectors the evaluation of edge losses is quite complicated. However, in a well designed collector the losses should be small and need not be predicted with great accuracy. Tabor (1958) recommends edge insulation of about the same thickness as bottom insulation. The edge losses are then estimated by assuming one-dimensional sideways heat conduction around the perimeter of the collector system. Thus for a collector of area $L_1 L_2$ and thickness L_3 , and with a layer of insulation L_i thick along the sides, if the edge loss coefficient-area product is $(UA)_{edge}$ then the edge loss coefficient, based on the collector area, A_c, is:

$$U_e = \frac{(UA)_{edge}}{A_c} = 2\frac{(L_1 + L_2)L_3}{L_1 L_2}\left(\frac{K_i}{L_i}\right)_{edge} \qquad (4.4)$$

The energy loss through the top is the result of convection and radiation between parallel plates and can be evaluated by determining the thermal resistances R_1 , R_2 and R_3 in Figure 4.4b. The energy transfer between the plate at T_p and the first cover at T_{c1} is the same as between any other two adjacent covers and is also equal to the energy lost to the surroundings from the top cover (under the assumptions listed). The loss through the top per unit area is then equal to the heat transfer from the absorber plate to the first cover.

$$q_{loss,top} = h_{p-c1}(T_p - T_{c1}) + \frac{\sigma(T_p^4 - T_{c1}^4)}{\frac{1}{\varepsilon_p} + \frac{1}{\varepsilon_c} - 1} \qquad (4.5)$$

If the radiation term is linearized, the radiation heat transfer coefficient can be used and the heat loss becomes :

$$q_{loss,top} = (h_{p-c1} + h_{r,p-c1})(T_p - T_{c1}) \qquad (4.6)$$

where

$$h_{r,p-c1} = \frac{(T_p + T_{c1})(T_p^2 + T_{c1}^2)}{\frac{1}{\varepsilon_p} + \frac{1}{\varepsilon_{c1}} - 1} \qquad (4.7)$$

The resistance, R_3, can then be expressed as

$$R_3 = \frac{1}{h_{p-c1} + h_{r,p-c1}} \qquad (4.8)$$

A similar derivation for the rate of heat transfer between the two cover plates gives

$$q_{loss,top} = (h_{c1-c2} + h_{r,c1-c2})(T_{c1} - T_{c2}) \qquad (4.9)$$

where

$$h_{r,c1-c2} = \frac{(T_{c1} + T_{c2})(T_{c1}^2 + T_{c2}^2)}{\frac{1}{\varepsilon_{c1}} + \frac{1}{\varepsilon_{c2}} - 1} \qquad (4.10)$$

Similarly the resistance, R_2, can be written as

$$R_2 = \frac{1}{h_{c1-c2} + h_{r,c1-c2}} \qquad (4.11)$$

In general, as many cover plates as desired can can be used but the practical limit seems to be three, and most collectors use one or two.

The emittances of the covers will, of course, be the same if they are made of the same material. However, economic advantages can sometimes be achieved by using a plastic cover between an outer cover of glass and the plate and in such a sandwich construction, the radiative properties of the two covers may be different.

The equation for the thermal resistance from the top cover to the ambient air has a form similar to the two preceding relations, but the convection heat transfer coefficient is for wind blowing over the collector. An equation for the wind heat transfer coefficient, h_w, is given by McAdams (1954) as :

$$h_w = 5.7 + 3.8V \tag{4.12}$$

The radiation resistance from the top cover accounts for radiation exchange with the sky at T_s. For convenience, this resistance is referenced to the ambient temperature, T_a, so that the radiation heat transfer coefficient can be written as :

$$h_{r,c2-a} = \varepsilon_{c2} \frac{\sigma(T_{c2} + T_s)(T_{c2}^2 + T_s^2)(T_{c2} - T_s)}{(T_{c2} - T_a)} \tag{4.13}$$

The resistance to the surroundings is then given by

$$R_1 = \frac{1}{h_w + h_{r,c2-a}} \tag{4.14}$$

For this two-cover system, the top loss coefficient from the collector plate to the ambient is :

$$U_t = \frac{1}{R_1 + R_2 + R_3} \tag{4.15}$$

The collector overall loss coefficient, U_L is then the sum of the top, bottom and edge loss coefficients.

$$U_L = U_t + U_b + U_e \tag{4.16}$$

Evaluation of the collector top loss coefficient as defined by Equation 4.15 is necessarily an iterative process because the unit radiation conductances are functions of the cover and plate temperatures, which are not known a priori. An empirical equation for calculating U_t for collectors with all covers of the same material, which is often sufficiently accurate and more convenient to use, has been developed by Agarwal and Larson (1981) following the basic procedure of Hottel and Woertz (1942) and Klein (1975). This new relationship is not only simpler to manipulate as compared to that due to Klein (1975), but it also provides an enhanced accuracy in the calculation of U_t over a wide range of different parameters. The equation is given by:

$$U_t = \left[\frac{N}{\left(\frac{C}{T_p}\right)\left(\frac{T_p - T_a}{N + f}\right)^{0.33}} + \frac{1}{h_w} \right]^{-1}$$

$$+ \frac{\sigma(T_p + T_a)(T_p^2 + T_a^2)}{\left[\varepsilon_p + 0.05N(1-\varepsilon_p)\right]^{-1} + \left(\frac{2N + f - 1}{\varepsilon_g}\right) - N} \quad (4.17)$$

where

$$f = (1 - 0.04h_w + 0.005h_w^2)(1 + 0.091N) \quad (4.18)$$

$$C = 250 \left[1 - 0.0044(\beta - 90)\right] \quad (4.19)$$

To use this empirical relationship or the more complicated exact equations to find U_t, it is necessary to know the mean plate temperature, $T_{p,m}$.

4.6 Temperature Distribution between Tubes and the Collector Efficiency Factor

The temperature distribution between two tubes can be derived if it is temporarily assumed that the temperature gradient in flow direction is negligible. Consider the plate-tube configuration as shown in Figure 4.5. The distance between the tubes is W, the tube diameter is D and the plate is thin with a thickness δ. Because the sheet material is a good conductor, the temperature gradient through the sheet is negligible. It will be assumed that the sheet above the bond is at some local base temperature, T_b. The region between the centerline separating the

tubes and the tube base can then be considered as a classical fin problem.

The fin is of length $(W-D)/2$. Considering an energy balance on an elemental region of width Δx and unit length in the flow direction gives

$$S\Delta x + U_L \Delta x (T_a - T) + \left(-k\delta\frac{dT}{dx}\right)\bigg|_x - \left(-k\delta\frac{dT}{dx}\right)\bigg|_{x+\Delta x} = 0 \qquad (4.20)$$

where S is the absorbed solar energy. Dividing through by Δx and finding the limit as Δx tends to zero gives

$$\frac{d^2T}{dx^2} = \frac{U_L}{k\delta}\left(T - T_a - \frac{S}{U_L}\right) \qquad (4.21)$$

The two boundary conditions necessary to solve this second-order differential equation are symmetry at the centerline and known root temperature;

$$\frac{dT}{dx}\bigg|_{x=0} = 0, \qquad T\big|_{x=(W-D)/2} = T_b \qquad (4.22a,b)$$

If $m^2 = U_L/k\delta$ and $\phi = T - T_a - S/U_L$, Equation 4.21 becomes

$$\frac{d^2\phi}{dx^2} - m^2\phi = 0 \qquad (4.23)$$

which has the boundary conditions

$$\frac{d\phi}{dx}\bigg|_{x=0} = 0, \qquad \phi\big|_{x=(W-D)/2} = T_b - T_a - S/U_L \qquad (4.24a,b)$$

The general solution is then

$$\phi = C_1 Sinh(mx) + C_2 Cosh(mx) \tag{4.25}$$

The constant C_1 and C_2 can be found by substituting the boundary conditions, Equation 4.24, into the general solution, which gives

$$\frac{T - T_a - S/U_L}{T_b - T_a - S/U_L} = \frac{Cosh(mx)}{Cosh[m(W-D)/2]} \tag{4.26}$$

The energy conducted to the region of the tube per unit length in the flow direction can now be found by evaluating Fourier's law at the fin base.

$$q'_{fin} = -k\delta \left. \frac{dT}{dx} \right|_{x=(W-D)/2}$$

$$= \frac{k\delta m}{U_L}[\delta - U_L(T_b - T_a)]tanh\left(m \frac{W-D}{2}\right) \tag{4.27}$$

But $k\delta m/U_L$ is just $1/m$. Equation 4.27 accounts for the energy collected only on one side of the tube. For both sides, the energy collected is

$$q'_{fin} = (W-D)[S-U_L(T_b - T_a)]\frac{tanh[m(W-D)/2]}{m(W-D)/2} \tag{4.28}$$

It is convenient to use the concept of a fin efficiency to rewrite Equation 4.28 as

$$q'_{fin} = (W-D)F[S- U_L(T_b - T_a)] \tag{4.29}$$

where

$$F = \frac{tanh[m(W-D)/2]}{m(W-D)/2} \tag{4.30}$$

The function F is the standard fin efficiency for straight fins with rectangular profile.

The useful gain of the collector also includes the energy collected above the tube region. The energy gain for this region is

$$q'_{tube} = D[S - U_L(T_b - T_a)] \qquad (4.31)$$

and the useful gain for the collector per unit of length in the flow direction is the sum of Equations 4.29 and 4.31

$$q'_u = [(W-D)F + D][S - U_L(T_b - T_a)] \qquad (4.32)$$

Ultimately, the useful gain from Equation 4.32 must be transferred to the fluid. The resistance of heat flow to the fluid results from the bond and the fluid to tube resistance. The useful gain can be expressed in terms of these two resistances as

$$q'_u = \frac{T_b - T_a}{\dfrac{1}{\pi D_i h_f} + \dfrac{1}{C_b}} \qquad (4.33)$$

The bond conductance, C_b, can be estimated from knowledge of the bond thermal conductivity, k_b, the bond average thickness, γ, and the bond width, b. On a per unit length basis,

$$C_b = \frac{k_b b}{\gamma} \qquad (4.34)$$

The bond conductance can be very important in accurately describing collector performance.

Whillier and Saluja (1965) have shown by experiments that simple wiring or clamping of the tubes to the sheet results in a significant loss of performance. They concluded that it is necessary to have good metal-to-metal contact so that bond conductance is greater than 30 W/mK.

In order to obtain an expression for the useful gain in terms of known dimensions, physical parameters, and the local fluid temperature, T_b must be eliminated from consideration. Solving Equation 4.32 for T_b, substituting it into Equation 4.33, and solving the result for the useful gain gives,

$$q'_u = WF' [S - U_L (T_f - T_a)] \qquad (4.35)$$

where F', is the collector efficiency factor given by

$$F' = \cfrac{\cfrac{1}{U_L}}{\cfrac{1}{U_L [D + (W-D)F]} + \cfrac{1}{C_b} + \cfrac{1}{\pi D_i h_f}} \qquad (4.36)$$

A physical interpretation for F' results from examination of Equation 4.35. At a particular location, F' represents the ratio of the actual energy gain to the useful energy gain that would result if the collector absorbing surface had been at the local fluid temperature. For this and most, but not all geometries, another interpretation for the parameter F' becomes clear when it is recognized that the denominator of Equation 4.36 is the heat transfer

resistance from the fluid to the ambient air. This resistance will be given the symbol $1/U_o$. The numerator is the heat transfer resistance from the absorber plate to the ambient air. F' is thus the ratio of these two heat transfer coefficients

$$F' = \frac{U_o}{U_L} \qquad (4.37)$$

The collector efficiency factor is essentially a constant for any collector design and fluid flow rate. The ratio of U_L to C_b, the ratio of U_L to h_f, and the fin efficiency parameter F are the only variables in Equation 4.36 that may be functions of temperature. For most collector designs F is the most important of these variables in determining F', but it is not a strong function of temperature.

The collector efficiency factor increases with increasing plate thickness and plate thermal conductivity, but decreases with increasing distance between flow channels. Also, increasing the heat transfer coefficient between the walls of the flow channels and the working fluid increases F', but an increase in the overall loss coefficient will cause F' to decrease.

4.7   Temperature Distribution in Flow Direction

Equation 4.35 gives the rate of heat transfer to the working fluid at a given point y along the plate

for specified collector and fluid temperatures.
However, in a real collector, the fluid temperature
increases in the direction of flow as heat is
transferred to it. An energy balance on the fluid
flowing through a single tube of length Δy can be
expressed as:

$$\left(\frac{\dot{m}}{n}\right) C_p T_f \Big|_y - \left(\frac{\dot{m}}{n}\right) C_p T_f \Big|_{y+\Delta y} + \Delta y q_u' = 0 \qquad (4.38)$$

Dividing through by Δy, finding the limit as Δy tends
to zero, and substituting Equation 4.35 for q_u' gives

$$\dot{m} C_p \frac{dT_f}{dy} - nWF' [S - U_L (T_f - T_a)] = 0 \qquad (4.39)$$

If it is assumed that F' and U_L are independent of
position, then the solution for the temperature at
any position y (subject to the condition that the
inlet fluid temperature is $T_{f,i}$) is

$$\frac{T_f - T_a - S/U_L}{T_{f,i} - T_a - S/U_L} = \exp\left(- \frac{n U_L WF' y}{\dot{m} C_p}\right) \qquad (4.40)$$

If the collector has a length L in the flow
direction, then the outlet fluid temperature, $T_{f,o}$ is
found by substituting L for y in Equation 4.40. The
quantity nWL is the collector area so that

$$\frac{T_{f,o} - T_a - S/U_L}{T_{f,i} - T_a - S/U_L} = \exp\left(- \frac{A_c U_L F'}{\dot{m} C_p}\right) \qquad (4.41)$$

4.8   Collector Heat Removal Factor and Flow Factor

To compare the performance of a real collector with the thermodynamic optimum, it is convenient to define a quantity that relates the actual rate of heat transfer to the working fluid to the rate of heat transfer at the minimum temperature difference between the absorber and the environment. The thermodynamic limit corresponds to the condition of the working fluid remaining at the inlet temperature throughout the collector. This can be approached when the fluid velocity is very high. This quantity is called the collector heat removal factor, F_R and mathematically is given by

$$F_R = \frac{\dot{m}C_p(T_{f,o} - T_{f,i})}{A_c[S - U_L(T_{f,i} - T_a)]} \tag{4.42}$$

The collector heat removal factor can be expressed as

$$F_R = \frac{\dot{m}C_p}{A_c U_L}\left[\frac{T_{f,o} - T_{f,i}}{S/U_L - (T_{f,i} - T_a)}\right]$$

$$= \frac{\dot{m}C_p}{A_c U_L}\left[\frac{(T_{f,o} - T_a - S/U_L) - (T_{f,i} - T_a - S/U_L)}{S/U_L - (T_{f,i} - T_a)}\right] \tag{4.43}$$

or

$$F_R = \frac{\dot{m}C_p}{A_c U_L}\left[1 - \frac{S/U_L - (T_{f,o} - T_a)}{S/U_L - (T_{f,i} - T_a)}\right] \tag{4.44}$$

which from Equation 4.41 can be expressed as

$$F_R = \frac{\dot{m}C_p}{A_c U_L}\left[1 - \exp\left(-\frac{A_c U_L F'}{\dot{m}C_p}\right)\right] \qquad (4.45)$$

It is convenient to define the collector flow factor, F'', as the ratio of F_R to F'. Thus,

$$F'' = \frac{F_R}{F'} = \frac{\dot{m}C_p}{A_c U_L F'}\left[1 - \exp\left(-\frac{A_c U_L F'}{\dot{m}C_p}\right)\right] \qquad (4.46)$$

This collector flow factor is a function of the single variable, the dimensionless collector capacitance rate, $\dot{m}C_p/A_c U_L F'$.

The quantity F_R is equivalent to a conventional heat exchanger effectiveness, which is defined as the ratio of the actual heat transfer to the maximum possible heat transfer. The maximum possible useful energy gain (heat transfer) in a solar collector occurs when the whole collector is at the inlet fluid temperature ; heat losses to the surroundings are then at a minimum. The collector heat removal factor times this maximum possible useful energy gain is equal to the actual energy gain Q_u.

$$Q_u = A_c F_R [S - U_L (T_i - T_a)] \qquad (4.47)$$

This is an extremely useful equation and it applies to most flat-plate collectors. With it, the useful energy gain is calculated as a function of the inlet fluid temperature. This is a convenient representation when analyzing solar energy systems,

since the inlet fluid temperature is usually known.
However, losses based on the inlet fluid temperature
are too small since losses occur all along the
collector from the plate and the plate has an ever-
increasing temperature in the flow direction.   The
effect of the multiplier, F_R , is to reduce the
useful energy gain from what it would have been had
the whole collector absorber plate been at the inlet
fluid temperature to what actually occurs.   As the
mass flow rate through the collector increases the
temperature rise through the collector decreases.
This causes lower losses since the average collector
temperature is lower and a corresponding increase in
the useful energy gain.   This increase is reflected
by an increase in the collector heat removal factor
F_R as the mass flow rate increases.   It is worth
noting that the heat removal factor F_R can exceed the
collector efficiency factor F'.   As the flow rate
becomes very large, the temperature rise from inlet
to outlet decreases toward zero but the temperature
of the absorbing surface will still be higher than
the fluid temperature.   This temperature difference
is accounted for by the collector efficiency factor
F'.

4.9   Natural Circulation Systems

A passive solar heater, that is, a natural circulation system is shown in Figure 4.6.   It is necessary that the entire storage tank be located above the collector upper outlet so as to facilitate liquid circulation.

Circulation in solar thermosyphon heaters occurs when the collector warms up enough to establish a density difference between the leg including the collector and the leg including the tank and the feed line from the tank to the collector.   As a result, the less dense liquid in the collector tubes rises to the highest point in the assembly, the top of the storage tank, and is replaced in the collector by the denser liquid, which flows from the bottom of the tank and is in turn heated.   The process repeats continuously forming what is termed a thermosyphon circulation pattern.

The density difference is a function of temperature difference, and the flow rate is then a function of the useful gain of the collector which produces the temperature difference.   Under these circumstances, these systems are self-adjusting, with increasing heat gain leading to increasing flow rates through the collector.

There are two alternative methods of modeling the performance of a collector in natural circulation systems.   The first is by analysis of the temperature

and density distributions and resulting flow rates
based on pressure drop calculations, as outlined by
Close (1962). The second is to assume a constant
temperature increase of water or any other fluid
flowing through the collector and calculate the flow
rate which will produce this temperature difference
at the estimated collector gain. The basic equations
are :

$$Q_u = A_c F_R [S - U_L (T_i - T_a)] \tag{4.48}$$

and

$$Q = m C_p (T_o - T_i) = m C_p \Delta T_f \tag{4.49}$$

Solving for the flow rate

$$m = \frac{A_c F_R [S - U_L (T_i - T_o)]}{C_p \Delta T_f} \tag{4.50}$$

This equation can be solved for m if it is assumed
that F' is independent of flow rate. Substituting
Equation 4.46 for F_R into Equation 4.50 and
rearranging gives

$$m = - \frac{U_L F' A_c}{C_p \ln \left[1 - \dfrac{U_L (T_o - T_i)}{S - U_L (T_i - T_o)} \right]} \tag{4.51}$$
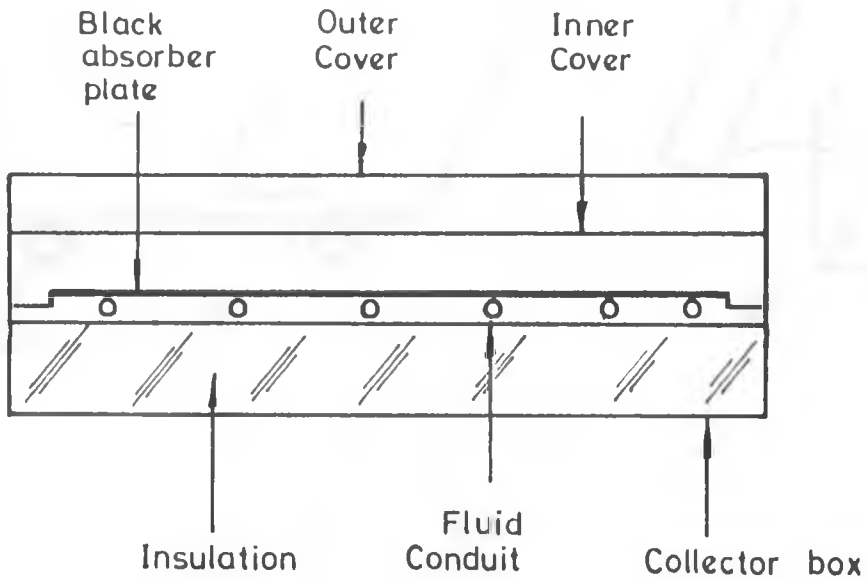
Figure 4.1   Cross-section of a basic
flat-plate solar collector.
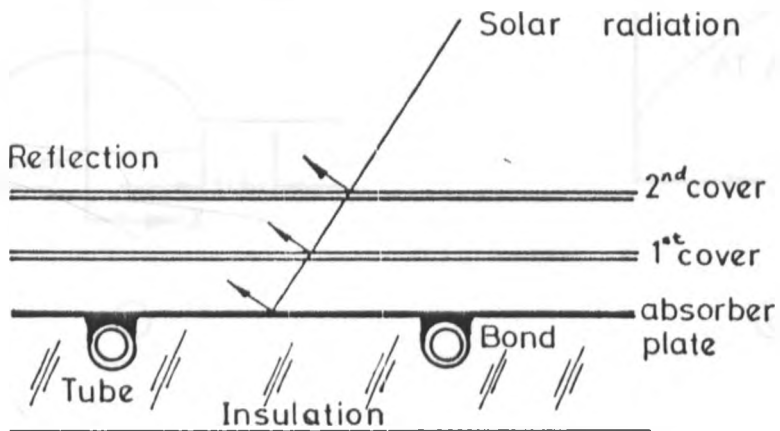
Figure 4.2   Sheet and tube solar collector.

FLUID

(a)

(b)

T

AT A FIXED Y

tube | Sheet | tube

X

(c)

T

AT A FIXED X

Y

(d)
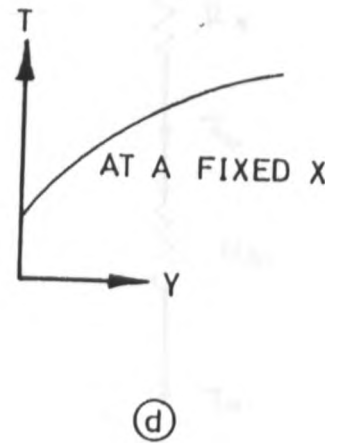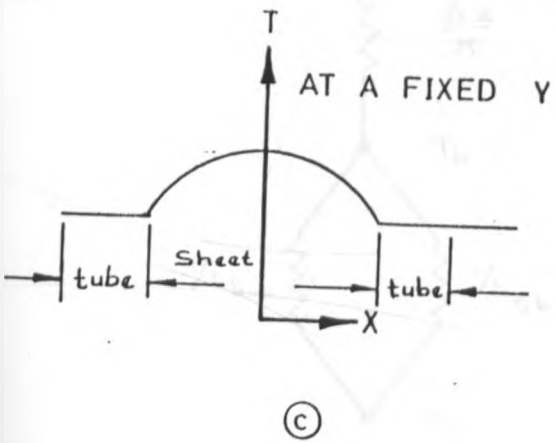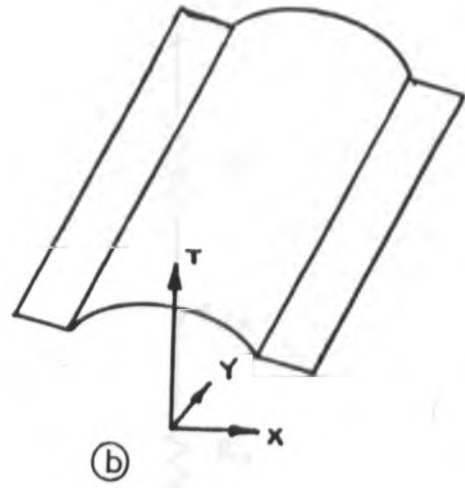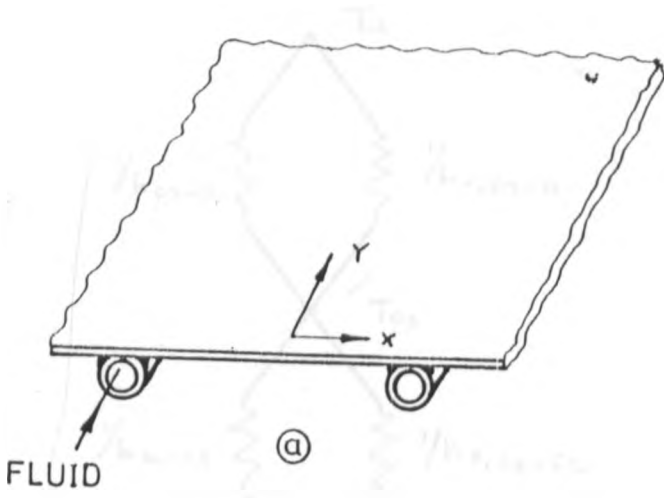
Figure 4.3   Temperature distribution on an
absorber plate.   [From Duffie and
Beckman (1980)]
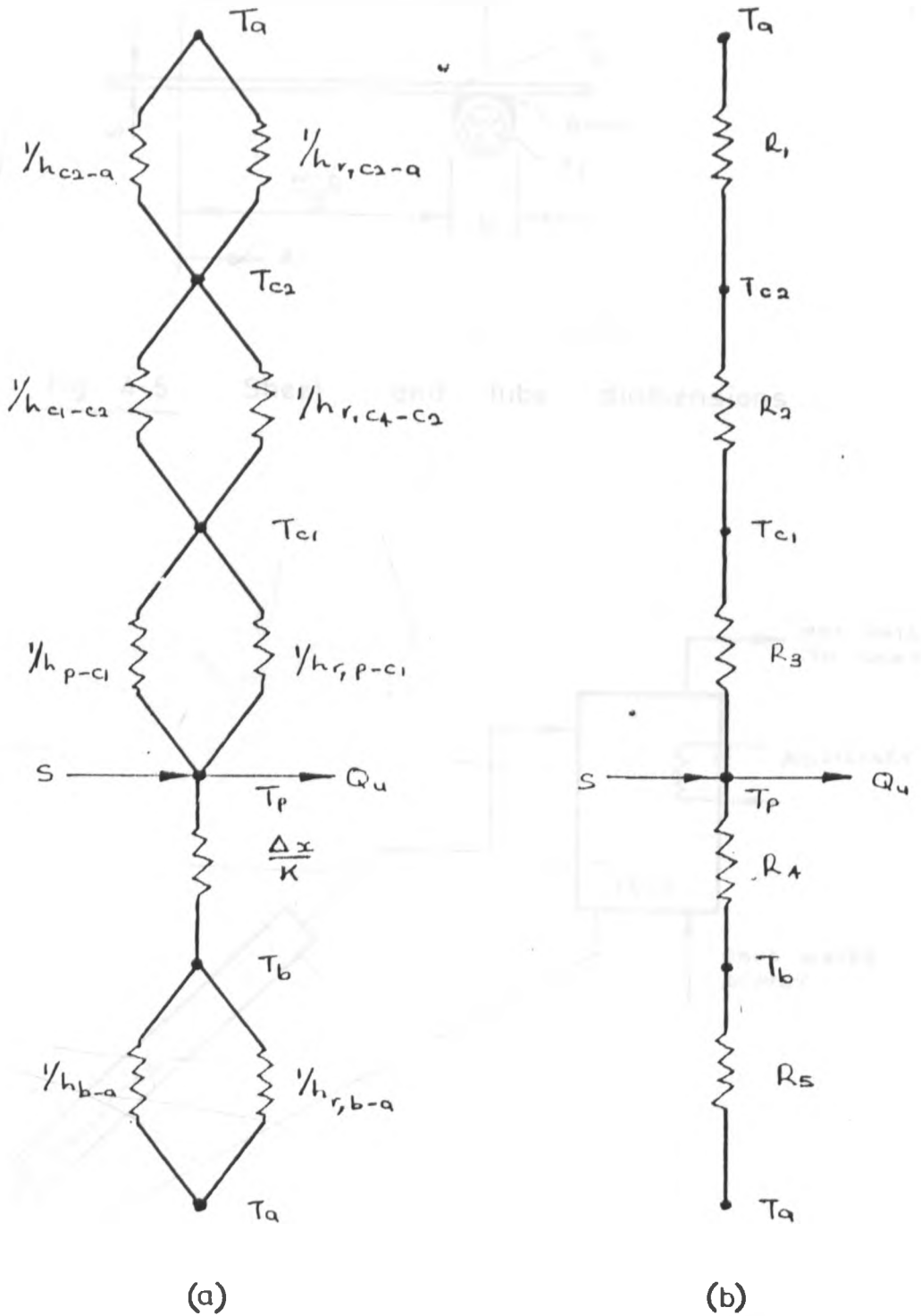
Figure 4.4   Thermal network for a two-cover
             flat-plate collector. (a) in terms
             of conduction, convection and
             radiation resistances, (b) in terms
             resistances between plates.
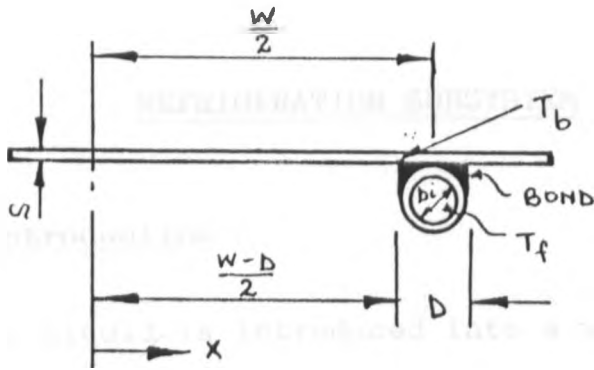
Fig. 4·5   Sheet   and   tube   diamensions.
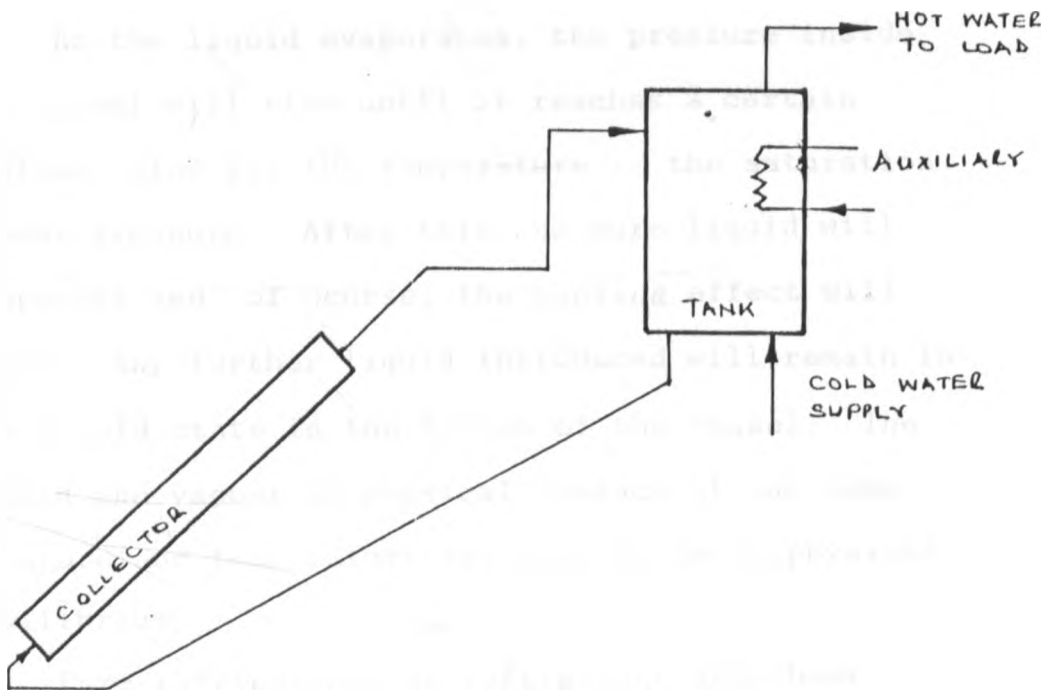
Fig. 4·6   Schematics   of   a   natural
circulation   system.

CHAPTER FIVE

REFRIGERATION SUBSYSTEM

5.1   Introduction

If a liquid is introduced into a vessel in which
there is initially a vacuum and whose walls are kept
at a constant temperature it will at once evaporate.
In the process the latent heat of vaporisation will
be abstracted from the sides of the vessel.   The
resulting cooling effect is the starting point of the
refrigeration cycle.

As the liquid evaporates, the pressure inside
the vessel will rise until it reaches a certain
maximum value for the temperature :- the saturation
vapour pressure.   After this, no more liquid will
evaporate and, of course, the cooling effect will
cease.   Any further liquid introduced will remain in
the liquid state in the bottom of the vessel.   The
liquid and vapour in physical contact at the same
pressure and temperature are said to be in physical
equilibrium.

Pure refrigerants or refrigerant-absorbent
combinations are used in a refrigeration process for
the artificial removal of heat energy from a space or
substance, producing in such a space or substance, a
temperature lower than that which would otherwise
exist under the natural influence of the environment.

5.2   Refrigerant Properties

For pure refrigerant of a two phase system in
equilibrium, the interdependence of the physical
properties of pressure and temperature are given by
Clapeyron's equations and the relationship between
the thermodynamic properties are given by the four
Maxwell equations amongst others.

For refrigerant-absorbent combinations, the
state of solution and the interdependence of the
physical properties are given by the phase rule,
which states that:

If equilibrium of phases in a system is not
influenced by gravity, electrical or magnetic forces
or by surface action and is only influenced by
temperature, pressure and concentration, then the
number of degrees of freedom F of the system is
related to the number of components C appearing in
all the phases at equilibrium and the number of
phases P by the equation

$$F = C - P + 2 \tag{5.1}$$

The number of degrees of freedom of the system
is the number of independent variables which may be
arbitrarily specified and which must be so specified
in order to fix the intensive state of a system at
equilibrium. This number is the difference between
the number of variables needed to characterize the
system and the number of equations that may be
written connecting these variables.

For the ammonia-water refrigeration system, there are two components, namely, ammonia and water and two phases: liquid solution and vapour. Then

F = 2 - 2 + 2 = 2

Hence only two of the three intensive properties of pressure, temperature and concentration are necessary to define the state of the solution when in equilibrium.

5.3   Characteristics of the Refrigerant-Absorbent Pair

The two materials that make up the refrigerant-absorbent pair should meet the following requirements to be suitable for absorption refrigeration :

(1) Absence of solid phase.

The refrigerant-absorbent pair should not form a solid phase of the range of composition and temperature to which it might be subjected. If solid forms, it presumably would stop flow and cause equipment shutdown.

(2) Volatility Ratio.

The refrigerant should be much more volatile than the absorbent so that the two can be easily separated. Otherwise, cost and heat requirements can prohibit separation.

(3)   Affinity.

The absorbent should have a strong affinity for the refrigerant under conditions in which absorption takes place [Buffington (1949)].   This affinity, (1) causes a negative deviation from Raoult's Law and results in an activity coefficient of less than unity for the refrigerant, (2) reduces the amount of absorbent to be circulated and, consequently, the waste of thermal energy from sensible heat effects and (3) reduces the size of the liquid heat exchanger that transfers heat from absorbent to pressurized refrigerant-absorbent solution in practical cycles. Calculations by Jacob, Albright and Tucker (1969) indicate that strong affinity does have disadvantages. This affinity is associated with a high heat of dilution; consequently, extra heat is required in the generator to separate refrigerant from absorbent.

(4)   Pressure.

Operating pressures, largely established by physical properties of the refrigerant, should be moderate.   High pressures necessitate use of heavy-walled equipment and significant electrical power may be required to pump the fluids from low side to high side.   Low pressures (vacuum) necessitate use of large volume equipment and special means of reducing pressure drop in refrigerant vapour flow.

(5)   Stability.

Almost absolute chemical stability is required, because fluids are subjected to rather severe conditions over many years of service.   Instability could cause undesirable formation of gases, solids or corrosive substances.

(6)   Corrosion.

Since the fluids or substances resulting from instability can corrode materials used in construction of equipment, corrosion inhibitors should be used.

(7)   Safety.

Fluids must be non-toxic and non-flammable if they are in an occupied dwelling.   Industrial process refrigeration is less critical in this respect.

(8)   Transport Properties.

Viscosity, surface tension, thermal diffusivity are important characteristics of the refrigerant and absorbent pair.   For example, low viscosity of the fluid promotes heat and mass transfer, and, to some extent, reduces pumping problems.

(9)   Latent Heat.

The refrigerant's latent heat should be high so that circulation rate of the refrigerant and absorbent can be kept at a minimum.

No known refrigerant-absorbent pair meets all the requirements listed.   Ammonia-water and water-lithium bromide come closest, and these are the only two pairs in extensive commercial use.

The ammonia-water pair meets most requirements, but it's volatility ratio is too low and it requires high operating pressures. Not withstanding ammonia-water is selected for this study because it can easily be found on the Kenya market since refrigeration applications require temperatures under $0^\circ C$ (273K) and the lithium bromide-water pair tends to form solid since the refrigerant turns to ice at $0^\circ C$, the pair cannot be used for low temperature refrigeration. Also, lithium bromide crystallizes out of solution at moderate concentrations, especially when it is air cooled, limiting the pair to applications where the absorber is water cooled. Ammonia-water on the other hand is not subjected to crystallization and it is considerably cheaper than water-lithium bromide, a factor that is important since refrigerant storage is being considered.

Advantages of water-lithium bromide pair include high safety, high volatility ratio, high affinity, high stability and high latent heat. However, using a combination of salts as the absorbent can reduce the crystallizing tendency enough to permit air cooling [Macriss (1969), Weil (1968) and Blytas and Daniels (1962)]. Hence its application is typically limited to air conditioning units. Other disadvantages of the water-lithium bromide pair include the low operating pressures it requires and the lithium bromide solution's high viscosity.

Proper equipment design can however overcome these
disadvantages.

Other important refrigerant-absorbent pair
include:

(1)   Ammonia-salts

(2)   Methylamine-salts

(3)   Alcohols-salts

(4)   Ammonia-organic solvents

(5)   Sulphur dioxide-organic solvents

(6)   Halogenated hydrocarbons-organic solvents.

Several of these appear suitable for a
relatively simple cycle and may not create as much as
crystallization problem as the water-lithium bromide
pair.   However, stability and corrosion information
on most of them is very sketchy.   Also, the
refrigerants, except for fluoro-refrigerants in the
last type, are somewhat hazardous.

5.4   Theory of Absorption Refrigeration

Absorption refrigeration cycles are
heat-operated cycles in which a secondary fluid, the
absorbent, absorbs the primary fluid, a gaseous
refrigerant, that has been vapourised in the
evaporator.

The basic absorption cycle consists of four heat
exchangers, namely, generator, condenser, evaporator
and absorber, a solution pump and two expansion valves.

The working fluid of the system is a solution of refrigerant and absorbent which has a strong chemical affinity for each other. Heat is added to this solution in the generator, as a result, the refrigerant is vapourised out of solution and a mixture weak in refrigerant concentration is left behind. The refrigerant vapour flows'to the condenser where it is liquified, while rejecting it's latent heat. The liquid refrigerant is then expanded from the high pressure side of the system (the generator and condenser) into the low pressure evaporator wherein vapourization of the refrigerant and hence cooling is effected. The vapourised refrigerant is next recombined in the absorber with the weak solution. Since the reabsorption process is exothermic, heat must be removed from the absorber to maintain a sufficiently low temperature such that a high chemical affinity between the refrigerant vapour and the solution is assured. The solution, now rich in refrigerant, is pumped back into the generator to complete the cycle. Additional details of the structure of this system may be found in Threlkeld (1970).

The main energy requirement for an absorption system is the heat supplied to the generator. Utilization of solar energy to supply this energy is the basis of design for a solar operated refrigeration system.

An absorption refrigeration system can be
continuous or intermittent in operation, depending on
whether the energy supply to the generator is
continuous or intermittent (e.g. solar) and also on
the storage facilities available in the system. A
line diagram of a continuous absorption system is
shown in Figure 5.1.

5.5   Theory of an Intermittent Solar Ammonia-Water
Refrigeration System

The theory as outlined here is as given by
El-Shaarawi and Ramadan (1986) and Jansen (1985).
Figure 5.2 shows the temperature-concentration
diagram for the theoretical constant temperature
refrigeration cycle which could be achieved by a
solar refrigerator. The initial concentration in the
generator is X_{s1} and the maximum generator (or
solution) temperature is t_g. Solar radiation
striking the generator raises the temperature and
pressure of the ammonia-water solution as indicated
by the path 1-2. At state 2 the system pressure is
equal to the saturation pressure of ammonia
corresponding to the condensing temperature.
Generation continues from state 2 to state 3 at
constant pressure as solar heating is continued.

The generated vapour passes to a water-cooled
condenser through a rectifier. State 3, the end of

the generation process, depends on the maximum temperature attainable in the flat plate collector. At this instant, when the state of the liquid ammonia in the condenser is at 2^* and the state of the solution in the generator is at 3, the generator and the condenser are isolated. The generator is cooled to ambient conditions so that the solution concentration, temperature and pressure are low and hence the generator is ready to operate as an absorber. The communication between the condenser and the absorber is now restored. A fraction of liquid ammonia in the condenser at 2^* flashes adiabatically into the absorber to change the solution state to 5. As a consequence of the flashing the temperature of the remaining quantity of ammonia in the condenser decreases, to bring it's state to 5^*. The condenser is now ready to operate as an evaporator. From 5^* to 1^*, the evaporator absorbs energy from the surroundings to provide the effective refrigeration and the rising vapours are reabsorbed in the absorber until the solution reaches the initial state 1. The increasing concentration of ammonia in the absorber causes a corresponding rise in the equilibrium pressure of the system, and a consequent increase in the boiling temperature of the refrigerant.

Figure 5.2 shows that the boundaries of the cycle are determined by three quantities: the

temperature of the heating medium used for generation, coolant temperature, and ammonia concentration at the beginning of generation.

The first of these is limited by the temperatures obtainable from a flat-plate solar collector. The second is fixed by the cooling medium used. The third quantity, however, can be varied over a wide range. Assuming that a higher initial ammonia concentration is used, the resultant cycle would have a slightly higher average evaporator temperature during evaporation, but a greater quantity of ammonia generated. This might appear advantageous since the evaporator temperatures would still be suitable for refrigeration applications. The same logic could be applied to still· higher ammonia concentrations. As the concentration increases, however, the absorption rate and cooling rate reduces. These important considerations place a practical limit on the initial ammonia concentration.

Commercial ammonia-water absorption systems usually operate with a high-temperature energy source (steam or a gas flame). The high-temperatures permit operation at low ammonia concentrations generally below 50 percent. The combination of high-temperature source and low concentration produces high cooling rates and low evaporator temperatures÷ low enough for food storage and ice production in the case of domestic refrigerators.

The temperature range available for generation in this investigation i.e. about 70°C to 90°C requires a bit higher ammonia concentrations (about 55 to 65 percent) if the cycle is to produce any usable results.

At the end of the regeneration process, state 3, the amount of liquid ammonia, m'_3 kg, condensed in the evaporator can be evaluated by applying the law of conservation of mass on the generator contents. Assuming that there is no water carry over into the condenser-evaporator, i.e., 100% rectification, then, the mass of ammonia condensed, m_{vc}, is given by

$$m_{vc} = m'_3 = m_{H_2O}\left[\frac{X_{s1}}{1-X_{s1}} - \frac{X_{s3}}{1-X_{s3}}\right]$$

$$= m_{s1}(1-X_{s1})\left[\frac{X_{s1}}{1-X_{s1}} - \frac{X_{s3}}{1-X_{s3}}\right] \qquad (5.2)$$

where m_{H_2O} is the assumed constant mass of water in the solution.

The amount of liquid ammonia remaining in the evaporator after flashing, m'_5, and which is available for cooling purposes, may be found as follows :
Equating the energy in the flashed-off ammonia and the heat lost by the remaining distillate gives,

$$-\bar{h}_{fg}\ dm' = -m'\ dh' \qquad (5.3)$$

where $\bar{h}_{fg}$ is the average latent heat of vaporisation between states 3 and 5, and h' is the enthalpy of the liquid refrigerant.

Rearranging and integrating give

$$\int_{m_3'}^{m_5'} \frac{dm'}{m'} = \frac{1}{\overline{h}_{fg}} \int_{h_3'}^{h_5'} dh'$$

$$\therefore \quad m_5' = m_3' \exp \frac{h_5' - h_3'}{\overline{h}_{fg}} \qquad (5.4)$$

where h_5' and h_3' are the enthalpies of the liquid
ammonia at states 5 and 3 respectively, determined
(as is $\overline{h}_{fg}$) from the ammonia tables in Appendix E.

The amount of ammonia flashed during the
refrigeration process, m_{fl}, is then given by

$$m_{fl} = m_3' - m_5' = m_{vc} \left[1 - \exp \frac{h_5' - h_3'}{\overline{h}_{fg}} \right] \qquad (5.5)$$

Also m_{fl} is given by :

$$m_{fl} = m_4 \frac{X_{s5} - X_{s4}}{1 - X_{s5}} \qquad (5.6)$$

The minimum evaporator temperature, t_5^*, is the
temperature of liquid ammonia in the condenser at the
end of the adiabatic flashing process.

This temperature can be evaluated with the help
of the two equations given by Venkatesh and Gupta
(1978):

$$X_{s5} = 0.007804 \, t_5^* + 0.55847 \qquad (5.7)$$

and

$$\exp\left(\frac{h_5^* - h_2^*}{\overline{h}_{fg}}\right) = 0.00331 \, t_5^* + 0.893 \tag{5.8}$$

Using Equations 5.8 through 5.11, a quadratic equation in t_5^* can be obtained and hence t_5^* can be calculated.

The effective cooling of the system, Q_c, that is, the energy absorbed by the vaporisation of the m_5' kg of ammonia, is given by

$$Q_c = m_5' \, h_{fg_5} = (m_{vc} - m_{fl}) h_{fg_5} \tag{5.9}$$

where h_{fg_5} is the latent heat of vaporisation of liquid ammonia at the evaporating temperature.

The energy absorbed by the generator contents during regeneration, Q_g, may be obtained from an energy balance on the generator contents during regeneration process 1-2-3 :

$$Q_g = m_3 u_3 - m_1 u_1 + \sum_1^3 h_v \, dm_{vg} \tag{5.10}$$

where u is the internal energy of the solution, m is the solution mass, and the summation represents the enthalpy of the ammonia-water vapour that leaves the generator during the process 1-3. Since the internal energy u of the liquid solution is nearly equal to the enthalpy, the equation may be rewritten as:

$$Q_g = m_3 h_3 - m_1 h_1 + \sum_1^3 h_v \, dm_{vg} \tag{5.11}$$

where $m_1 h_1$ and $m_3 h_3$ are the enthalpies of the

solution in the collector-generator at states 1 and 3 respectively, and $h_v dm_{vg}$ is the enthalpy of an incremental mass dm_{vg} of the ammonia-water vapour distilled from the collector-generator.

Most of the heat added goes to increase the internal energy of the solution during the process 1-2.

The mass m_g is readily found from the change in solution concentration, and h_g and h_1 are determined from the aqua-ammonia chart in Appendix F. The specific enthalpy of the liberated vapour, h_v, is also determined from this chart. In order to determine dm_{vg}, it is necessary to develop a relationship between dm_{vg} and dm_{vc}, the mass of anhydrous ammonia in the ammonia-water vapour mass generated dm_{vg}. This is done by a mass balance on the rectifier.

In Figure 5.3, ammonia-water vapour dm_{vg}, enters the rectifier and a lesser amount dm_{vc} of anhydrous ammonia leaves on the right, the difference in mass consisting of the mass of condensate returned to the generator. If the concentration of ammonia in the vapour which enters the rectifier is X_v and the concentration of ammonia in the condensate is X_s (the same as the solution concentration), an ammonia balance on the rectifier yields

$$X_v dm_{vg} - X_s (dm_{vg} - dm_{vc}) = dm_{vc}$$

from which

$$dm_{vg} = \frac{1 - X_s}{X_v - X_s} \, dm_{vc} \qquad\qquad (5.12)$$

where the concentration of ammonia in the vapour, X_v, is found from the aqua-ammonia chart in Appendix F.

The term $\sum h_v dm_{vg}$ in Equation 5.11 is evaluated by calculating dm_{vg} from Equation 5.12 for a number of points along process 2-3. Plotting dm_{vg} against the vapour enthalpy h_v (the dependent variable), the area under the curve may be conveniently determined using Simpson's rule, yielding the term $\sum h_v dm_{vg}$.

Finally, the cooling ratio, η, is defined as

$$\eta = \frac{Q_c}{Q_g} \qquad\qquad (5.13)$$
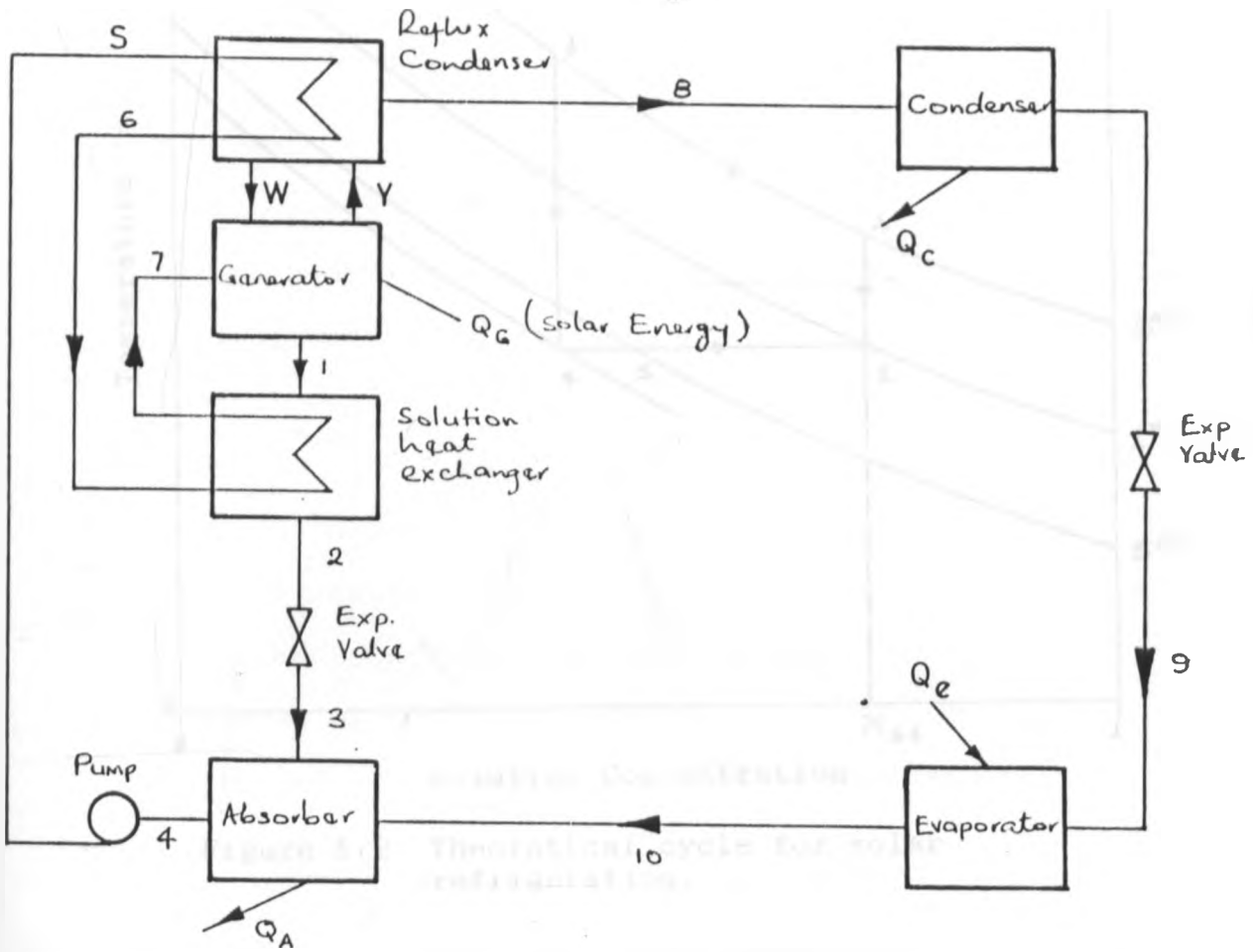
Fig. 5·1 Schematic of the ammonia - water system
A continous absorption refrigeration system.
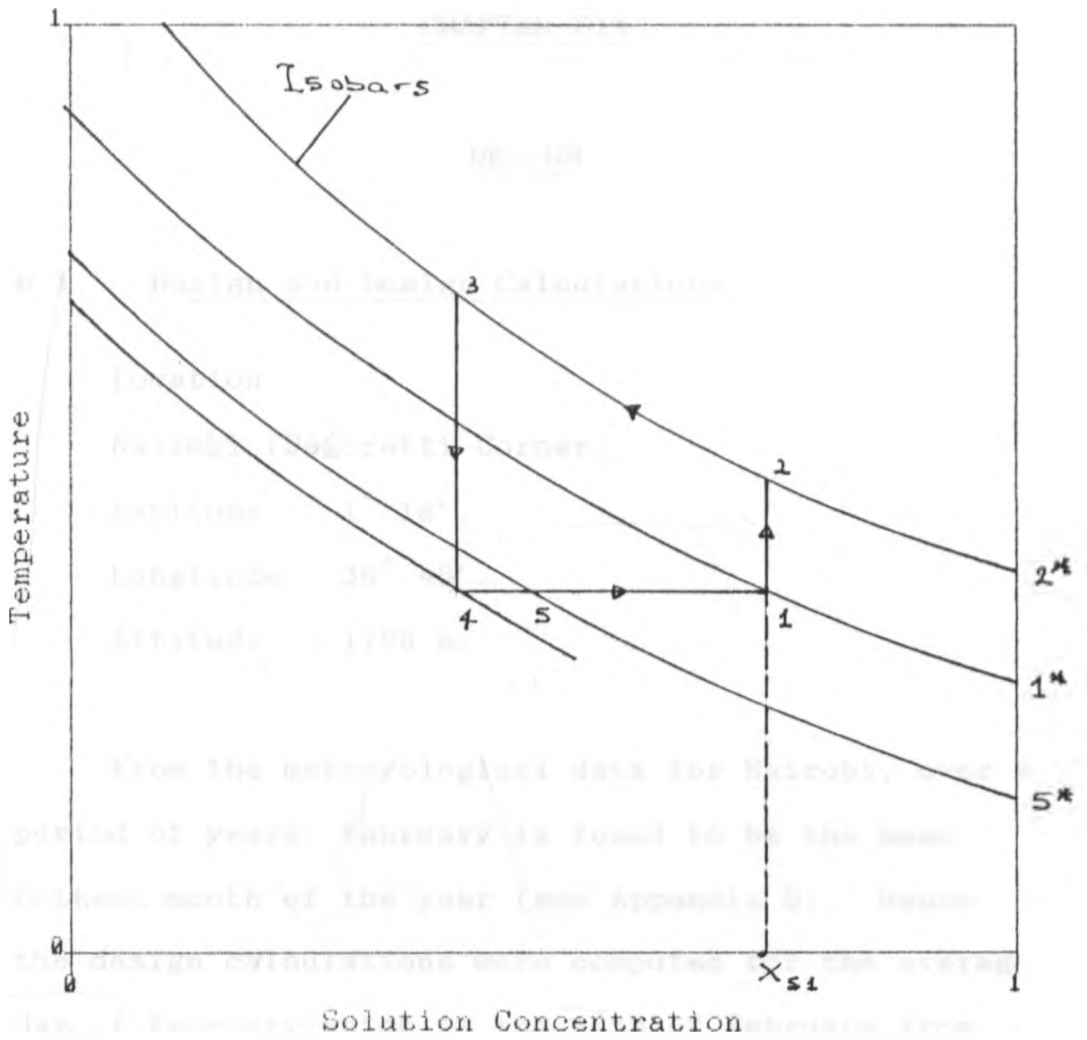
Figure 5.2   Theoretical cycle for solar
refrigeration.
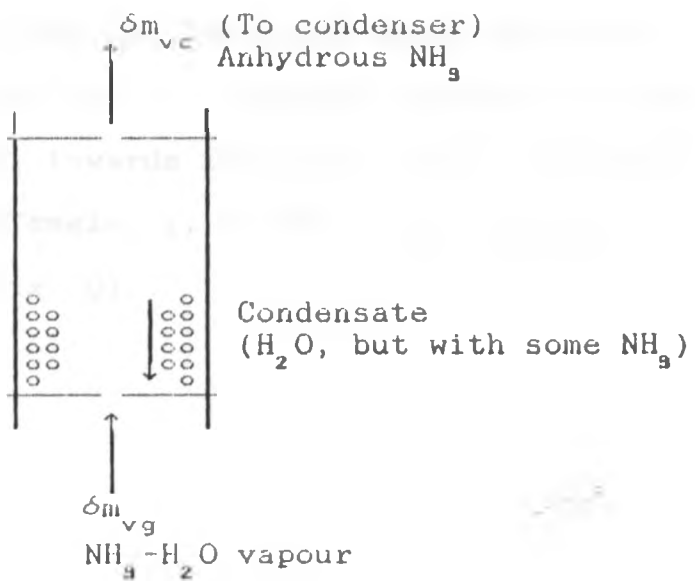
Figure 5.3   Mass balance on the rectifier.

CHAPTER SIX

DESIGN

6.1   Design and Design Calculations

Location :

Nairobi (Dagoretti Corner)

Latitude   : $1° \ 18'$.

Longitude : $36° \ 45'$.

Altitude   : 1798 m.

From the meteorological data for Nairobi, over a
period of years, February is found to be the mean
hottest month of the year (see Appendix D).   Hence
the design calculations were computed for the average
day of February which is the 16th of February from
Klein (1976).

Sample insolation calculations were computed at
10.00 am solar time for the fixed solar collector
sloped at an angle of $5°$, (because Nairobi is close
to the equator), towards the north, that is, with a
surface azimuth angle, γ, of $180°$ (see computer
program, Appendix C).

6.2   Collector-Absorber Design

Collector Specifications :

Number of glass covers, N	2.
Cover to cover spacing	25 mm.
Plate to cover spacing	25 mm.
Ambient temperature, T_a	20°C.
Mean plate temperature, T_p	100°C.
Collector tilt, β	5°.
Wind heat transfer coefficient, h_w	10 $Wm^{-2}K^{-1}$.
Collector length	90 cm.
Collector width	108.24 cm.
Collector thickness	90 mm.
Back insulation thickness	50 mm.
Edge insulation thickness	50 mm.
Back insulation conductivity (glass wool)	0.045 $Wm^{-1}K^{-1}$
Edge insulation conductivity (wood)	0.123 $Wm^{-1}K^{-1}$
Plate emittance, ε_p	0.90.
Tube spacing, W	100 mm.
Tube diameter (outside), D	13.7 mm.
Plate thickness, δ	1 mm.
Plate thermal conductivity (copper)	384 W/mK.
Heat transfer coefficient inside tubes (Computed below)	1070 W/m^2K.
Bond conductance, C_B	30 W/m^2K.

Calculating the top loss coefficient from
Equation 4.17, therefore,

C = 250[1-0.0044(5-90)] = 345.5

$$f = [1-0.04(10)+0.0005(10)^2][1+0.091(2)] = 1.3002$$

$$\therefore U_t = \left[\frac{2}{\left(\frac{345.5}{373}\right)\left(\frac{373-293}{2+1.3002}\right)^{0.33}} + \frac{1}{10} \right]^{-1}$$

$$+ \frac{5.67\times10^{-8}(373+293)(373^2+293^2)}{[0.9+0.005(2)(1-0.9)]^{-1} + \frac{2(2)+1.3002-1}{0.88} - 2}$$

$$\therefore U_t = 3.2966 \ W/m^2K.$$

The back loss coefficient, U_b, is given by

$$U_b = \frac{0.045}{0.050} = 0.9 \ W/m^2K.$$

The edge loss for the collectors is given by

$$U_e = \frac{(UA)_e}{A_c} = \frac{(0.123/0.05)(1.9824)(0.09)}{0.09\times1.0824}$$

$$= 0.4505 \ W/m^2K.$$

Therefore, the collector overall loss coefficient is

$$U_l = 3.2966+0.9+0.4505 = 4.6471 \ W/m^2K.$$

The fin efficiency factor, F, is given by

Equation 4.30, therefore,

$$m = \left(\frac{4.6471}{384\times0.001}\right)^{1/2} = 3.4788 \ m^{-1}$$

$$\therefore F = \frac{\tanh[3.4788(0.1-0.0137)/2]}{3.4788(0.1-0.0137)/2} = 0.993$$

The Heat Transfer Coefficient inside the collector tubes, h is computed as follows:

In view of the low velocities in many solar convection apparatuses, the velocity produced by buoyant forces, that is, free convection will also affect the convection heat exchange. In this so called mixed-flow region when Gr/Re^2 is between 1 and

10 and $L/D_H > 50$, the heat transfer coefficient for flow in horizontal ducts and ducts inclined not too far from the horizontal can be evaluated from the relation [Metals and Eckert (1964) and Brown and Gauvin (1965)]:

$$Nu = 1.75 \left(\frac{\mu_b}{\mu_v}\right)^{0.14} \left[\frac{Re_D \, Pr.D}{L} + 0.012\left[\frac{Gr_D^{1/3} \, Re_D \, Pr.D}{L}\right]^{4/3}\right]^{1/3}$$

where

$$Gr_D = \frac{\rho^2 \, g\beta(T_v - T_b)D^3}{\mu^2}$$

For the mean temperature of the solution in the collector tubes of:

$$T_m = \frac{24+80+100}{3} = 68\,^\circ C$$

From the specific volume of saturated ammonia-water solution table [ASHRAE (1985)], the density of the solution is

$$\rho = \frac{1}{1.356\times10^{-3}} = 737.46 \text{ kg/m}^3$$

Using correlations given in Perry (1984), the viscousity, μ and the thermal conductivity, k for an ammonia-water solution of concentration 0.6 $kgNH_3/kg$ solution were computed as:

μ_b = viscousity at bulk temperature of $68\,^\circ C$ =

= 2.567×10^{-4} N.s/m^2

μ_v = viscousity at wall temperature of $100\,^\circ C$ =

= 1.559×10^{-4} N.s/m^2

Thermal conductivity, k = 0.479 W/mK

Assuming a mean flow rate in the collector tubes of 0.005 kg/s

From $G = \dfrac{\dot{m}}{A} = \dfrac{0.005 \times 4}{\pi (0.0127)^2} = 39.47 \ \text{kg/m}^2\text{s}$

$\therefore \quad Re_D = \dfrac{GD}{\mu} = \dfrac{39.47 \times 0.0127}{2.567 \times 10^{-4}} = 1952.74$

From the thermal expansitivity, β given by

$$\beta = \frac{1}{\nu}\left(\frac{\delta \nu}{\delta T}\right)_P = \frac{2}{(\nu_1 + \nu_2)} \frac{\nu_2 - \nu_1}{T_2 - T_1}$$

where ν_1 and ν_2 are the specific volume of the ammonia-water solution at $24°C$ and $80°C$ respectively.

$$\beta = \frac{2}{(1.274 + 1.39) \times 10^{-3}} \frac{(1.39 - 1.274) \times 10^{-3}}{(80 - 24)}$$

$$= 1.555 \times 10^{-3} \ K^{-1}$$

$\therefore \quad Gr_D = \dfrac{(737.46)^2 \times 9.81 \times 1.555 \times 10^{-3}(100-68)(0.0127)^3}{(2.567 \times 10^{-4})^2}$

$$= 8.25 \times 10^{+6}$$

$$Pr = \frac{C_p \mu}{k} = \frac{4190 \times 2.567 \times 10^{-4}}{0.479} = 2.25$$

Therefore

$$\frac{Gr}{Re^2} = \frac{8.25 \times 10^{+6}}{(1952.74)^2} = 2.16$$

and

$$\frac{L}{D} = \frac{0.9144}{0.0127} = 72$$

Hence the correlation can be applied.

$\therefore \ Nu_D = \dfrac{hD}{k} = 1.75 \left[\dfrac{2.567 \times 10^{-4}}{1.555 \times 10^{-4}}\right]^{0.14} \left[\dfrac{1952.74 \times 2.25 \times 0.0127}{0.9144} + \right.$

$$\left. + 0.012 \left[\frac{(8.25 \times 10^6)^{1/3}(1952.74)(2.25)(0.0127)}{0.9144}\right]^{4/3}\right]^{1/3}$$

$$= 28.44$$

$\therefore \quad h = \dfrac{0.479 \times 28.44}{0.0127} = 1070 \ \text{W/m}^2\text{K}$

The collector efficiency factor, F', is given by
Equation 4.36.

$\therefore$ F' =

$$\frac{1/4.6471}{.1\left[\frac{1}{4.6471[.0137+.993(.1-.0137)]}+\frac{1}{30}+\frac{1}{\pi(.0127)(1070)}\right]}$$

= 0.97

6.3 Design Considerations of the Condenser-Evaporator

Apart from the design of the collector-absorber,
the next critical component of the system is the
condenser-evaporator. In order to design the
condenser, it is necessary that the amount and the
rate of generation of the ammonia vapour to be
condensed be known. For these quantities to be
determined, it was necessary to dynamically simulate
the thermal performance of the system on a computer.

Because of the coupled performance of the
condenser and the generator i.e. the system
generation pressure being equal to the saturation
pressure of ammonia corresponding to the cooling
water temperature, and also because a storage
condenser is being considered, it is not necessary to
compute the heat transfer coefficient using either
the LMTD or NTU method. This is so because the rate
of the cooling water flow is so adjusted that the
difference between the inlet and outlet water

temperature is limited to about $2°C$ temperature rise, so as to give a constant cooling water temperature during condensation.

Also it is worth noting that since the regeneration/condensation process takes about two to three hours, there is ample time for the ammonia vapour generated to be condensed. Also, because of the condensed refrigerant is being stored in the condenser tubes, the interface between the condensate and the generated vapour acts also as a condensing surface. Because of the condenser storage there will be a little subcooling of the condensed refrigerant but since the condensing temperature is almost equal to the cooling water temperature, it is a good assumption that there will be no subcooling of the condensed ammonia.

Hence, the major design considerations for this storage condenser are (i) ensuring as much as possible a constant temperature of the cooling water and (ii) the volume capacity of the condenser must be large enough to store all the condensed vapour. The rate of generation of ammonia from the solar generator being slow because of the low temperatures obtainable from solar flat-plate collectors, will give ample time for condensation of the generated vapour. Although the surface area available for condensation decreases as vapour is condensed and stored in the condenser tubes, the area available for

condensation is such that it will always be
sufficient for condensation since the amount of
ammonia generated for any time period decreases with
the time as the solution becomes weaker in ammonia as
generation proceeds.

6.3.1 Liquid Storage Calculations

The energy storage capacity of the aqua-water
storage unit at uniform temperature operating over a
finite temperature difference is given by

$$Q_s = (mC_p)_s \Delta T_s \tag{6.1}$$

where Q_s is the total heat capacity for a cycle
operating through the range ΔT_s, with m kilograms of
solution in the unit.

For a non-stratified tank, an energy balance on
the tank yields

$$(mC_p)_s \frac{dT_s}{d\tau} = Q_u - L - (UA)_s (T_s - T_a') \tag{6.2}$$

where Q_u and L are rates of addition or removal of
energy from the collector and to the load.

6.3.2 Component Models

For flat-plate collectors, Equation 4.47 is
appropriate. The flat-plate equation can be written
as :

$$Q_u = A_c F_R [S - U_L (T_\iota - T_a)]^+ \tag{6.3}$$

where the + sign implies a controller is present and
only positive values should be used.

Assuming the storage unit is a fully mixed
sensible heat unit, its performance is given by
Equation 6.2.

$$Q_u - L - (UA)_s (T_s - T_a) = (mC_p)_s \frac{dT_s}{d\tau}$$

These equations are the basic equations to be solved
in the analysis of systems such as a simple solar
liquid heater with collector and storage tank. L is
a time dependent rate of removal of energy to meet a
load, which in this study is the vapourization of
ammonia out of solution. S and T_a are also time
dependent.

6.3.3 System Models

System models are the assemblies of appropriate
component models. The net effect of this assembly is
to produce a set of coupled algebraic and
differential equations, having time as the
independent variable. These equations include
meteorological data as forcing functions that operate
on the collector, and possibly also on the load as in
this case, depending on the application. The
equations can be manipulated and combined

algebraically or they can be solved simultaneously without formal combinations. Each process has some advantages in solar process simulation.

As a example of a simple system that yields a single differential equation, consider the solar aqua-ammonia heater with an unstratified storage unit generating ammonia vapour. Equation 6.3 for the collector can be combined with Equation 6.1 for the tank to give

$$(mC_p)_s \frac{dT_s}{d\tau} = A_c F_R [S - U_L (T_s - T_a)]^+$$
$$- (UA)_s (T_s - T_a) - \int h_v \, dm \qquad (6.4)$$

where

$$L = \int h_v \, dm \qquad .$$

is the energy quantity of the ammonia vapour generated out of solution.

Once the collector parameters, the storage size and loss coefficient, the magnitude of the load, and the meteorological data are specified, then the storage tank temperature can be calculated as a function of time.

Various methods are available to numerically integrate equations like Equation 6.4. Using simple forward difference method, and expressing the temperature derivative $dT_s/d\tau$ as $(T_s^+ - T_s)/\Delta\tau$, an expression for the change in storage tank temperature for the time period in terms of known quantities is :

$$T_s^+ = T_s + \frac{\Delta\tau}{(mC_p)_s} \left[A_c F_R [S - U_L (T_s - T_a)]^+ \right.$$

$$\left. - (UA)_s (T_s - T_a) - \int h_v \, dm \right] \quad (6.5)$$

The above equation has been solved for the case in study. (see computer program, Appendix C)

6.4 Design Computations of the Condenser-Evaporator

For the case in study, using an initial aqua-ammonia solution mass of 12.kg and an initial solution concentration of 0.6 kg ammonia/kg solution, it was computed that 4.50 kg of NH_3 would be condensed in two hours by which time the generation would have been over (see program output, Appendix C).

For ammonia liquid at $24°C$, density $= 600$ kg/m^3. Hence condenser minimum capacity should be

$$= \frac{4.50}{600} = 7.5 \times 10^{-3} \, m^3.$$

Available for condenser construction are tubes of 25.4mm id., 27.94mm od. and 1150mm long.

∴ Minimun number of tubes is given by

$$N_{min} = \frac{7.5 \times 10^{-3} \times 4}{\pi (.0254)^2 \times 1.15} = 13$$

Hence the condenser was made of a one-pass, 16, 25.4mm id., 27.94mm od. and 1150mm long tube on a square pitch of 50.8mm in a shell of square cross-section of 0.0645m^2.

7.1 DESCRIPTION OF APPARATUS

The main features of the experimental refrigerator are diagrammatically shown in Figure 7.1. Photos of the refrigerator are shown in Plates 1 to 4. Because of the corrosive effects of ammonia, all parts of the system in contact with ammonia were made from steel and iron components.

The apparatus comprised of the following components :

(i) Flat-Plate Collector(s)

A flat-plate collector array consisting of two flat-plate collectors each made of a 1mm thick copper sheet of area 914.4mm by 800mm and painted black. Eight 12.7mm inner-diameter steel furniture tubes at 100mm intervals were soldered onto each of the plates to give good thermal contact between the tubes and the collector plate. The top and bottom ends of the 12.7mm pipes were connected to 25.4m diameter galvanised steel pipe headers. The rear of the plate was insulated by 50mm thick asbestos glass wool. There were two glass covers in front of the collecting surface. The glass was of commercial quality and was 2.5mm thick. The total solar

radiation collecting surface area was $1.463m^2$ for the two collectors.   The whole collector assembly was enclosed in a galvanised steel sheet box.   The flat-plate collector assembly is shown in Figure 7.2.

(ii)   Generator Storage Tank

Generator storage tank supported above the top of the collector to store the required quantity of aqua-ammonia and to facilitate the natural convection in the circuit which commences when the solar radiation strikes the flat-plate collectors.   This storage tank was a cylindrical vessel made out of a 2mm thick mild steel sheet.   It was of 152.4mm inner diameter and 600mm in height.   The external surface of the tank was thermally insulated with asbestos.

(iii)   Rectifying Column

The rectifying column prevents water from being carried over to the condenser.   It was a cylindrical vessel of 12.7mm diameter, 320mm in height and 2mm thick.   It consisted of seven sieve plates as the baffle plates.   The generator storage tank with rectifying column are shown in Figure 7.3.

(iv)   Condenser-Evaporator

The condenser-evaporator section consisted of a vertical, one-pass, tube-in-shell heat exchanger of 1300mm height and a square cross-section of 6.45×10^{-2}

m^2 area, containing sixteen 25.4mm diameter steel
furniture tubes on 50.8mm centre to centre square
bundle. During regeneration, the heat exchanger
performed as a condenser which was cooled by a flow
of water whose flow rate could be adjusted to ensure,
as near as possible, a constant pressure generation
process. However, during the refrigeration process,
stagnant water was used as the refrigeration load by
filling part of the shell surrounding the tubes with
water.

(v) Instrumentation and Controls

Thermocouples were installed at several points
in the generator-collector and the condenser-
evaporator assemblies, (see Figure 7.1), to measure
the surface temperatures and solution temperatures at
various stages. Also, two pressure gauges were
fitted, one on the condenser-evaporator and the other
on the generator-collector, to record pressures in
the system.

The valves A and B (see Figure 7.1) were used
respectively to control the direction of flow of
ammonia vapour during the generation of the ammonia
during the day and its reabsorption during the night
in aqua-ammonia solution that had become weak during
the day. Valve C was used for purging the liquid
residues from the evaporator at the end of the

refrigeration period. Valve D was used for vacuuming the apparatus and valve E was used for charging the system with the ammonia (see Figure 7.1).

7.2   Assembly and Charging

The different components of the experimental test rig were assembled to form a closed unit for the working fluid using 12.7mm diameter galvanized steel pipes threaded on both ends. In order to have an air-tight unit as far as possible, PTFE thread seal tape was used on the threads before being screwed into the different elbows, tees and sockets.

After the assembly was completed, the apparatus was pressure tested using water and a hand pump to determine whether it would be able to withstand a maximum working pressure of 11 bars. The hand pump was connected to valve E and pressurized with water through this valve. After the pressure in the unit reached the desired maximum, the valve was closed and the joints examined for leakage of water.

After the leakages were sealed, the unit was vacuumed using a small rotary vacuum pump connected to valve D. This was necessary to facilitate charging the unit with water, and also because if air is not removed from the unit it would hamper the condensation of the ammonia vapour that was to be generated.

Finally, the rig was charged with water and
ammonia gas. First, after the vacuuming operation, a
known quantity of de-ionised water was charged into
the unit. This was done by opening the vacuuming
valve D, and because of the very low pressure in the
unit, water was sucked in through a flexible charging
tube connected between the charging valve E and the
cylinder. The charging of ammonia into the unit had
to be done through valve E because that was the
lowest point of the unit so that the pressurized
ammonia gas could come into direct contact with the
water at the point of entry into the unit. This
facilitated a higher absorption rate of ammonia in
the water. Also, as the absorption of ammonia
proceeded, the aqua-ammonia solution formed became
less and less dense as the ammonia concentration
increased. And since the charging was being done at
the lowest point in the unit, this led to a natural
convection current being set in the system with the
resultant effect that the denser fluid flowed to the
bottom of the unit.

At the end of the charging operation, the
temperature of the solution and the pressure in the
system were used to estimate the final concentration
of the aqua-ammonia solution formed. The enthalpy-
concentration chart for ammonia-water solution
(Appendix F) gives the pressure and the corresponding

temperature for any concentration of ammonia in the solution.

The charging operations had to be done during the nights when the ambient temperatures are at their lowest so as to facilitate the cooling of the collector-absorber because the absorption of ammonia in water is an exothermic process. The charging had to be at a very low rate to provide ammonia with ample time to dissolve in the water and also to prevent the solution temperature (as a result of the exothermic absorption) from becoming too high. Hence, as a result of this low rate of charging, the charging operation took about 4 to 5 hours. Once the solution had been charged into the unit, performance tests were carried out.

7.3   Experimentation: Procedure of Data Acquisition

At the commencement of the regeneration process in the morning, valves B, C, D and E (see Figure 7.1) were closed and valve A was opened. The valve connecting the cooling water reservoir to the condenser was opened and water filled up the shell-side of the condenser and continued to flow counter-currently relative to the direction of flow of the ammonia vapour in the condenser tubes during the whole of the regeneration period.

Radiation falling upon the surface of the collector plates causes the solution in the collector tubes to heat up, and circulation of the solution is up the tubes, and into the upper header, then to the storage cylinder. The bubbles of the ammonia and warmer solution rise to the free surface of the solution in the storage cylinder, forcing the heavier cold solution through the external line back into the lower feeder. Ammonia vapour bubbles out of solution into the upper header to the storage cylinder, then the rectifying column and into the condenser-evaporator. At the lower temperature of the condenser-evaporator, the ammonia vapour condenses. Regeneration continues into the mid-afternoon until the sun begins to set, and this marks the end of the regeneration. At the end of regeneration period, the condenser is isolated from the collector-generator by closing valve A and the temperature of the collector-generator allowed to cool to the ambient temperature.

Just before the commencement of the refrigeration period, the cooling water that had filled the shell of the condenser was drained until about 5.5kg of water was left in the shell of the condenser and then the drain valve was closed. This water in the shell of the evaporator-condenser was used as the load during the refrigeration process.

At about mid-night when the weak solution in the collector should have cooled to the ambient

temperature, the refrigeration period is started by opening valve B so that liquid ammonia vapourizes and flows back to the generator-absorber,where it is reabsorbed by the weak solution. The evaporation of the ammonia extracts heat from the water in the shell of the condenser-evaporator.

Six tests were performed in the concentration range 0.53 to 0.58 kg NH_3/kg solution and with different initial solution mass.

During the regeneration period an Eppley pyranometer was used to record the insolation at half-hourly intervals. At the same time, the pressure in the system was recorded from the readings on the two pressure gauges (P in Figure 7.1). The ambient temperature was also recorded and the various temperatures in the system were recorded by a six-point temperature recorder connected to the affixed thermocouples in the system. These measure the inlet and outlet temperatures of the solution in the collector and the inlet and outlet cooling water temperatures.

During the refrigeration period, the ambient temperature, the evaporator pressure, the absorber pressure and the load (water) temperatures were recorded at half-hourly intervals.

7.4 Problems Encountered During the Fabrication and Assembly of the Experimental Test Rig

The fabrication process started with the making of the two flat-plate solar collectors. Firstly, the required number of holes, in this case eight, of diameter corresponding to the external diameter of the tubes, were drilled exactly on a straight line on each of the feeders to the collector tubes. The problem encountered was in the arrangement and alignment of the collector tubes into the holes in the feeders in such a way that they are parallel to one another. After the alignment all the tube joints to the feeders were welded to form a unit, and the tubes were then soldered onto the copper plate.

Another problem encountered was how to bond the collector tubes onto the the thin copper plate so as to give good thermal contact without destroying the plate. Soldering was selected, but this has to be done manually by heating a copper anvil on a paraffin burner until it became red hot and then using it to melt the soldering stick so as to fill the groves around the tubes between the copper plate and tubes with solder. This took rather a long process for all the sixteen tubes but it was the best procedure in order to prevent too much heat been applied to the copper plate which would have led to plate wobbling.

The other major problem encountered was in the assembly of the different components of the rig

together as shown in the plates 1-4. This was assembled in such a way as to be air-tight as much as possible and also to be able to withstand an operating pressure of about 11 bars gauge pressure. In order to assemble the components together, 12.7mm diameter galvanised steel pipes threaded on both ends were used in connecting the components together via a series of tees, elbows and sockets. Due to the many joints there was an increased likelihood of leakages. In order to prevent the leakages PTFE thread seal tapes were wound on the threads before being screwed into the sockets, elbows and tees.

Another point to note is that when there was a leakage in any part of the system, virtually the whole of the test rig had to be disassembled, more tape added on the threads and then reassembled. This was such a crucial problem that it took about three months for the rig to be in a usable form.

Plate 1: Front view of the test rig.

Plate 2:   Left side view of the test rig with
a clear view of the solarimeter.

Plate 3: Right side view of the test rig
with the student in the background.

Plate 4: Back view of the test rig with a close
view of the temperature recorder.

Figure 7.1   Schematic diagram of the intermittent
solar absorption refrigeration system.
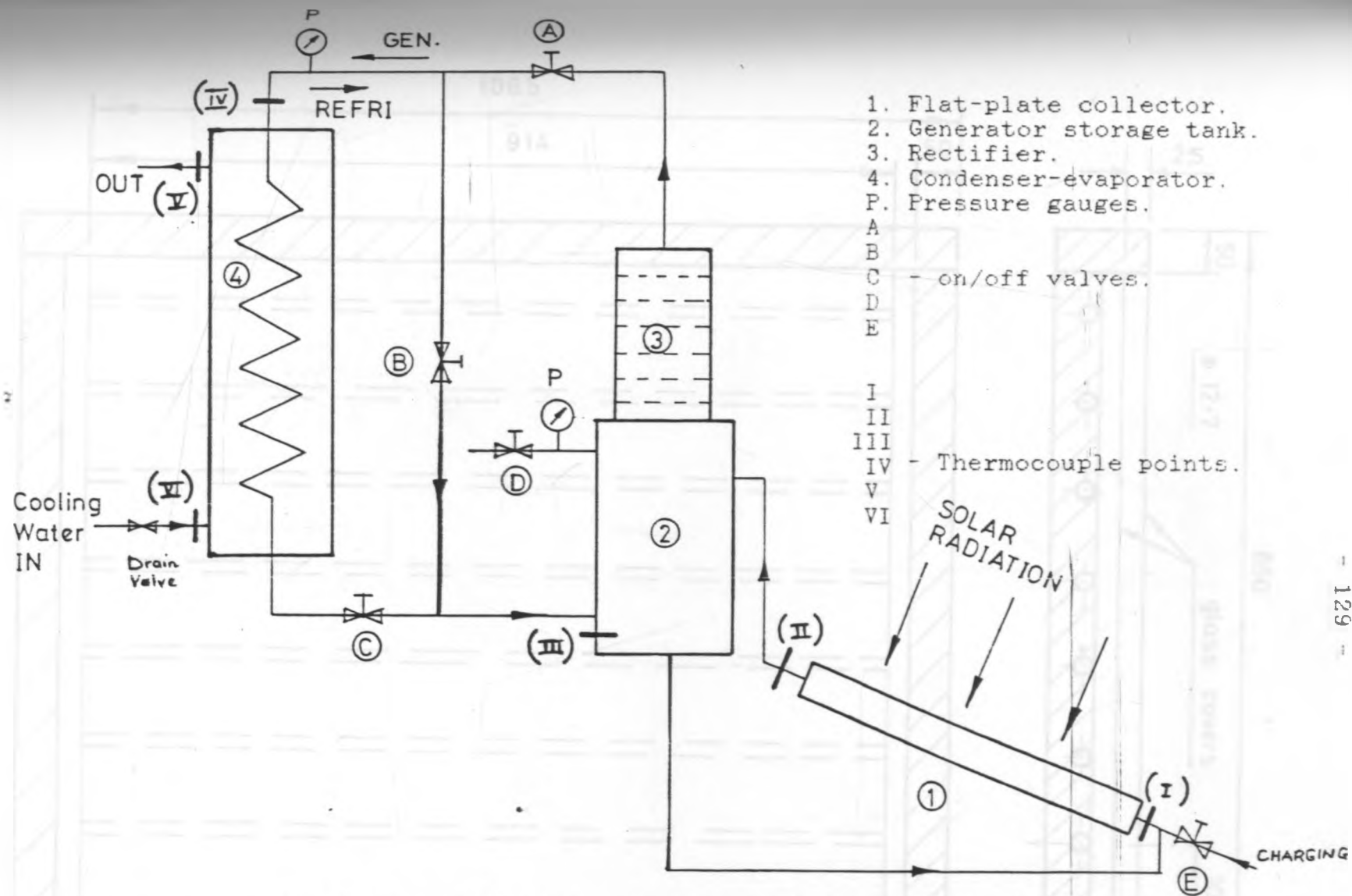
1. Flat-plate collector.
2. Generator storage tank.
3. Rectifier.
4. Condenser-evaporator.
P. Pressure gauges.
A
B
C - on/off valves.
D
E

I
II
III
IV - Thermocouple points.
V
VI
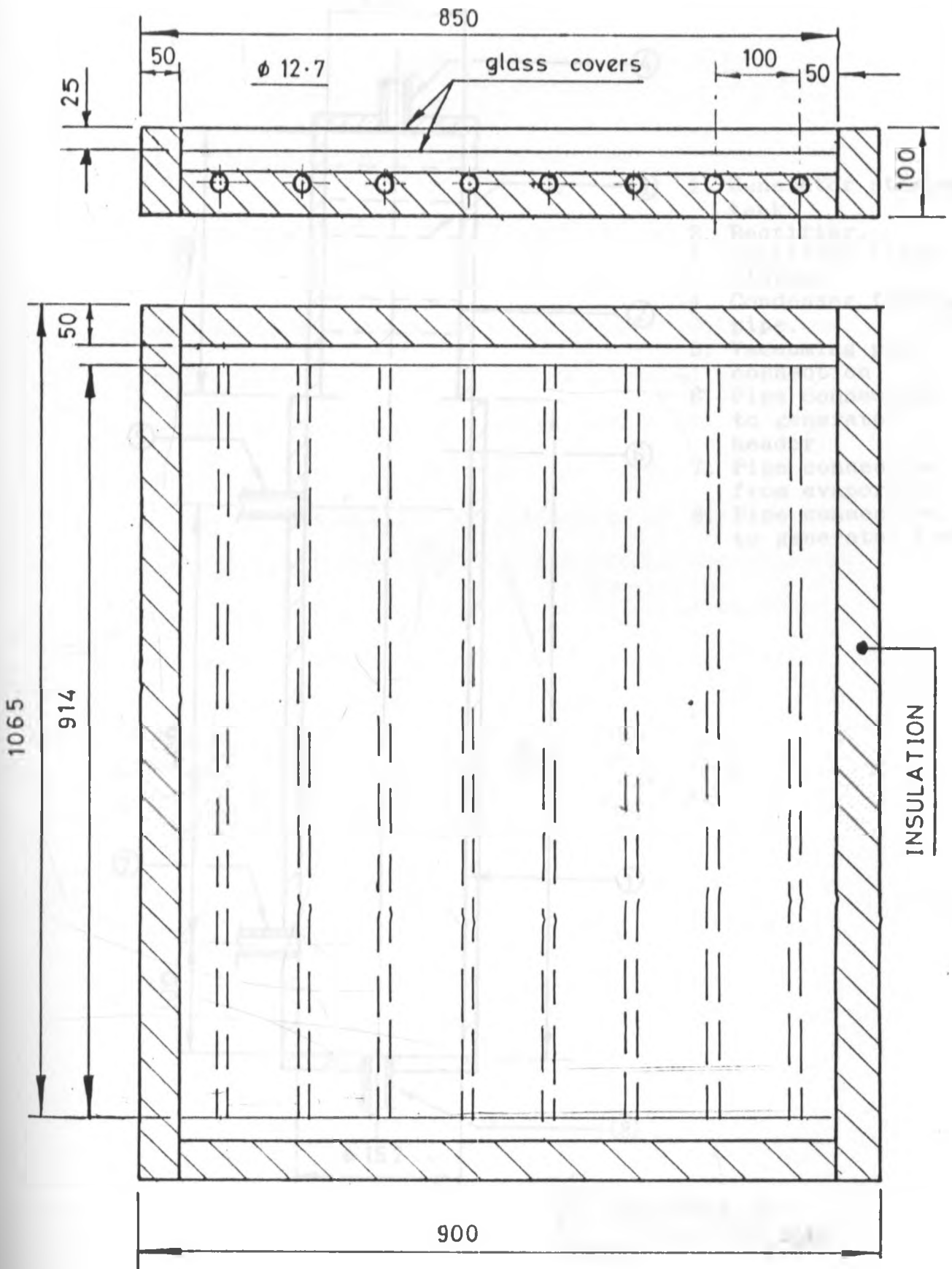
Fig. 7·2   FLAT   PLATE   COLLECTOR   ASSY.

all   dimensions   in   mm   unless   otherwise
stated .
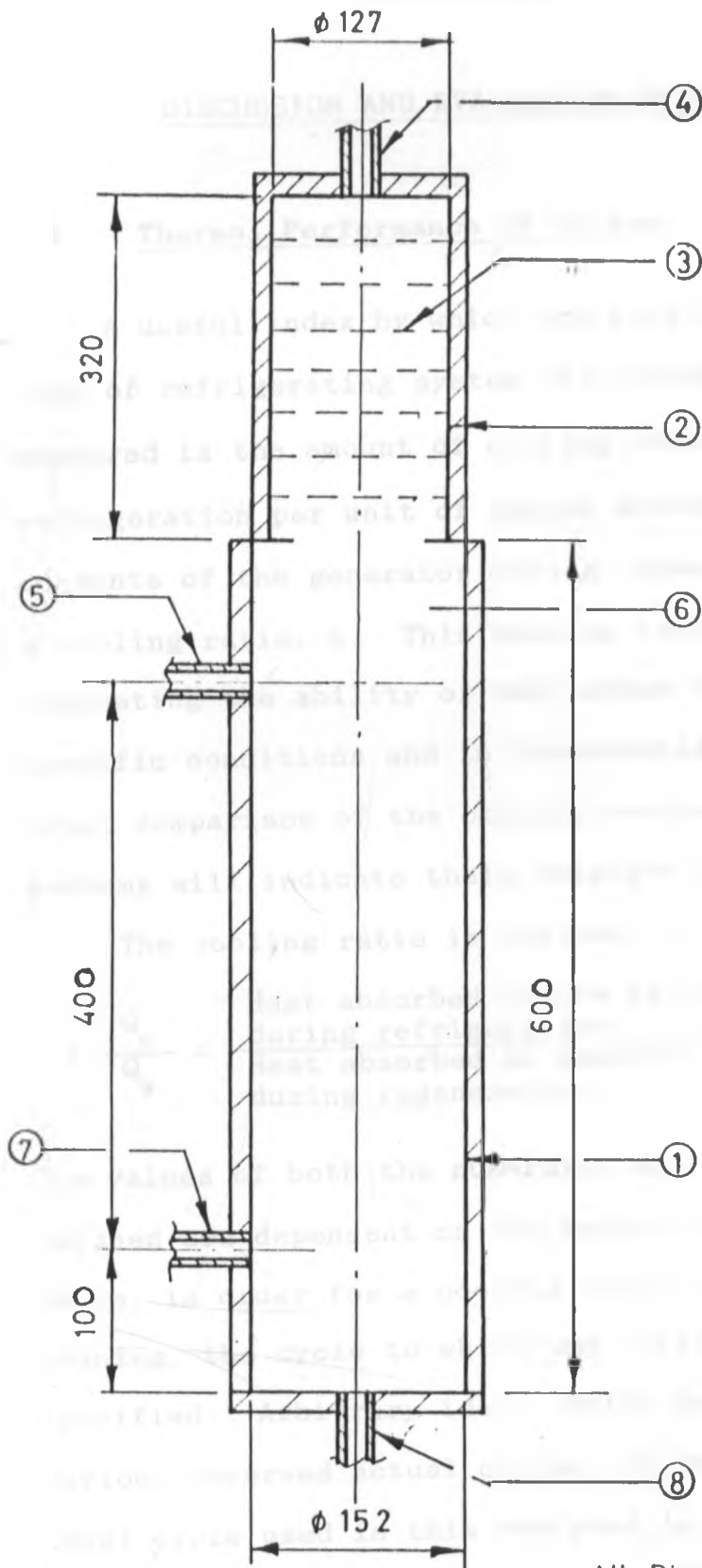
1. Generator storage tank.
2. Rectifier.
3. Rectifier sieve plates.
4. Condenser feeding pipe.
5. Vacuuming pipe connection.
6. Pipe connection to generator header.
7. Pipe connection from evaporator.
8. Pipe connection to generator feeder

All Dimensions In MM Unless Otherwise Stated.

Figure 7.3   Generator storage tank and rectifier.

CHAPTER EIGHT

DISCUSSION AND EVALUATION OF RESULTS

8.1   Thermal Performance of System

A useful index by which the performance of the
type of refrigerating system discussed herein can be
measured is the amount of cooling obtainable during
refrigeration per unit of energy absorbed by the
contents of the generator during regeneration, i.e.,
a cooling ratio, η.   This cooling ratio is useful in
indicating the ability of the system to perform under
specific conditions and in interpreting experimental
data; comparison of the cooling ratios of various
systems will indicate their relative practicality.

The cooling ratio is defined as

$$\eta = \frac{Q_c}{Q_g} = \frac{\text{Heat absorbed by the refrigerant during refrigeration.}}{\text{Heat absorbed by generator contents during regeneration.}}$$

The values of both the numerator and denominator as
defined are dependent on the nature of the cycle.
Hence, in order for a cooling ratio to have full
meaning, the cycle to which the ratio applies must be
specified.   Arbitrary ideal cycles patterned after
various observed actual cycles can be chosen.   The
ideal cycle used in this analysis is as shown in
Figures 8.9 to 8.13; the cooling ratio derived from
it are designated η_L.

8.2   Variation of the Theoretical Ideal Cooling
Ratio, η_t, with Parameters

The major parameters affecting the value of the
cooling ratio, η_t, for a particular system are :

(1)   the relative amounts of refrigerant and
absorbent charged to the unit;

(2)   the temperature of the generator contents at the
end of the regeneration process, and

(3)   the condensing temperature which fixes the
pressure in the system at that of the pure
refrigerant after condensation has started.

The temperature of the refrigerant during
refrigeration is an additional parameter.   This is
fixed by the initial concentration of the charged
solution and the initial temperature of solution at
the start of the regeneration process.   The effects
of these parameters on the calculated cooling ratios
are presented in Figures 8.1 and 8.2.   These curves
show the variation of the cooling ratio with the
final generator temperature at various condensing
temperatures of the refrigerant at two different
concentrations.

All of the cooling ratios are calculated on the
assumption that the initial generator temperature is
the same as that of the absorber at the end of the
reabsorption process; i.e., the equilibrium
temperature of the absorber when the last of the
refrigerant is vapourised.   This initial temperature

is thus fixed by the initial concentration of the
ammonia in the solution. It is also assumed that
there is no carry over of the absorbent, i.e., water
into the condenser. However, practically, there will
always be some water carry over into the condenser
because of the high volatility of water even though
some rectification will occur in the rectifier above
the generator by partial condensation. The effect of
the distillation of water into the condenser is to
slightly lower the cooling ratio.

The effects on η_t of changes in operating
variables of the system with a particular charge, and
the effects of changes in charge concentration, are
shown by the η_t curves. After the start of
regeneration, no refrigerant was vapourised and
condensed, and $\eta_t = 0$ until the vapour pressure of
the refrigerant over the solution reached a value
equal to the saturation pressure at the condensing
temperature. The η_t increased as the refrigerant was
vapourised and reached a maximum after which
additional heat went largely into heating the
refrigerant-depleted solution. The effect of an
increase in the condensing temperature, at a given
final generator temperature, was to increase the
pressure in the system and thus increase the
equilibrium concentration of the refrigerant in the
absorber. Hence a higher percentage of the heat
absorbed by the generator contents went into heating

the absorbent and unvapourised refrigerant, and η_L was reduced as a result of the increase in the condensing temperature.

In continuous absorption refrigeration systems, the use of heat exchangers permits overall performance ratios of 0.5 to 0.7, depending on the temperature levels involved. In simple intermittent units, however, heat absorbed by the absorbent and the refrigerant left in the generator at the end of regeneration must be rejected to the atmosphere and lost. Thus the performance ratios are substantially lower, and the η_L value represents an upper limit on the performance to be expected from a particular unit.

8.3   Discussion of Experimental Results

Table 8.1 shows the operating data for solar regeneration of ammonia-water experimental unit and results for five of the tests. Examples of such results are shown in Figures 8.3a to 8.8b. Examples of the actual cycle and comparison with the corresponding theoretical cycles are shown in Figures 8.9 to 8.13.

The heat input to the aqua-ammonia solution in the generator during the regeneration process was calculated from an energy balance on the generator during the heating period in a manner similar to that

described previously for Q_g, but with measured
temperatures and changes in concentration (i.e., the
amount of refrigerant condensed). The refrigeration
effects were calculated from the mass of condensate
in a manner similar to that used for Q_c, assuming
that the condensate is pure refrigerant. η is then
the ratio of the refrigeration effect to the net
generator heat input, ε is the ratio between the heat
input to the generator contents and the total
measured direct solar radiation on the effective
collector area during the regeneration process and
the $(COP)_{overall}$ is the ratio of the refrigeration
effect to the incident daily insolation for the
period regeneration was on, i.e., the product of η
and ε.

8.3.1 Comparisons between the Actual Experimental Cycle and the Theoretical Ideal Cycle

The actual cycle differs from the corresponding
theoretical cycle in a few notable ways.

Firstly, the actual pressure at which generation
occurred was greater than the theoretical pressure.
This difference between the actual and theoretical
pressures corresponded to the difference in
temperatures between the condensing vapour and the
cooling water. This temperature difference was
necessary in order that the heat of condensation

could be transferred to the cooling water. The
condensing temperature fixed the pressure in the
system, and thus the equilibrium concentration in the
generator. At a particular generator temperature, a
high condensing pressure (and temperature) resulted
in a high refrigerant concentration in the generator;
at the increased concentration, a smaller percentage
of the total heat input went into vapourising the
refrigerant. As a result the actual value of the
final generator concentration (X_a) was greater than
the theoretical value (X_o) for the same value of
maximum solution temperature $(t_a$ or $t_o)$; i.e. the
actual mass of condensate was less than the
theoretical quantity. This resulted in the actual
cooling ratio, η, being less than the theoretical
value.

Two factors in these experiments contributed to
the differences in these temperatures.

(1) The liquid refrigerant accumulated in the
condenser tubes, progressively filling it as
regeneration proceeded. Part of the effective
condenser area was the interface between the
condensate and the vapour. The condensate formed at
that surface or draining down to that surface from
the walls of the condenser lost heat by conduction
through the bulk of the condensate and metal
container walls to the coolant. Thus there was a
temperature gradient through the liquid, from the

interfacial condensing temperature to the lower bulk
temperature, which tended to be maintained by the
density gradient existing in the opposite direction.
Hence, there was a difference between the true
condensing temperature and the measured condensate
temperatures which increased as the quantity of
liquid refrigerant increased.

(2) Heat of condensation and sensible heat of
cooling of the liquid had to be removed from the vapour
stream in the condenser and the tube connecting the
generator and condenser. As the effective area
decreased, the driving force increased to transfer
this heat; the interfacial temperature, i.e., the
condensing temperature, therefore increased relative
to the coolant temperature.

Secondly, at the end of the cooling process of
the generator (process 3-4), the solution
concentration (X_3) and pressure (P_4) were higher than
the corresponding theoretical values (X_6 and P_7).
Such a deviation between the actual and theoretical
cycle was one of the reasons that made the actual
effective cooling less than its corresponding
theoretical value.

Thirdly, it was actually difficult to prevent a
small quantity of water from being carried over
during regeneration to the condenser-evaporator. The
presence of the water in the condensate produced
three effects. First, it caused the minimum

temperature attained by the refrigerant to be higher than its corresponding theoretical value. The water in the condensate also had to be cooled during the flashing process from the temperature of condensation to the highest temperature at which absorption of heat took place and ammonia had to be evaporated to achieve this. Secondly, it produced a lower effective cooling since the water in the condensate had to be cooled during both the flashing and the subsequent cooling process. A third consequence of water in the condensate was that at the end of the absorption the cycle was not completed, and provision had to be made to purge the residual solution in the evaporator back to the generator-absorber in order to return the solution to its original concentration.

8.3.2 Generation Pressure Versus Time

From Figures 8.3a to 8.8a, the curves of the generation pressure against time indicate that they follow a generalised pattern of a fairly horizontal base, then a steep rise and afterwards a fairly horizontal peak.

The horizontal base corresponds to a ''heat up period'' at the start of the generation process, when the heat absorbed goes to heat the solution at constant pressure until the temperature of the solution attained is the temperature corresponding to

the solution initial concentration at the particular
pressure. This temperature is that attained at the
end of the reabsorption process during the night
prior to generation. This can be explained by the
fact that since the reabsorption of ammonia in the
weak solution is exothermic, the absorber temperature
at the end of the reabsorption process was well above
the ambient temperature. However, since the
—absorption process occurred for only about 4 to 5
hours during the night, at the start of the
regeneration at about 8.00 am the following morning,
the solution in the collector-generator would have
cooled down to the ambient temperature and hence this
initial ''heat up period'' was necessary to heat up
the solution to the temperature at the end of the
reabsorption during the previous night.

The steep portion of the curves corresponds to
the sensible heating of the solution at constant
concentration. And the horizontal top part of the
curves correspond to the boiling of the solution when
ammonia vapourises out of solution and it's condensed
at this constant pressure. This pressure is
determined by the temperature of the cooling water in
the condenser and is the saturation pressure of the
ammonia vapour corresponding to the condensation
temperature. It was observed that the bubble point
of the solution, i.e., the initiation of the boiling
of ammonia out of the solution, occurred at a slightly

lower pressure than this peak horizontal pressure.
This was the point that was used to indicate the
theoretical condensing temperature and it corresponds
to the cooling water temperature at the initiation of
boiling.   But because of the temperature gradient
that was set up in the condenser tubes after the
initiation of condensation between the cooling water
and the condenser surface, the actual condensing
temperature was higher than the cooling water
temperature.

8.3.3 Effect of Initial Solution Concentration on System Performance

From Figures 8.9 to 8.13, it can be observed
that the temperature at which the solution boils
depends on the initial solution concentration as well
as the cooling water temperature.   For a constant
generation pressure, which is dependent on the
cooling water temperature, the temperature at which
ammonia starts coming out of solution increases as
the initial solution concentration decreases.
However, the effect of the initial solution
concentration on the system performance is not quite
apparent.   If the case of constant energy absorbed by
the generator-collector contents, Q_9, for different
initial solution mass is considered, it is discovered
that the lower the initial concentration, the higher

the maximum generator temperature. However, as the solution temperature increases, the lower the rate at which ammonia comes out of solution and a lot of the heat goes to increase the internal energy of the ammonia depleted solution. Also, as the solution temperature increases and the concentration decreases, the amount of water generated with the ammonia increases. Hence, as the initial solution concentration decreases for a constant Q_g, the effect is that the mass of ammonia condensed decreases and hence a reduction in the cooling ratio. On the other hand, as the initial concentration is increased, the final generator temperature decreases but the mass of ammonia condensed increases. This leads to a slightly higher average evaporator temperature during refrigeration and a higher cooling ratio. This might appear advantageous, however, as the initial concentration increases, the reabsorption rate during refrigeration and the cooling rate decreases. These important considerations place a practical limit on the initial ammonia concentration.

From this investigation, it would seem that the optimum range of the initial solution concentration should be 0.58 to 0.63 kg ammonia/kg solution.

8.3.4 Effect of the Initial Solution Mass on the System Performance

The higher the initial solution mass, for a constant initial solution concentration, the higher the mass of ammonia in the solution. However, a larger quantity of heat energy is required to heat up a solution of a larger mass than one of a smaller mass through the same temperature rise. For the case of a constant heat energy absorbed by the generator contents, Q_g, for solutions of the same initial concentration but different initial solution masses, the maximum temperature attained in the generator decreases as the initial solution mass increases.

The effect of the initial solution mass on the system performance is not intuitive obvious because the quantity of ammonia condensed is dependent on both the initial solution mass and the final generator temperature, which are in turn dependent on one another. However, the higher the initial solution mass, the lower the final generator temperature and vice versa.

8.3.5 Refrigeration Phase

Figures 8.14 and 8.15 show the variation of the absorber pressure, the evaporator pressure and the load temperature with time during the refrigeration process for two of the experiments. The load was

stagnant water of 5.5kg mass filling part of the shell surrounding the condenser-evaporator tubes.

The minimum temperature attained by the water was $8^{\circ}C$, through a temperature decrease of $14^{\circ}C$. The slope of the load curve decreases towards the right, indicating that the cooling rate decreases as the refrigeration proceeds. This can be explained by the fact that since the absorption of ammonia in the weak solution in exothermic, the temperature of the solution increases as well as the absorber pressure. This leads to a decrease in the rate of absorption of ammonia in the weak solution and hence a decrease in the cooling rate of the water.

A lower load temperature could have been attained in the refrigerator, if not for the following two reasons. Firstly, the quantity of water used as the load was quite high. This was due to the limitation imposed by the way the condenser-evaporator was constructed. The other reason was heat capacity effect of the evaporator-condenser. Because of the bulk of the component, most of the energy that could have been abstracted from the water was absorbed from the materials of construction of the unit, which in this case was mild steel.

Table 8.1   Results of Tests.

Test Number	1	2	4	5	6
Date	02-03--1989	03-03--1989	05-03--1989	07-08--1989	08-03--1989
1 Intial Solution Conc. X_{a1} (%)	50.7	53.2	48.5	37.1	58.0
2 Final Solution Conc. X_{a3} (%)	33.1	36.7	34.0	30.1	45.7
3 Maximum Solution Temp T_3 (°C)	95.2	86.8	91.5	100.0	69.0
4 Maximum Generator Pressure (Bars)	10.031	9.722	9.575	9.722	9.281
5 Initial Mass of Soln. m_{a1} (kg)	9.736	9.615	9.515	10.652	13.810
6 Average Cooling Water Temperature (°C)	23.0	21.5	21.0	21.5	20.0
7 Mass of NH_3 Condensed m_{vc} (kg)	2.56	2.51	2.09	1.07	3.13
8 Heat Added To Soln. During Regeneration Q_g (kJ)	6921.9	6247.8	5873.2	5124.8	7288.4
9 Effective Cooling Obtained, Q_c (kJ)	2912.5	2858.3	2391.7	1207.6	3604.1
10 Obtained Cooling Ratio, $\eta = Q_c/Q_g$	0.421	0.457	0.407	0.236	0.495
11 Solar Heating Ratio $\varepsilon = Q_c/I$	0.258	0.240	0.243	0.288	0.347
12 Overall COP $(COP)_{sys} = Q_g/I$	0.109	0.110	0.099	0.068	0.171
13 Cooling Capacity $= Q_c/A_c$ (kJ/m^2)	1990.7	1953.7	1634.7	825.4	2463.4
14 Measured Minimum Load (Water) Temp. (°C)	9.5	10.0	12.0	16.0	8.0

Final Generator Temperature, Deg.C
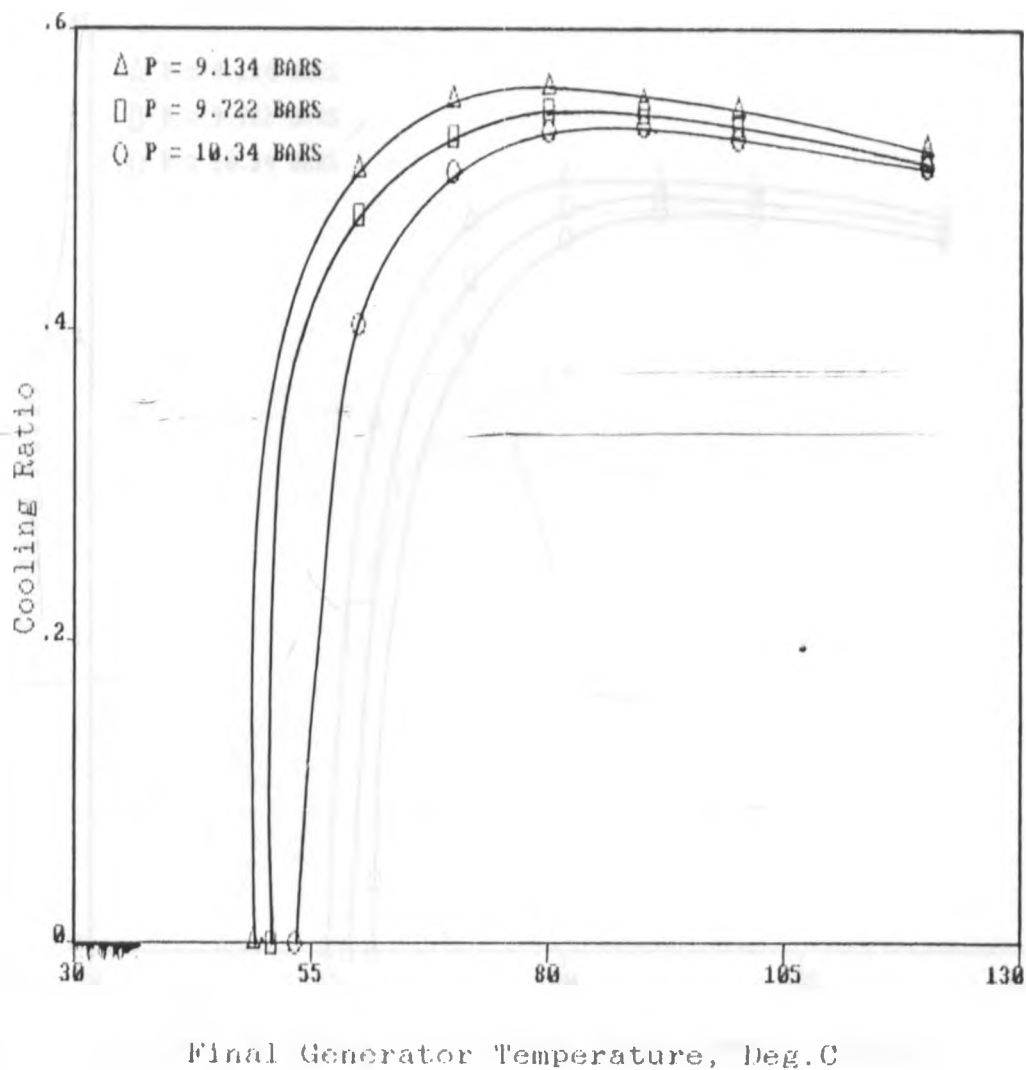
Figure 8.1   Theoretical cooling ratio, z_i, versus
final generator temperature, T_3, at
various condensing temperatures for
$T_1 = 20$ C and $X_{31} = 0.6$ kg NH_3/kg Sol.

Final Generator Temperature, Deg.C
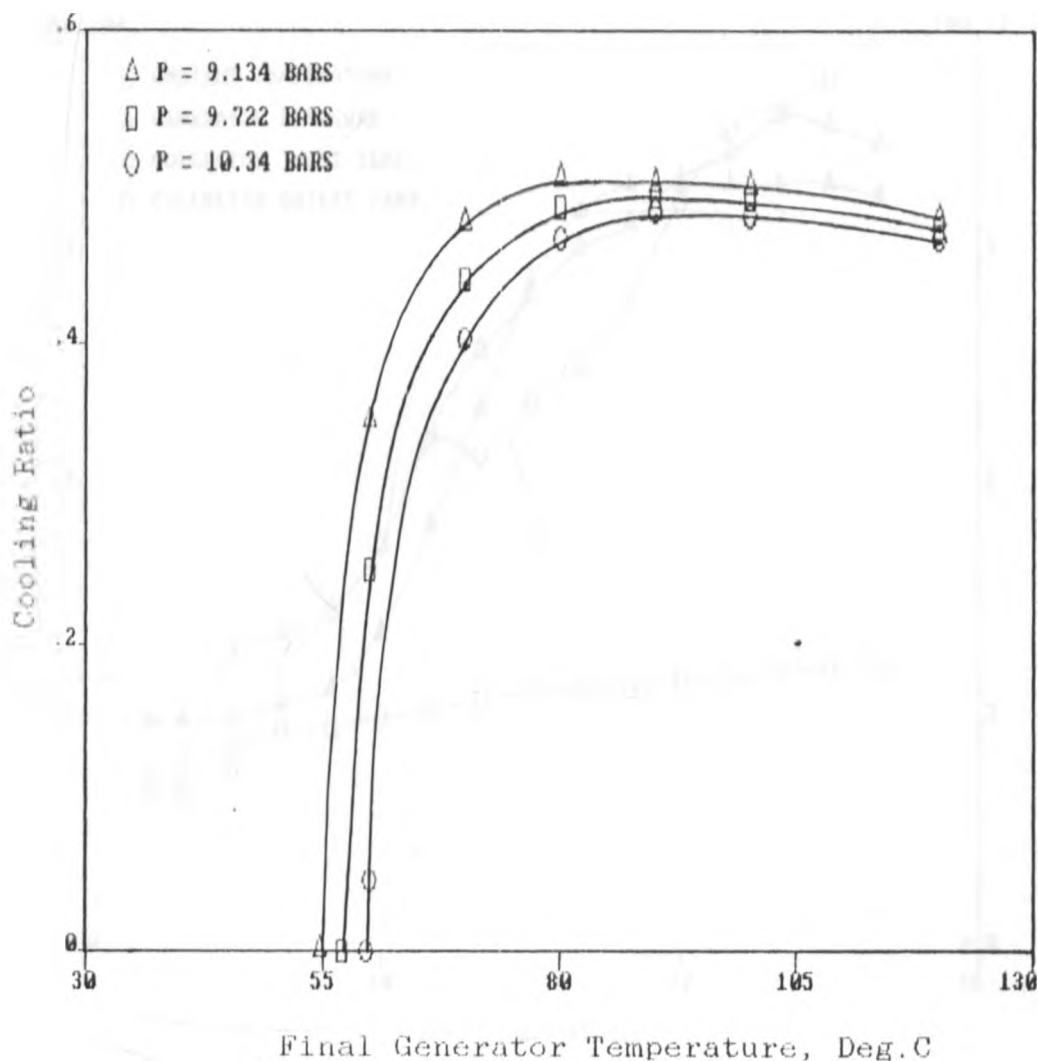
Figure 8.2   Theoretical cooling ratio, η_i, versus
final generator temperature, T_3, at
various condensing temperatures for
$\bar{T}_1 = 26 °C$ and $X_{s1} = 0.55$ kg NH_3/kg Sol.
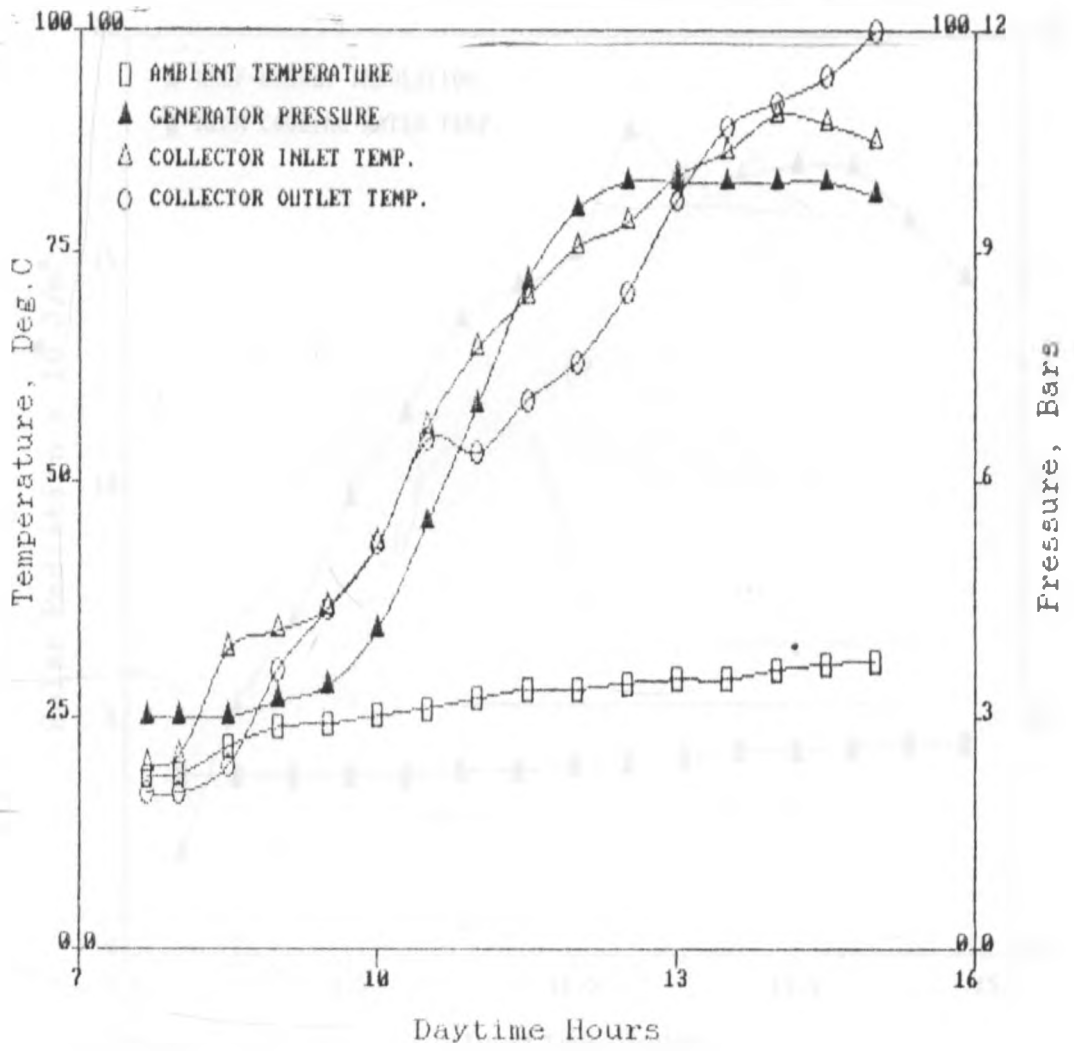
Figure 8.3a Observations during regeneration
for test 1.
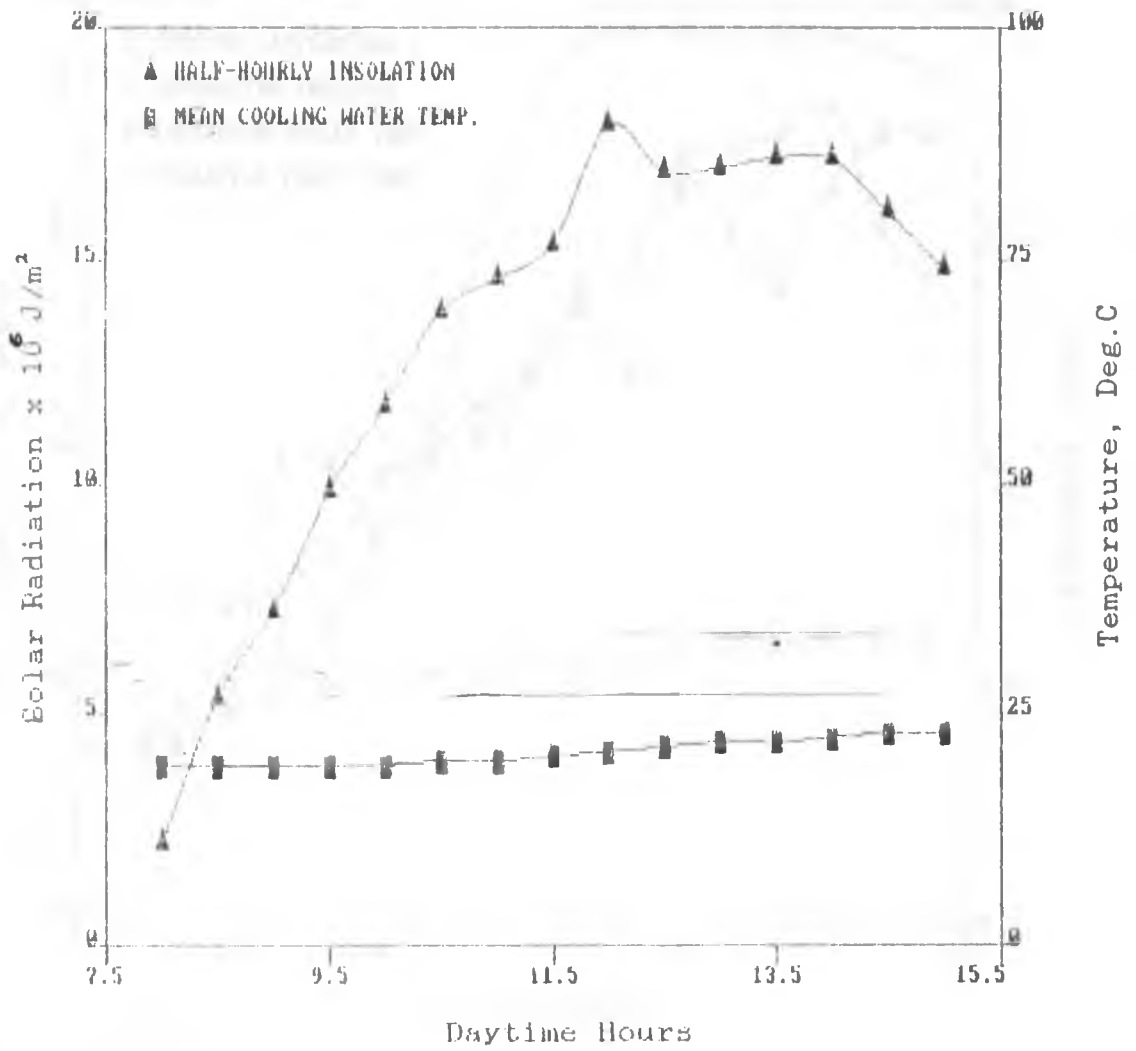
Figure 8.3b   Insolation level and cooling water temperature during regeneration for test no. 1.
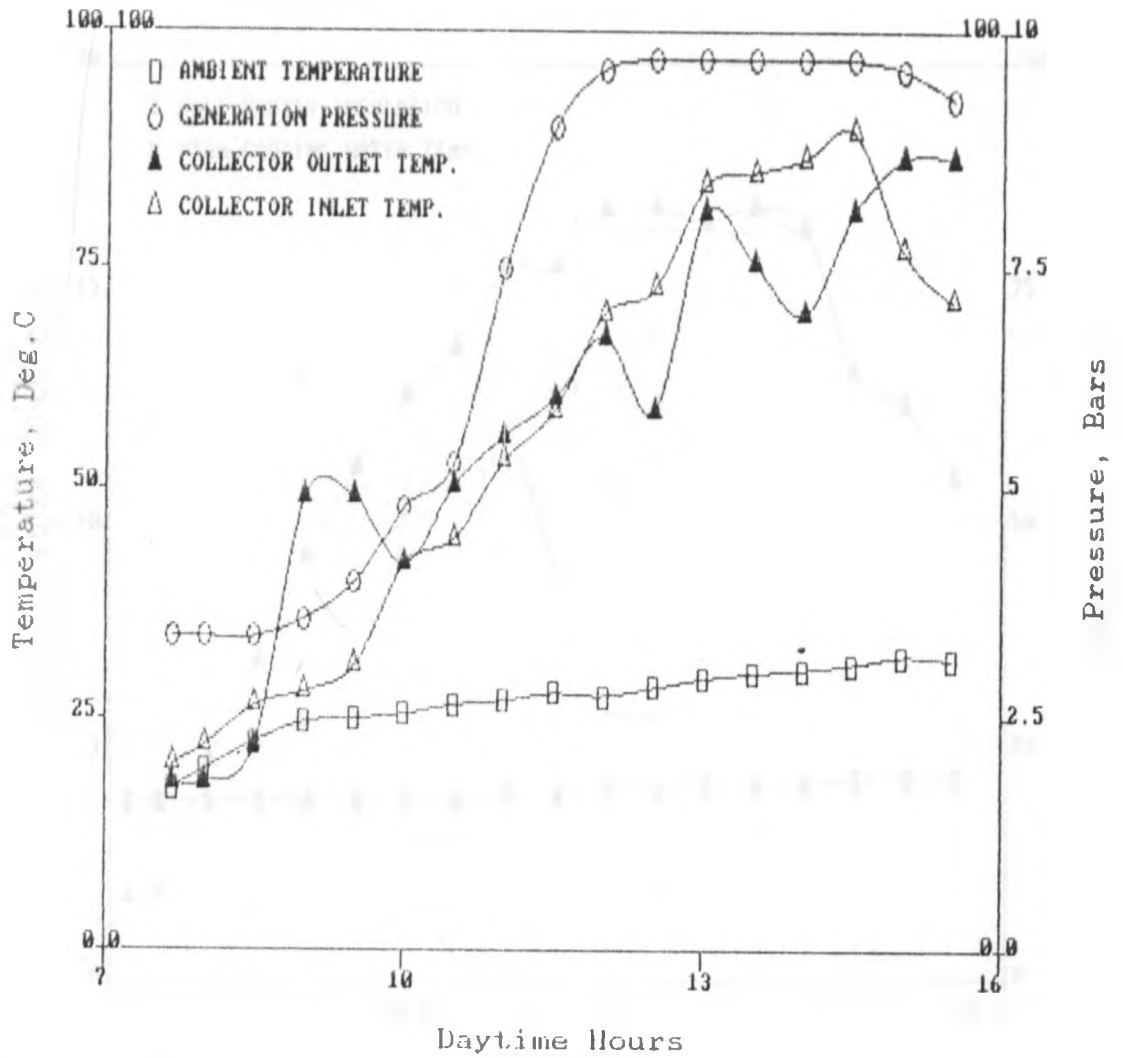
Figure 8.4a Observations during regeneration
for test no. 2.
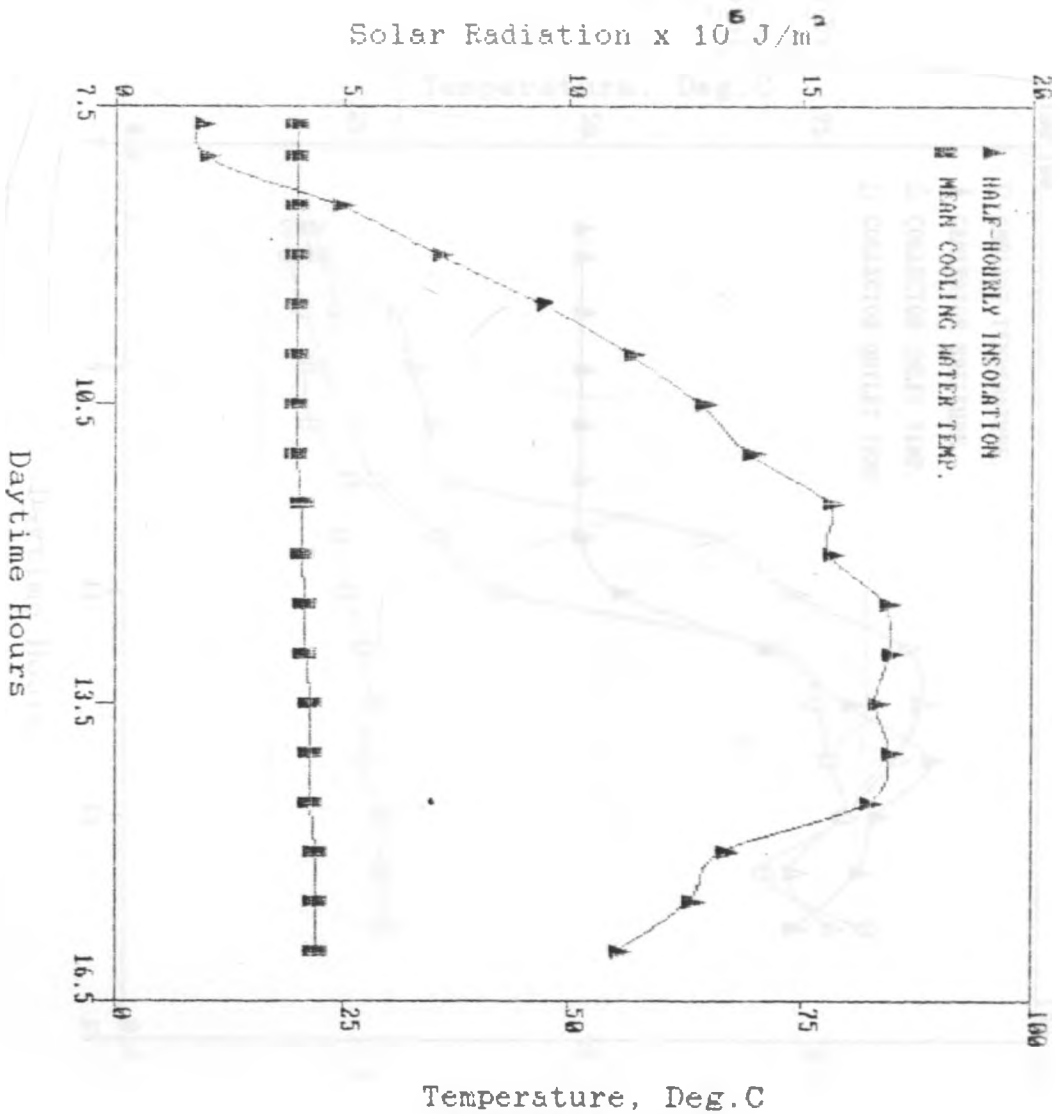
Figure 8.4b   Insolation level and cooling water temperature during regeneration for test no. 2.

Solar Radiation x 10^5 J/m^2

Temperature, Deg.C

Daytime Hours

- ▲ HALF-HOURLY INSOLATION
- ■ MEAN COOLING WATER TEMP.
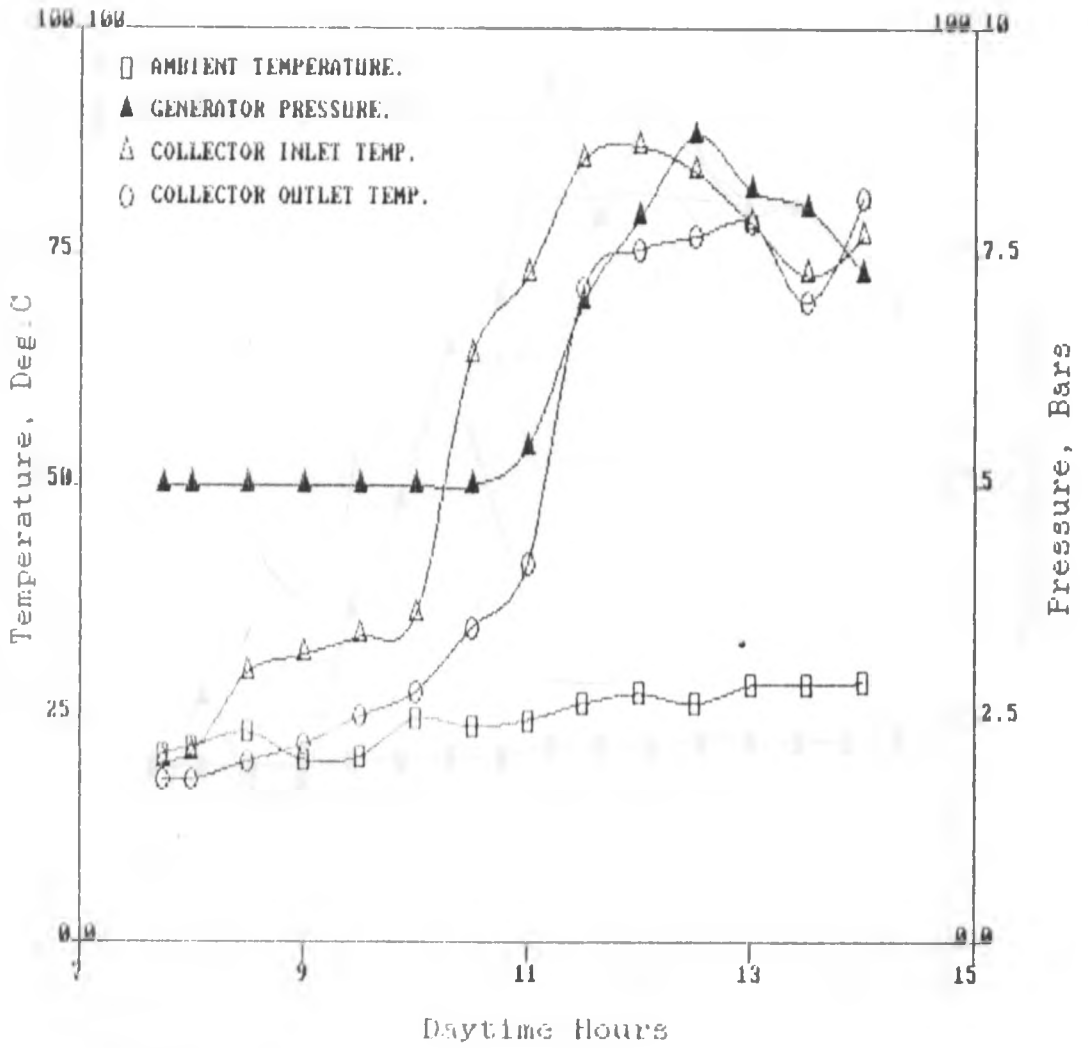
Figure 8.5a Observations during regeneration
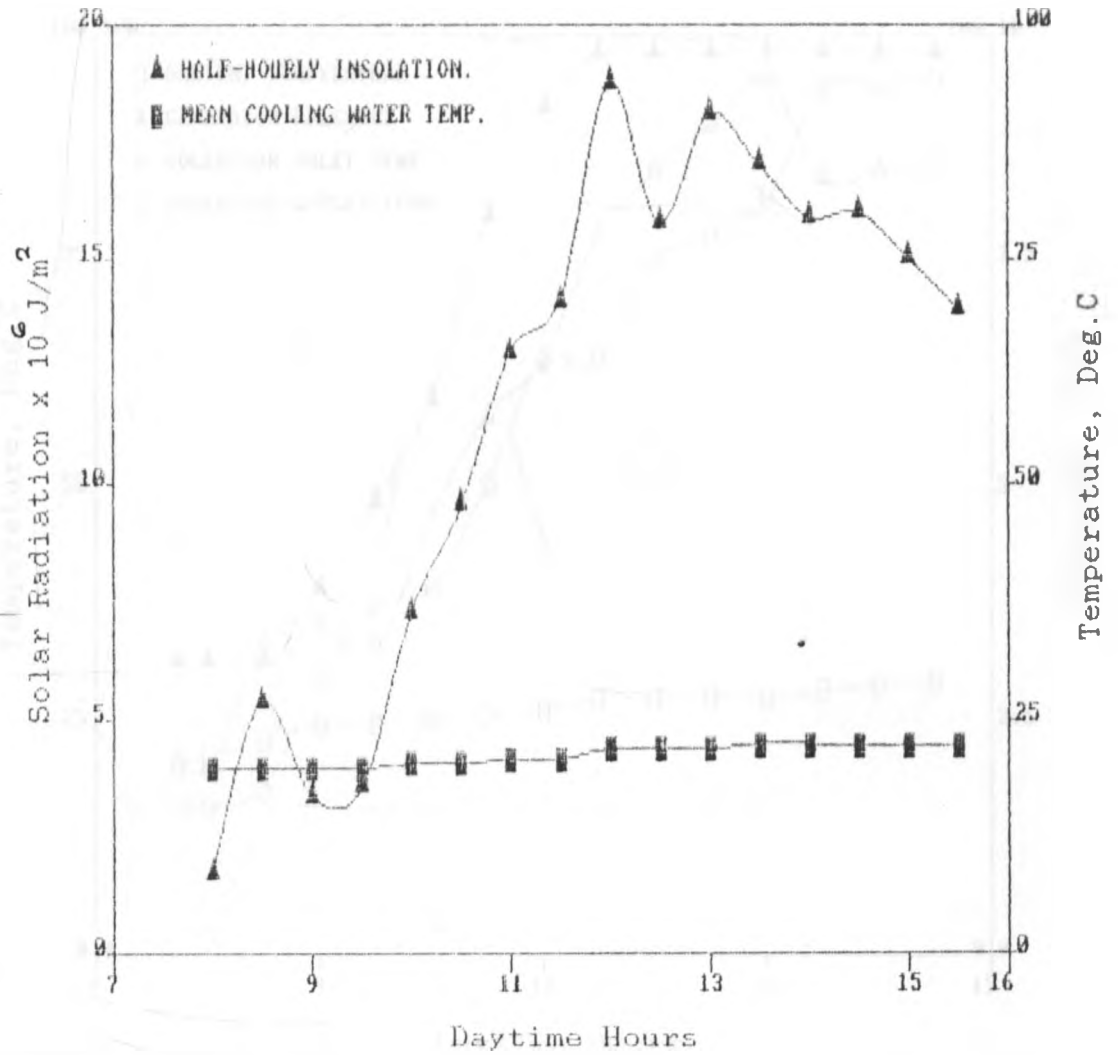
for test no. 3.

Figure 8.5b   Insolation level and cooling water
              temperature during regeneration for
              test no. 3.
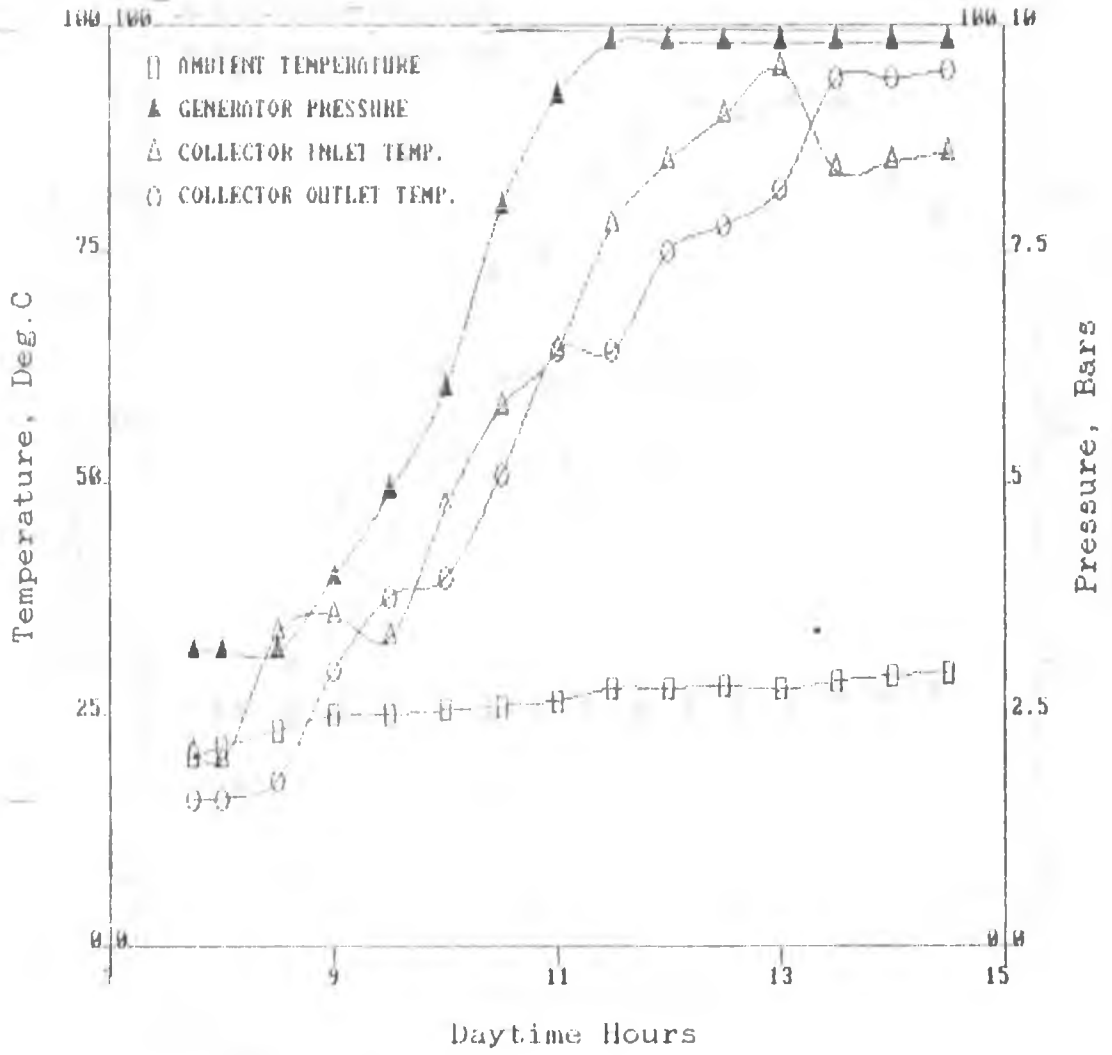
Figure 8.6a Observation during regeneration
for test no. 4.
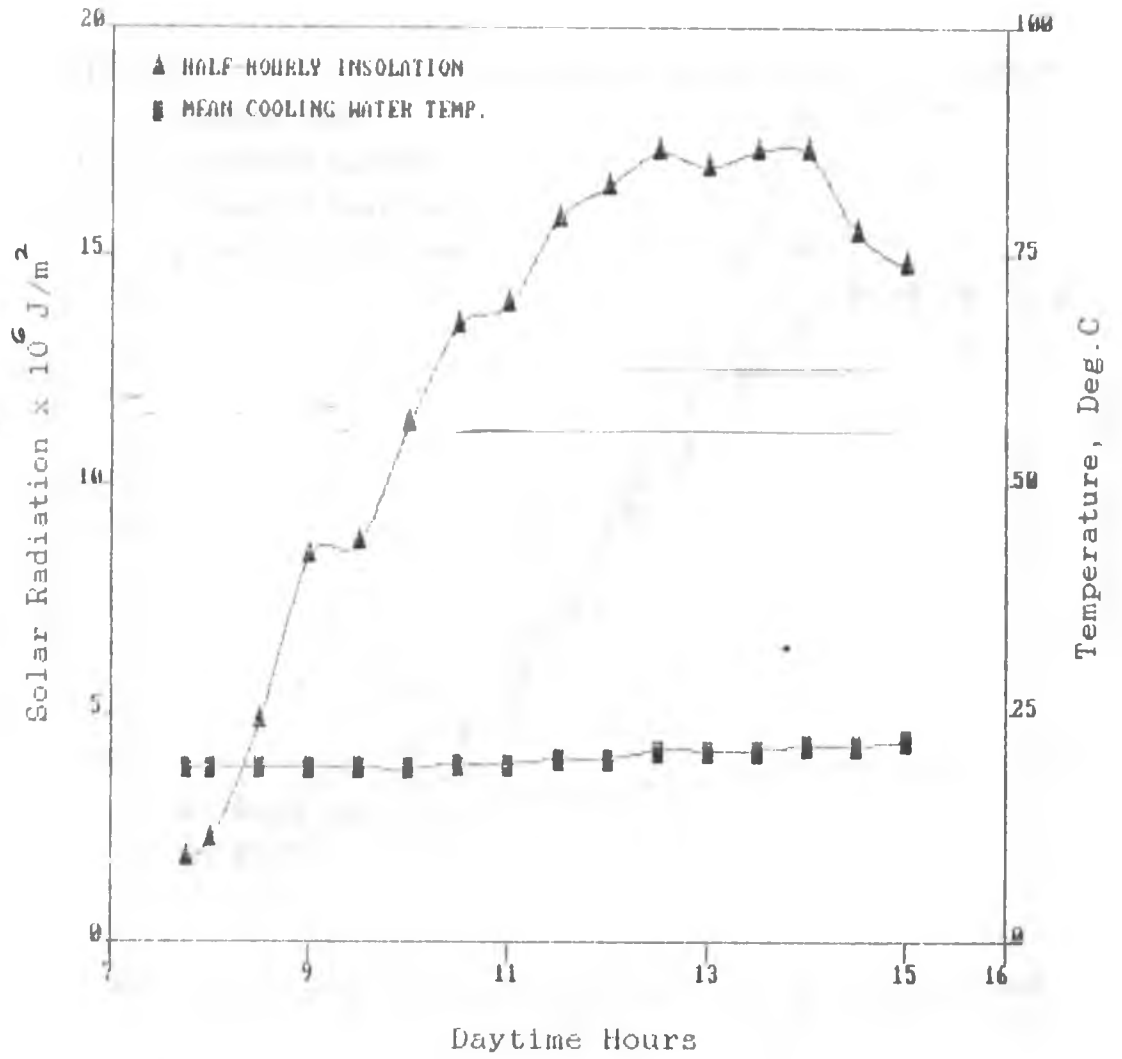
Figure 8.6b   Insolation level and cooling water
                temperature during regeneration for
                test no. 4.
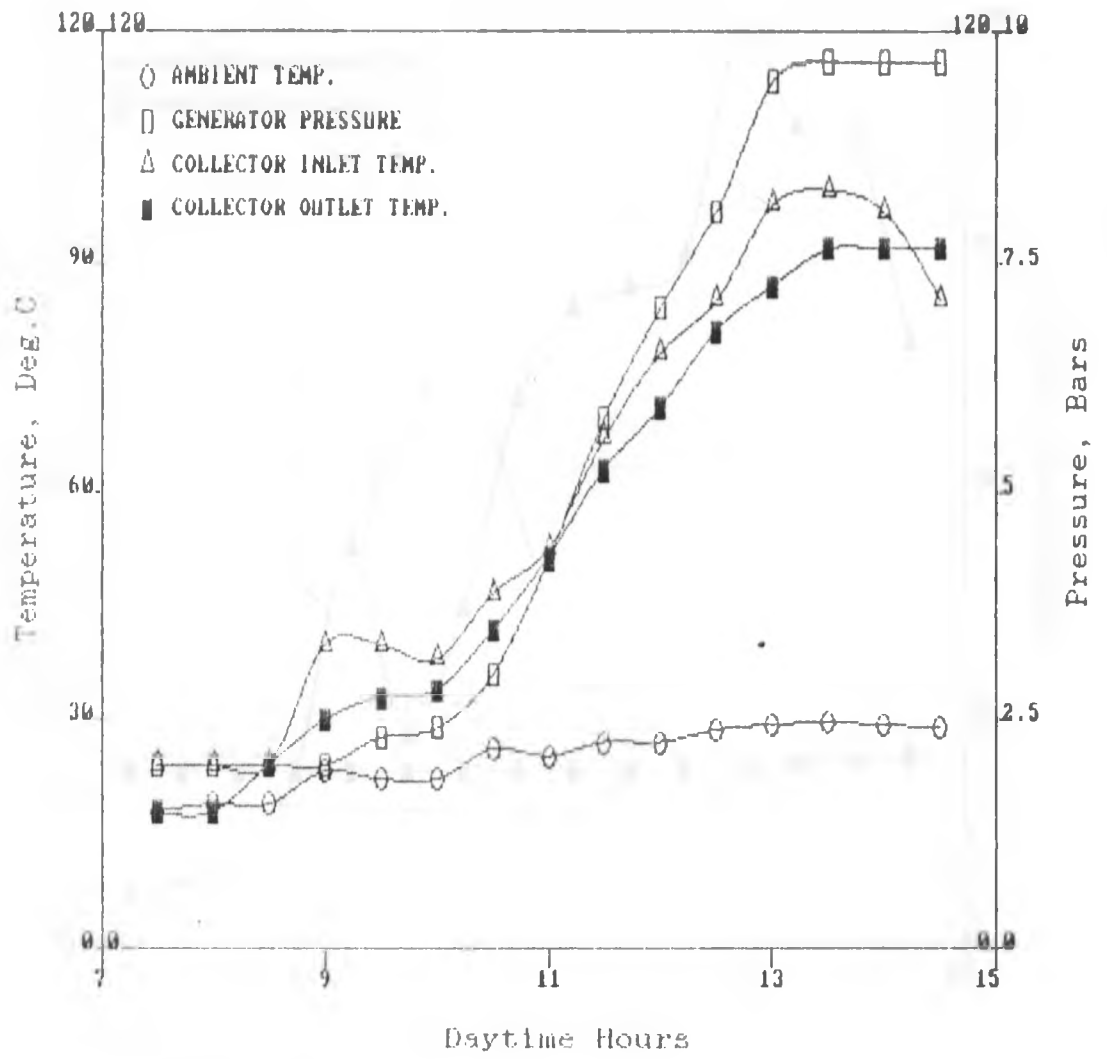
Figure 8.7a Observations during regeneration
for test no. 5.
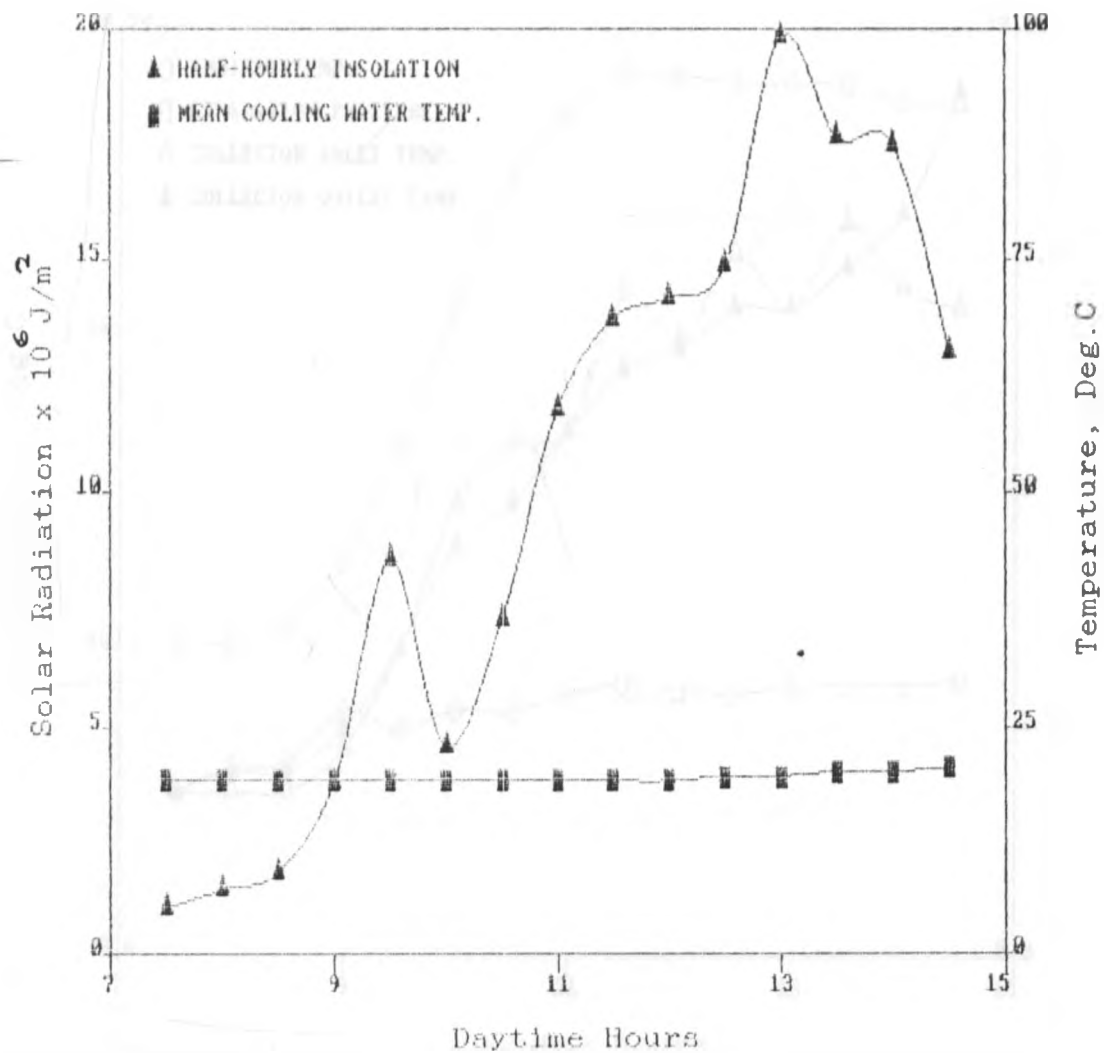
Figure 8.7b   Insolation level and cooling water
              temperature during regeneration for
              test no. 5.
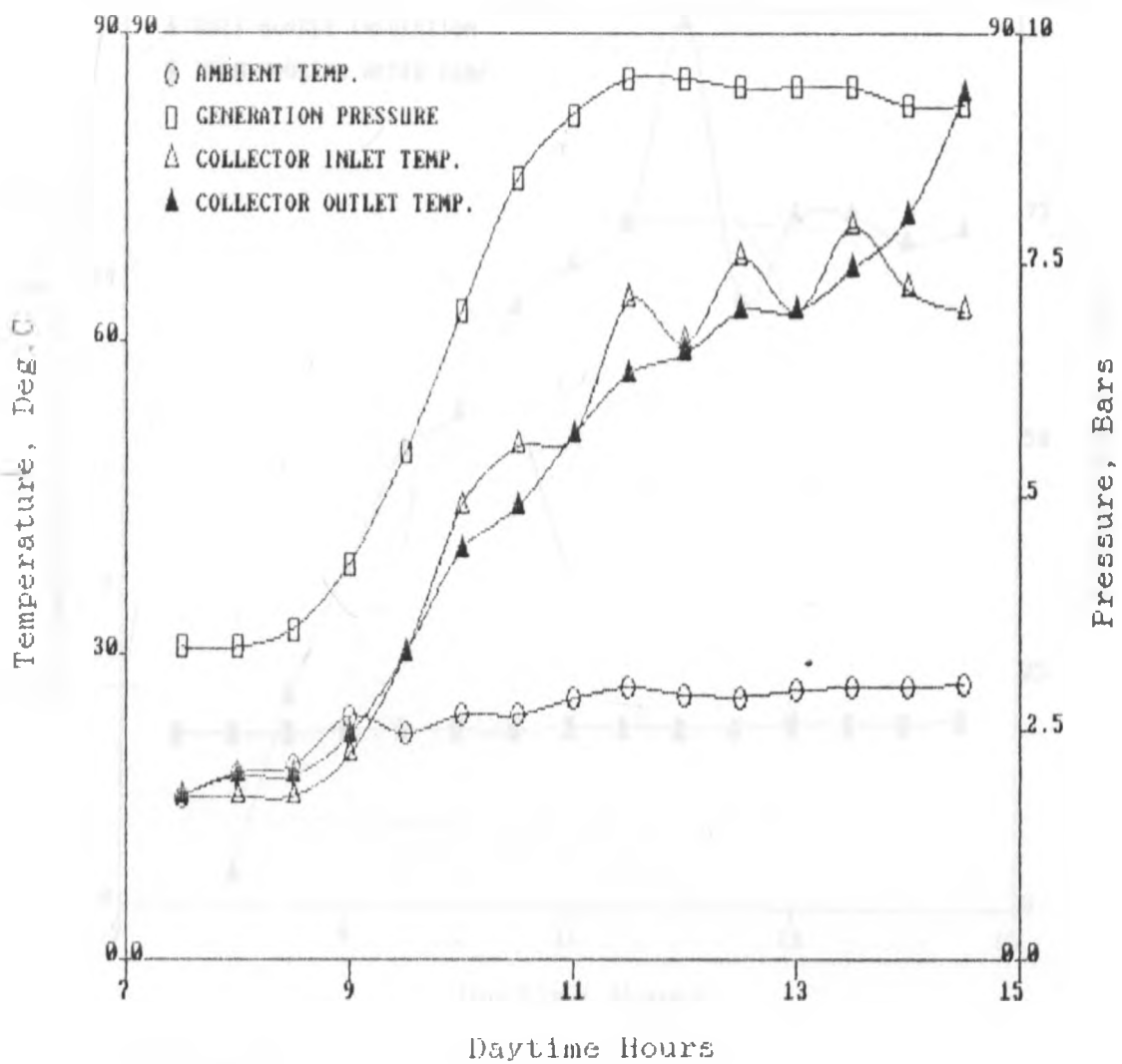
Figure 8.8a Observations during regeneration
for test no. 6
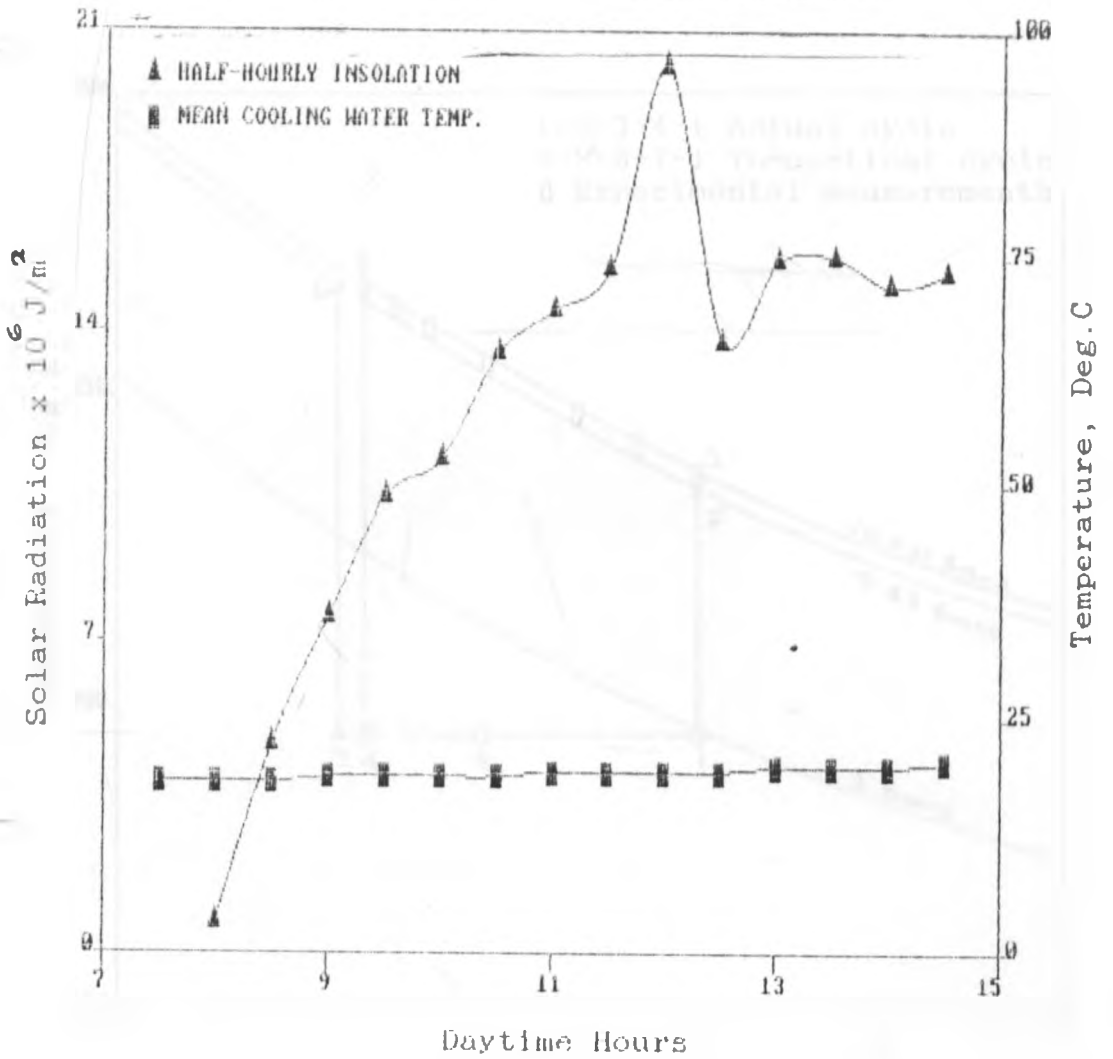
Figure 8.8b   Insolation level and cooling water
               temperature during regeneration for
               test no. 6.
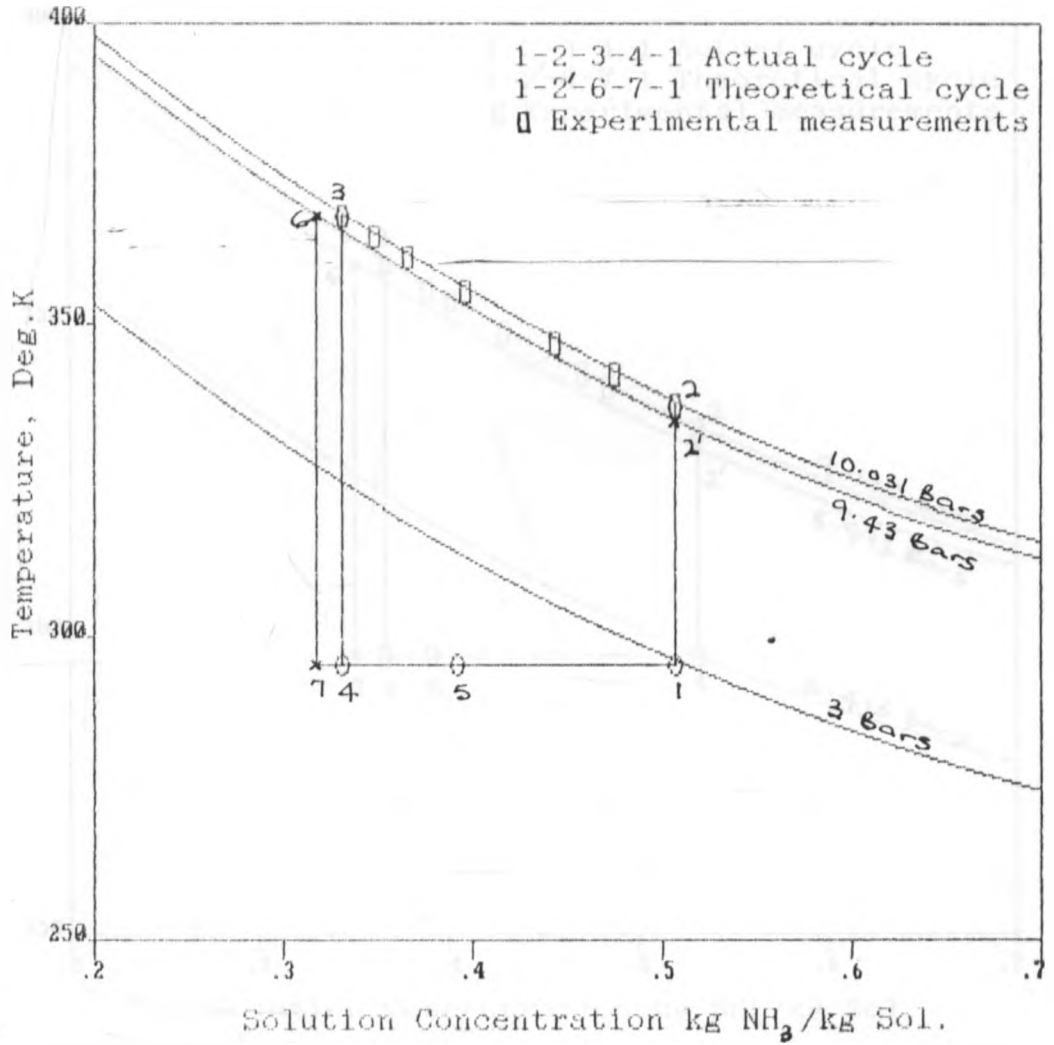
Figure 8.9 Actual cycle compared with the
theoretical cycle for test no. 1.
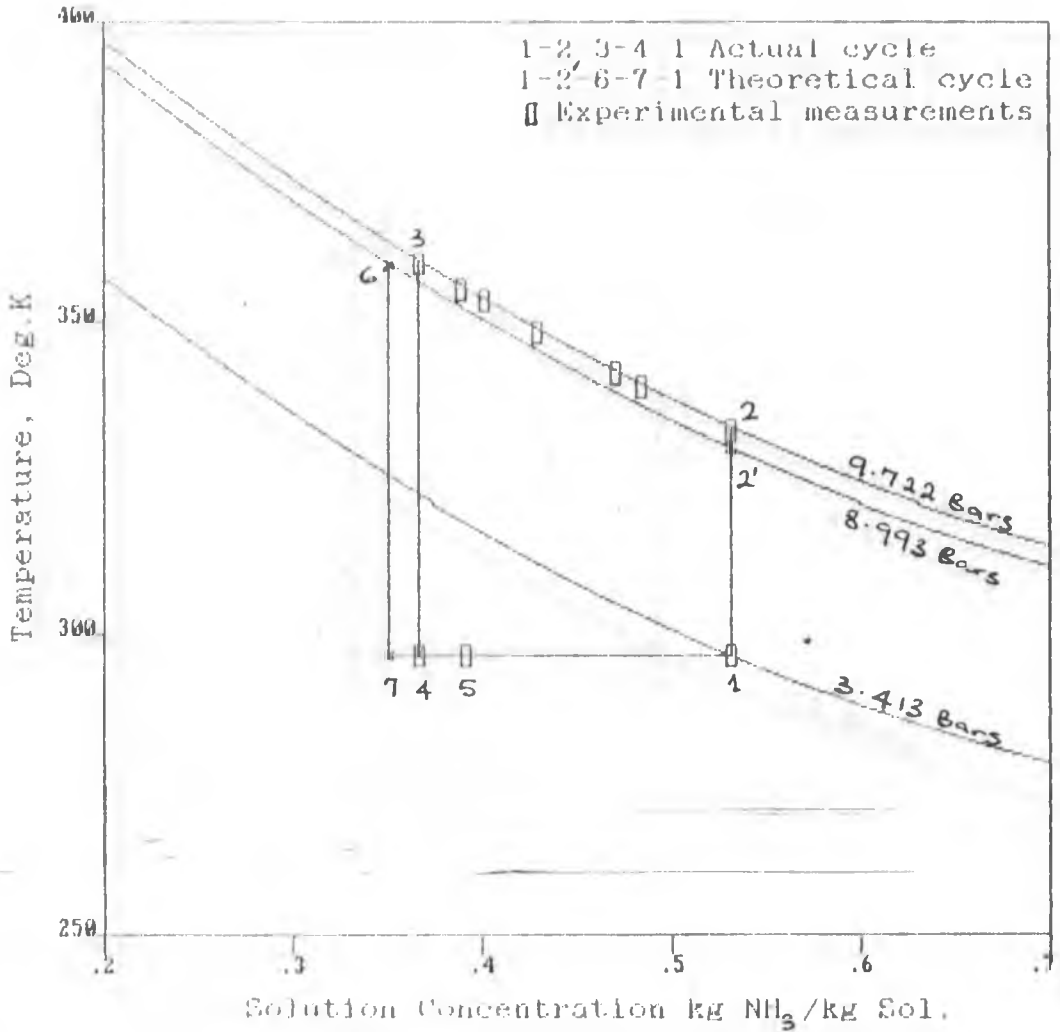
Figure 8.10   Actual cycle compared with the
theoretical cycle for test no. 2.
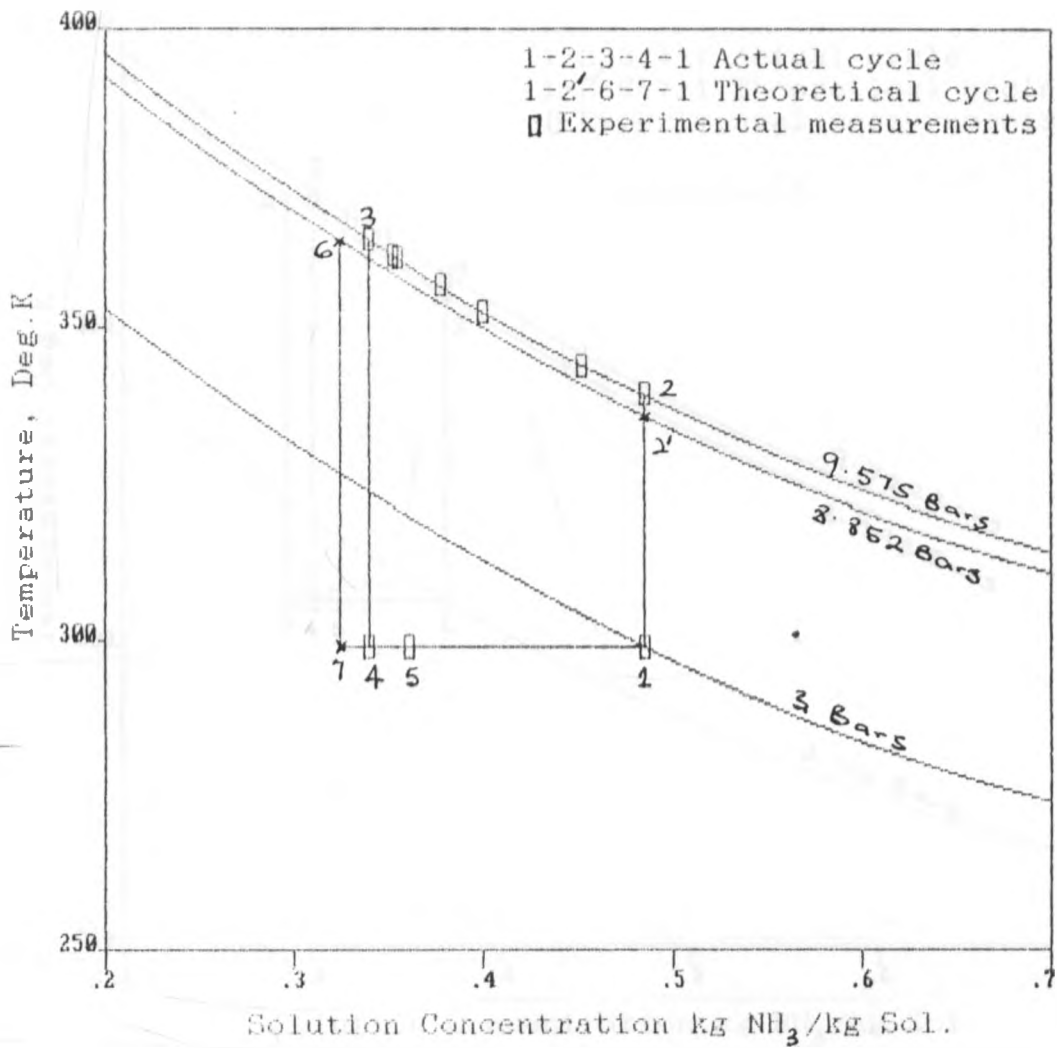
Figure 8.11 Actual cycle compared with the
theoretical cycle for test no. 4.
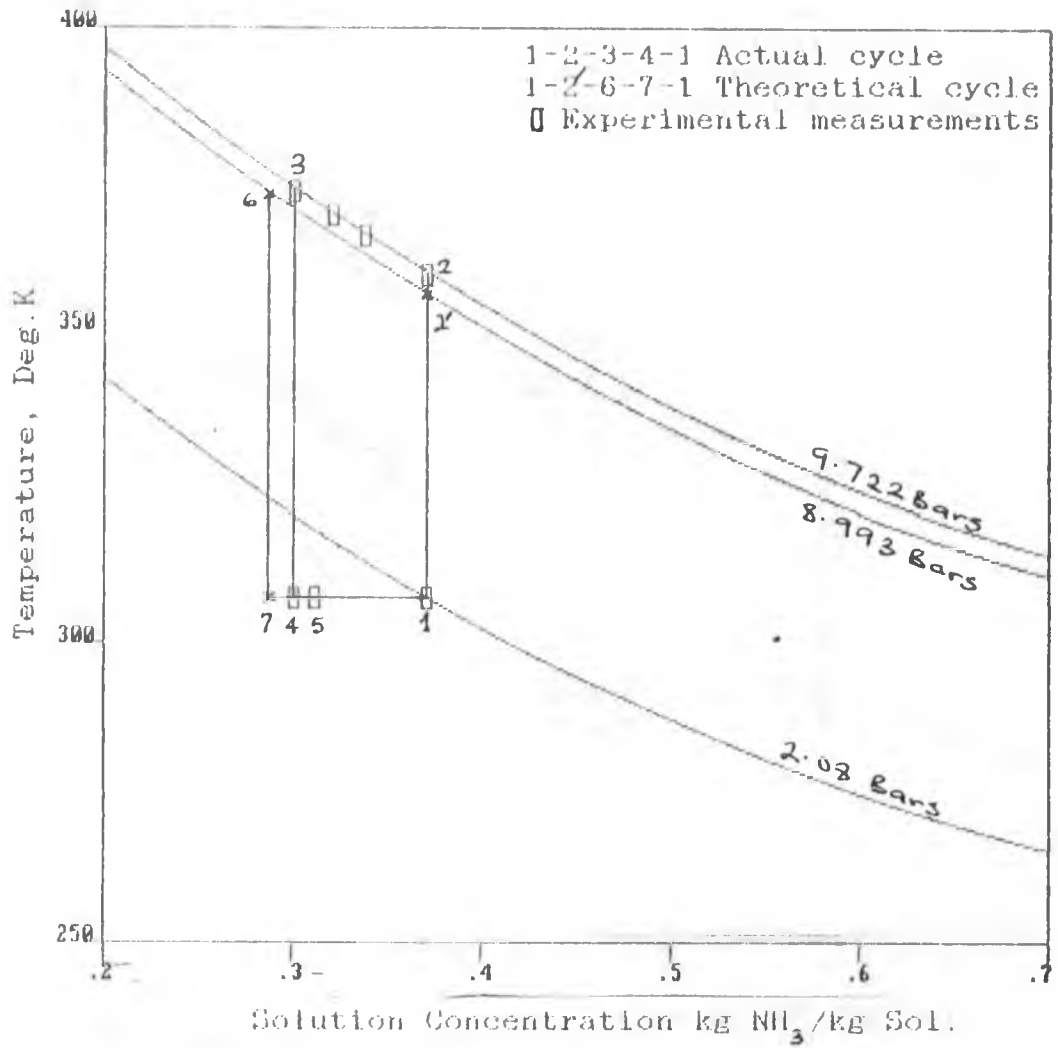
Figure 8.12 Actual cycle compared with the
theoretical cycle for test no. 5.
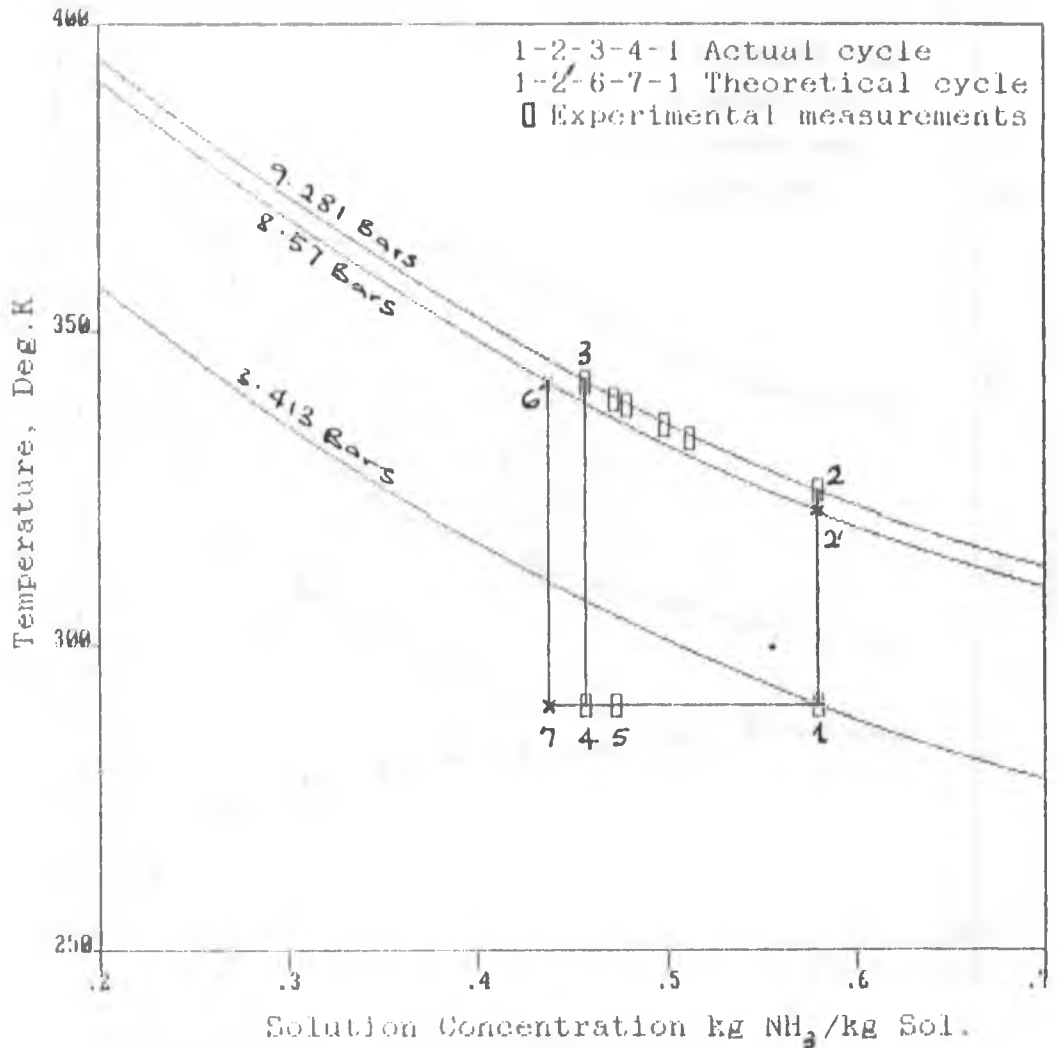
Figure 8.13   Actual cycle compared with the
theoretical cycle for test no. 6.
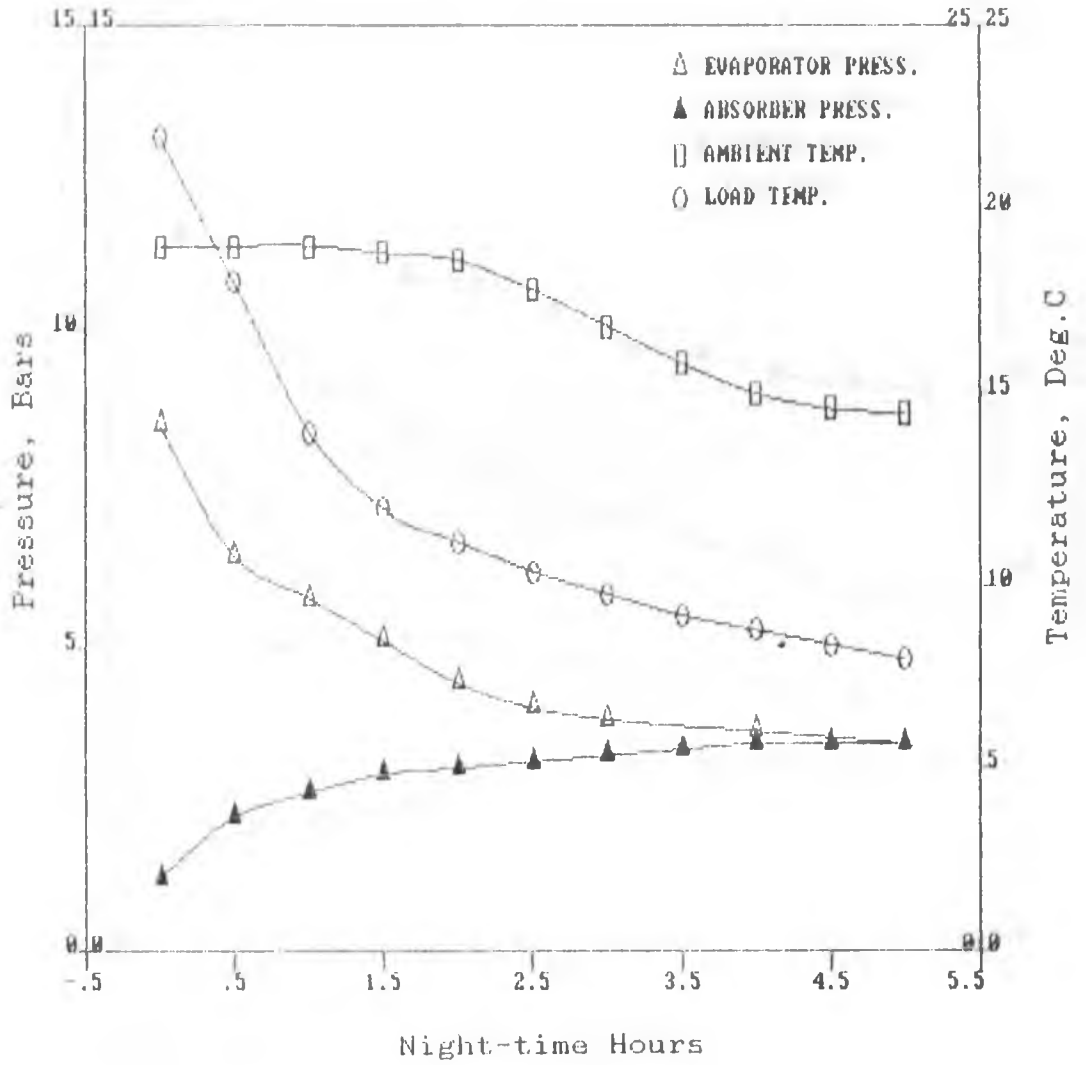
Figure 8.14 Observations during refrigeration
for test no. 1.
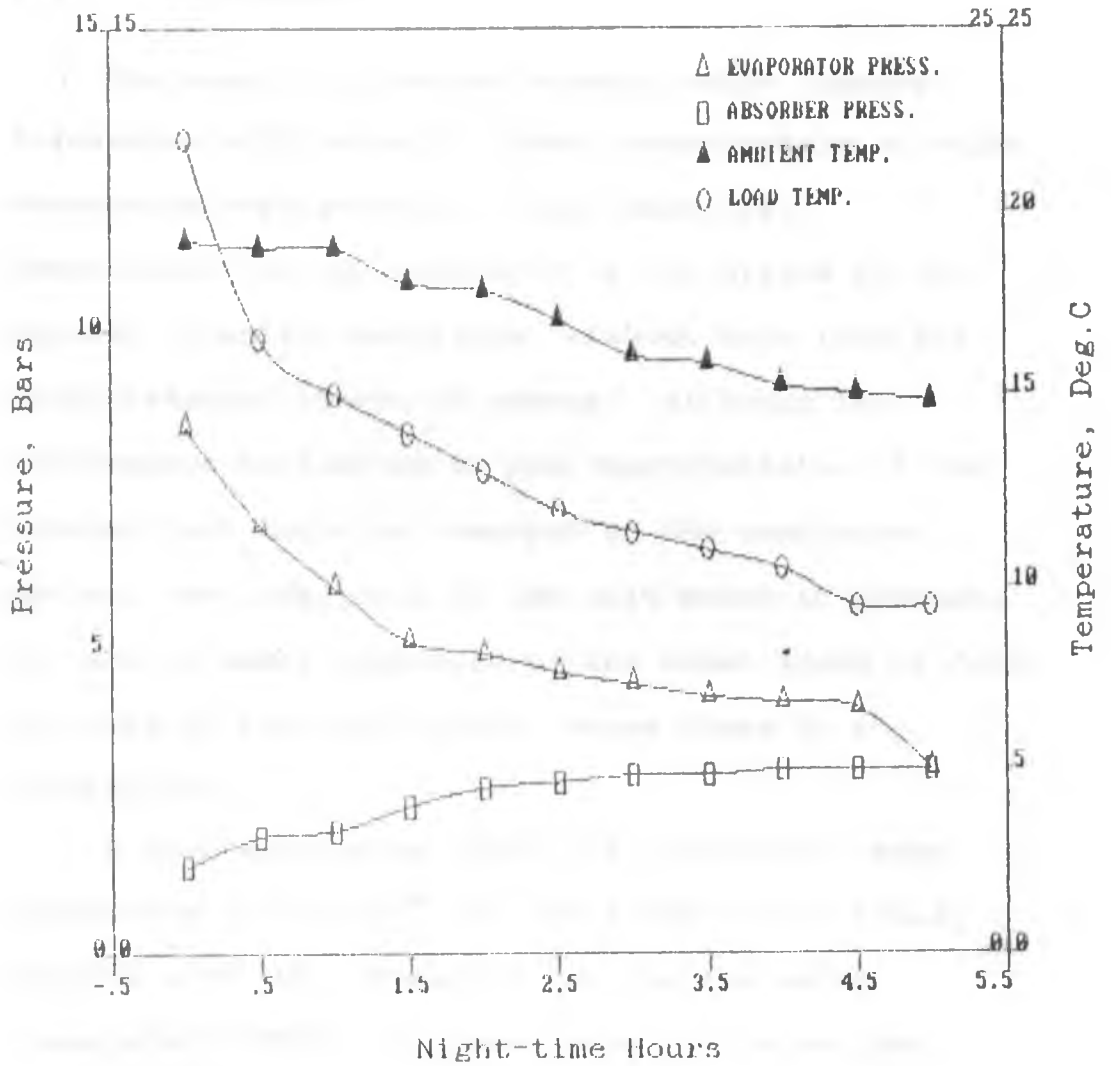
Figure 8.15   Observations during refrigeration

for test no. 6.

CHAPTER NINE

CONCLUSIONS AND RECOMMENDATIONS

9.1   Conclusions

The results, obtained herein, which compare favourably with those of other investigators of solar absorption refrigeration, (see Table 9.1), demonstrate the applicability of the system in the Nairobi climatic conditions, without help from any other external source of energy. Although the performance is limited by the characteristic of the intermittent cycle as compared to the continuous cycles, the simplicity of the unit makes it adequate for use in small household(s) and other types of food chillers in the rural areas, where there is no electricity.

A good insolation level, (a cummulative mean insolation of 15.8×10^6 Jm^{-2} at 2.00pm local time), coupled with the relatively low cooling water temperature ($20°C$), and the range of the ambient temperature variation being small (20-$27°C$), enabled the system to give good overall performance ratio. This leads to the conclusion that an intermittent aqua-ammonia absorption refrigerator can give satisfactory performance in an equatorial climate like Kenya.

From this investigation, it can also be concluded that the optimum range of the initial solution concentration should be 0.58 to 0.63 kg ammonia/kg solution in order to give a satisfactory performance. This is so because of the temperature range available for generation in this investigation i.e. about 70°C to 100°C, which is a consequence of the limitation of the design of flat-plate solar collectors.

It was also discovered that the higher the maximum solution temperature attained in the solar collector-generator, the better the cooling ratio as a result of more ammonia being generated and condensed. But, it should also be noted that this temperature is dependent on the initial solution concentration and the initial solution mass. Also, the lower the minimum evaporator temperature during refrigeration, the higher the cooling ratio and this gives a better overall performance ratio for the system.

The ammonia-water combination gives the best performance under the assumption that no water is transferred to the condenser. In practice, it is difficult to prevent a liquid absorbent such as water from being transferred to the condenser during regeneration. This transfer reduces the cooling ratio. Improvements in system performance should be attainable by design modifications.

Ammonia and water constitute a particularly advantageous combination for absorption refrigeration systems with solar regeneration. This is attributed to both the pressure-temperature-concentration relationships of the combination and the high latent heat of ammonia. Higher latent heats result in smaller equipment sizes as well as good thermodynamic performance.

9.2   Recommendations

(1)   Investigations should be carried out to determine how the changes in solution concentration as generation proceeds affect the heat transfer coefficient in the collector tubes, and therefore the collector design parameters such as the collector efficiency factor, F' and the collector heat removal factor, F_R. This knowledge will aid the proper designing of the collector-generator with a view of optimizing the system performance, since the insolation levels are fixed for any particular location.

(2)   During the experimentation it was discovered that it was not necessary to have a multi-tube condenser provided that the rate of the cooling water flow could be adjusted to give constant generation pressure. Hence, it is recommended that in future work the condenser should be of the single tube-in-shell type.

(3)   In order to obtain refrigeration temperatures below $0°C$, a separate evaporator should be used for refrigerant storage apart from the condenser.   If this is done, it will be possible to have a condenser with better effectiveness by having refrigerant condensation outside the tube.   This would reduce the heat capacity effect of the evaporator during the refrigeration and ensure a generation pressure closer to the theoretical generation pressure.

(4)   Proper design of the rectifier to prevent water vapour from being carried over with the refrigerant distillate would increase the cooling significantly.

Table 9.1 Comparison of Research Done on Ammonia-Water
Combination.

Researcher	Williams et al. (1957)	Chinnappa (1961)	Chinnappa (1962)	Farber (1970)	Swartman et al. (1970)
Ammonia-Water Concentration	0.56	0.48	0.46	0.48-0.6	0.58 - 0.70
Generator	Solar Concentrators	Electric Heating in Oil	Flat-Plate Collector	Flat - Plate Collector	Flat - Plate Collector
Solution Temperature	129°C	82-134°C	99°C	66°C	87°C
Condenser Cooling Medium	Water 27-30°C	Water 25-28°C	Water 30-36°C	Water	Water 37°C
Evaporator Temperature	19°C below amb.	-10°C	-21°C	Below 0°C	
Ambient Temp. Variation	20°C		30-35°C		Up to 27°C
Cooling Ratio	0.36 - 0.41	0.287 - 0.374	0.238 - 0.279	.	
Auxiliaries			Vapour lift pump (bubble)	Pumps, anti-freeze	
Overall COP	0.16		0.06	0.1	0.05-0.14

Table 9.1   Comparison of Research Done on Ammonia-Water
Combination (Continued).

Researcher	Eisenstadt et al. (1959)	Murungi (1982)	El-Shaarawi et al. (1986)	Staicovici (1986)	Onasanya (1989)
Ammonia-Water Concentration	0.4 - 0.7	0.672	0.63	0.43	0.58
Generator	Hot water from flat-plate collector	Solar Concentrator	Flat-plate collector	Flat-plate collector	Flat-plate collector
Solution Temperature	Water, 60-82°C	156°C	83-95°C	90°C	69°C
Condenser Cooling Medium	Water	Air	Water, 29°C	Water 25-28°C	Water, 20°C
Evaporator Temperature	-10-7°C	15°C	-2°C	-17- -12°C	8°C
Ambient Temp. Variation		20-27°C	30- 37°C	30 - 32°C	20 - 27°C
Cooling Ratio	0.14-0.47	0.47	0.49-0.51		0.495
Auxiliaries					
Overall COP				0.09-0.152	0.17-0.19

APPENDIX A

ELEMENTARY PHASE EQUILIBRIA

A.1 Definitions

The molar concentration c_i of component i is given by

$$c_i = \frac{\rho_i}{M_i} \tag{a.1}$$

where ρ_i is the density of component i and M_i is the molecular mass.

The total molar concentration of the mixture is given by

$$c = \sum_{i=1}^{n} c_i \tag{a.2}$$

The mol fraction in the liquid x_i or the vapour y_i is defined by

$$y_i (\text{or } x_i) = \frac{c_i}{c} \tag{a.3}$$

A.2 Binary Systems

In a mixture of vapours the partial pressure, p_A, of component A is that pressure which would be exerted by A alone in a volume appropriate to the concentration of A in the mixture at the same temperature. Since $p = \sum p_A$, then for an ideal

mixture the partial pressure, p_A, is proportional to the mol fraction of A in the vapour phase:

$$p_A = y_A p \qquad\qquad (a.4)$$

Two laws relate the partial pressure in the vapour phase to the concentration of component A in the liquid phase.

(a) Henry's law which states that the partial pressure p_A is directly proportional to the mol fraction x_A of component A on the liquid phase.

$$p_A = \text{constant} * x_A \qquad\qquad (a.5)$$

This holds for dilute solutions only where x_A is small.

(b) Raoult's law which states that the partial pressure p_A is related to the mol fraction x_A and the vapour pressure of pure component A at the same temperature.

$$p_A = p_A^{\circ} x_A \qquad\qquad (a.6)$$

where p_A° is the vapour pressure of pure component A at the same temperature. This holds for high values of x_A only.

If a mixture follows Raoult's law it is said to be "ideal" and values of y can be calculated for various values of x from a knowledge of the vapour pressures of the two pure components at various temperatures.

Few mixtures behave in an "ideal" manner. If the ratio of the partial pressure p_A to the mol fraction in the liquid phase x_A is defined as the

'volatility', then for a binary mixture of components A and B,

volatility of $A = \dfrac{p_A}{x_A}$, volatility of $B = \dfrac{p_B}{x_B}$ (a.7)

The ratio of these two volatilities is known as the 'relative volatility', α, given by :

$$\alpha = \frac{p_A x_B}{p_B x_A}$$ (a.8)

Substituting Equation (a.6) for an 'ideal' mixture, the relative volatility is just the ratio of the vapour pressures of the pure components A and B at the chosen temperature. Values of α vary somewhat with temperature and tables for different binary systems are available in chemical engineering handbooks.

Consider a container initially filled with a binary liquid mixture having a mol fraction x_o of the more volatile component and held at constant pressure, p, and temperature, T_1 (Fig. A.1). What happens when the liquid mixture is heated at constant pressure can be shown conveniently on a temperature-composition diagram (Fig. A.1). In this diagram the mol fraction of the more volatile component in the liquid is plotted as the abscissa and the temperature at which the mixture boils as the ordinate.

The initial conditions in the container are denoted by point Q. The container is now heated at

constant pressure. When the temperature reaches T_2 the liquid will start to boil as shown by point R. Some vapour is formed of composition y_0 as shown by point S. This initial vapour is rich in the more volatile component. If the experiment is repeated for the complete range of values of x then a series of points such as R and S can be determined. The locus of points like R is a curve AXTRB which is known as the 'buble point' or 'boiling point' curve. The locus of points like S is a curve AWYSB which is known as the 'dew point' curve.

If the container is heated further the composition of the liquid will change, because of the loss of the more volatile component to the vapour. The boiling point will therefore rise tö some temperature T_3. Both the liquid and the vapour phases become richer in the less volatile component with the liquid having a composition represented by point T and the vapour having a composition represented by point V. Since no material is lost from the container, the proportion of liquid to vapour must be given by

$$\frac{L}{V} = \frac{UV}{TU} = \frac{y - x_0}{x_0 - x} \tag{a.9}$$

The ratio y/x at constant temperature is referred to as the equilibrium ratio, K.

$$K = y/x \tag{a.10}$$

Combining Equations (a.9) and (a.10):

$$x = \frac{x_o \left[\frac{L}{V} + 1\right]}{K + \frac{L}{V}}$$

(a.11)

On further heating to a temperature of T_4, all the liquid is vapourized to give a vapour of the same composition as the original liquid (point W). The last drop of liquid to disappear is very rich in the less volatile component (x_L) (point X).

In the design of evaporation equipment for liquid mixtures, thermodynamic equilibrium is usually assumed. However, clearly this must be an approximation since temperature and concentration differences must exist for evaporation to occur. Equilibrium is invariably assumed to exist at vapour-liquid interfaces, i.e., where the phases remain in intimate contact with one another. However, it is possible to conceive a situation where the vapour bubble formed rise to the surface and into a vapour space such that there is no longer any close contact with the liquid phase. Further evaporation of the liquid must occur with a heavier (less volatile) liquid than originally designed for. There will be a corresponding rise in the boiling point, the effective temperature driving force for evaporation will be reduced and the available surface area may become insufficient to accomplish the required duty. Such a separation of the vapour from the liquid may occur to some extent when evaporating

a mixture on the shell side of a kettle reboiler,
especially at low circulation rates. Alternatively,
it could also occur within tubes where there is
stratification or poor distribution of the flows.
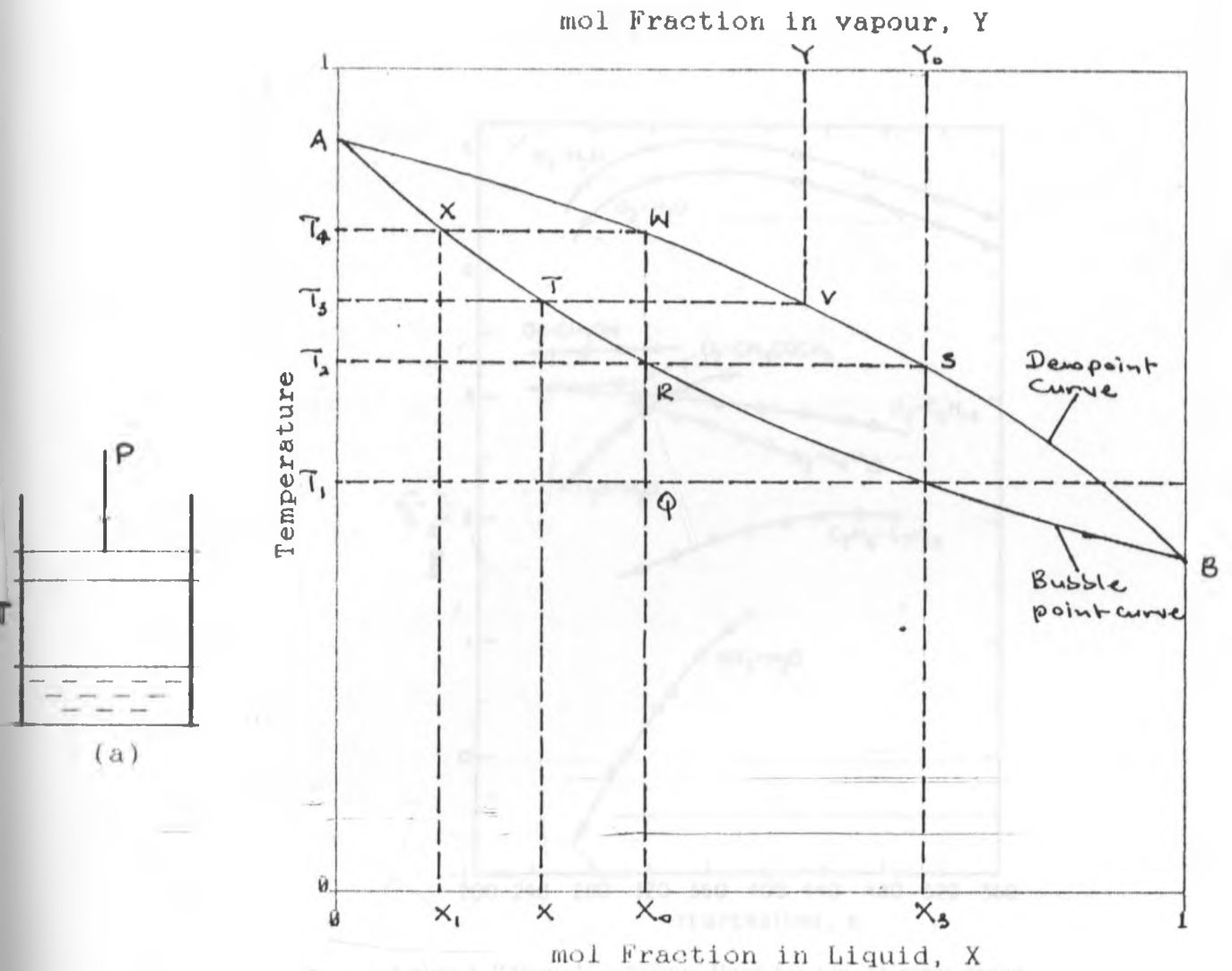
Figure A.1 Elementary phase equilibria
for binary systems.
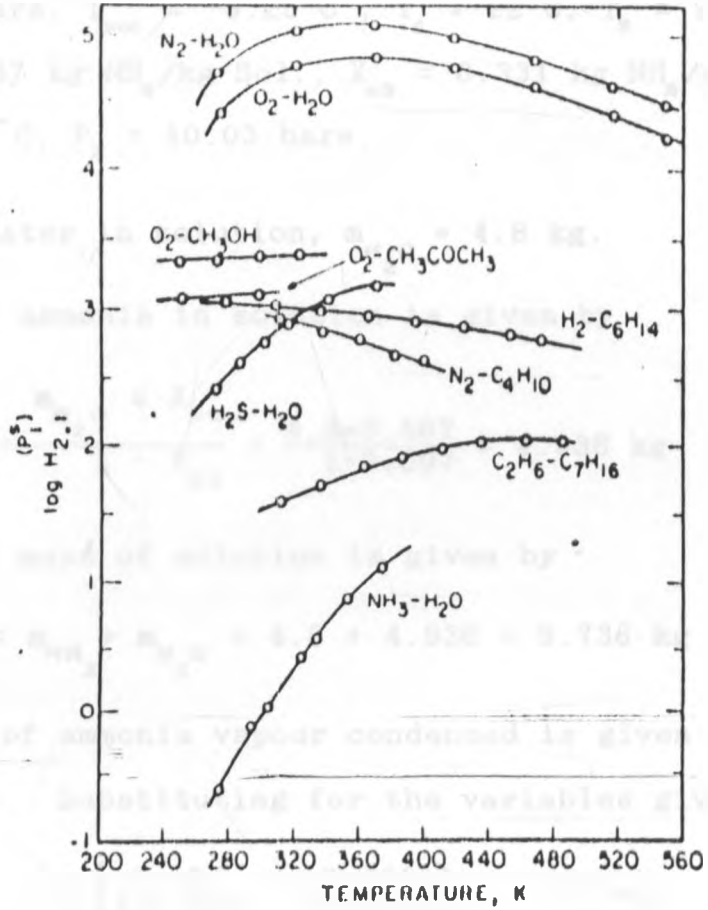
Figure A.2 Henry's constants (bar) for typical gases range over five orders of magnitude. The effect of temperature differs qualitatively from one system to another.

[From Prausnitz et al.]

APPENDIX B

COMPUTATION OF THE COOLING RATIO, η

Sample calculation of the cooling ratio, η is computed for data of Test no. 1.

Data:

P_{s1} = 3 bars, T_{sat} = -9.25°C , T_1 = 22°C, T_3 = 95.2°C

X_{s1} = 0.507 kg NH_3/kg Sol., X_{s3} = 0.331 kg NH_3/kg Sol.

T_2 = 64.4°C, P_2 = 10.03 bars.

Mass of water in solution, m_{H_2O} = 4.8 kg.

∴ Mass of ammonia in solution is given by

$$m_{NH_3} = \frac{m_{H_2O} \times X_{s1}}{1 - X_{s1}} = \frac{4.8 \times 0.507}{1 - 0.507} = 4.936 \text{ kg}$$

∴ Initial mass of solution is given by ·

$$m_{s1} = m_{NH_2} + m_{H_2O} = 4.8 + 4.936 = 9.736 \text{ kg}$$

The mass of ammonia vapour condensed is given by Eq. (5.5). Substituting for the variables gives

$$m_{vc} = 4.8 \left[\frac{0.507}{1 - 0.507} - \frac{0.331}{1 - 0.331} \right] = 2.56 \text{ kg}$$

The mass of NH_3 remaining, m_5', in the evaporator after a portion is flashed off during the refrigeration phase is given by Eq. (5.7).

The enthalpy h_5' of the liquid NH_3 at the evaporator temperature of -9.25°C corresponding to the saturation pressure of 3 bars is read from Appendix E as

h'_5 = 138.82 kJ/kg

The enthalpy h'_9 at the condenser temperature of 25°C corresponding to the generation pressure of 10.03 bars is also read from Appendix E as

h'_9 = 298.9 kJ/kg

— The average latent heat of evaporation is found (from Appendix E) to be

$$\bar{h}_{fg} = \frac{(1433.86-138.82) + (1465.85-298.9)}{2}$$

$$= 1230.995 \text{ kJ/kg}$$

$$\therefore m'_5 = 2.561 \text{ exp } \frac{138.82-298.9}{1230.995} = 2.249 \text{ kg}$$

The heat extracted in the evaporator is given by Eq. (5.12). Substituting

$$\therefore Q_c = 2.249(1433.86-138.82) = 291\overset{\bullet}{2}.5 \text{ kJ}$$

The solution enthalpy at the end of regeneration, h_9, is found from the NH_9-H_2O chart (Appendix F) at X_{s9} = 0.331 and T_9 = 95.2°C.

h_9 = 214 kJ/kg

$\therefore m_9 h_9$ = (9.736-2.561)×214 = 1535.45 kJ

Similarly at state 1,

h_1 = -150 kJ/kg

$\therefore m_1 h_1$ = 9.736× -150 = -1460.4 kJ

The term $\sum h_v \delta m_{vg}$ must now be evaluated (see Section 5.5). Using the Trapezoidal rule, the area

$\sum h_v \delta m_{vg}$ = 3926.07 kJ

The heat absorbed by the system is given by Eq.(5.14)

$$\therefore \ Q_g \ = \ 1535.45 - (-1460.4) + 3926.07 \ kJ$$

$$= \ 6921.9 \ kJ.$$

The cooling ratio is given by Eq.(5.16).

$$\therefore \ Q_c \ = \ \frac{2912.5}{6924.9} \ = \ 0.421$$

The overall efficiency, $(COP)_{system}$, is defined as

$$(COP)_{system} \ = \ \frac{Q_c}{I} \ = \ \frac{\text{Heat absorbed by refrigerant}}{\text{during refrigeration}} \ \frac{\text{during refrigeration}}{\text{Incident total insolation on the}} \\ \text{effective area of collector.}$$

$$= \ \frac{2912.5}{18305 \times 1.6 \times 0.9144} \ = \ 0.109$$

COMPUTER PROGRAM

A computer program has been developed to simulate the performance of an aqua-ammonia absorption refrigerator powered by two-cover flat-plate collector. The computations were based on the theories outlined in chapters three, four, five and six.

The program received the information about the material, the configuration and orientation of the collectors, the weather data, the initial solution mass and concentration, the operating pressure and the bubble point of solution. The output from the program predicted the hourly insolation on the sloped collector surface and the absorbed radiation by the collector. Next, using the absorbed hourly radiation, it computed the aqua-ammonia solution temperature, and the quantities of ammonia generated and condensed at the end of each hour.

The diurnal temperature variation was also calculated on an hourly basis by the program considering the minimum occuring at sunrise and the mximum two hours after noon. Straight line interpolation was used before the maximum and the same slope but negative in sense was used after the maximum until sunset.

```
      PROGRAM HTTRAP
C
C  HTTRAP SIMULATES THE PERFORMANCE OF AN INTERMITTENT
C  AQUA-AMMONIA ABSORPTION REFRIGERATOR POWERED BY A
C  TWO-COVER FLAT PLATE SOLAR COLLECTOR.
C
C  THIS PROGRAM WAS DEVELOPED BY B. A. ONASANYA,
C  MECHANICAL ENGINEERING DEPARTMENT, UNIVERSITY OF
C  NAIROBI.    JUNE, 1988.
C
C  HTTRAP CONSISTS OF ONE MAIN PROGRAM AND SEVEN SUBROUTINES:
C  SOLINSO, COVER, INTERHV, INTERXV, SIMINT, QUADEQ, AND X
C
C  VARIABLES USED ARE AS FOLLOWS:
C  AC: THE AZIMUTH ANGLE OF THE COLLECTOR (THE POINT
C       BEING DUE SOUTH, EAST NEGATIVE, AND WEST POSITIVE),
C       DEGREES.
C  ALPHAB: ABSORPTANCE OF THE ABSORBER PLATE, DECIMAL.
C  ALPHAC: AN ARRAY REPRESENTING ABSORPTANCE OF THE COVER
C          PLATE AT DIFFERENT HOURS OF THE DAY, DECIMAL.
C  EXTCOE: EXTINCTION COEFFICIENT OF THE COVER PLATE, 1/M
C  HBAR: DAILY TOTAL TERRESTRIAL RADIATION ON HORIZONTAL
C        SURFACES OF UNIT AREA, J/M**2-DAY.
C  N: NUMBER OF GLASS COVERS
C  NHR: NUMBER OF DAYTIME HOURS, ROUNDED TO THE NEAREST
C       WHOLE NUMBER.
C  NTHDAY: THE NTH DAY OF THE YEAR, JANUARY 1 BEING THE
C          FIRST DAY.
C  GREFL: THE REFLECTANCE OF THE SURFACE IN FRONT OF THE
C         COLLECTOR.
C  REFLD: DIFFUSE REFLECTANCE OF THE COVER PLATE, DECIMAL.
C  SC: THE SLOPE OF THE COLLECTOR SURFACE (HORIZONTAL
C      PLANE BEING ZERO), DEGREES.
C  SSHD: SUNSET HOUR ANGLE, DEGREES.
C  TAU: AN ARRAY REPRESENTING SHORTWAVE TRANSMITTANCE
C       OF THE COVER PLATE AT DIFFERENT HOURS OF THE
C       DAY, DECIMAL.
C  TEMP: AN ARRAY REPRESENTING TEMPERATURES AT DIFFERENT
C        HOURS OF THE DAY, DEGREE K
C  THIKC: THICKNESS OF THE COVER PLATES, M
C  TMAX: THE MAXIMUM TEMPERATURE OF THE DAY, DEGREE K
C  TMIN: THE MINIMUM TEMPERATURE OF THE DAY, DEGREE K
C  XLATD: LATITUDE (NORTH POSITIVE), DEGREES.
C  XIBAR: AN ARRAY REPRESENTING THE HOURLY TOTAL RADIATION
C         RECEIVED BY A TILTED COLLECTOR FOR EACH DAYTIME
C         HOUR, J/M**2-HOUR
C  XIDIFS: AN ARRAY REPRESENTING THE HOURLY DIFFUSE SKY
C          RADIATION RECEIVED BY A TILTED COLLECTOR FOR
C          EACH DAYTIME HOUR, J/M**2-HOUR
C  XIDIFG: AN ARRAY REPRESENTING THE HOURLY DIFFUSE GROUND
C          RADIATION RECEIVED BY A TILTED COLLECTOR FOR
C          EACH DAYTIME HOUR, J/M**2-HOUR
```

```
C  XIDIR : AN ARRAY REPRESENTING THE HOURLY DIRECT
C          RADIATION RECEIVED BY A TILTED COLLECTOR FOR
C          EACH DAYTIME HOUR, J/M**2-HOUR
C  XNR : INDEX OF REFRACTION
C
       COMMON /CB1/PI,N,XNR,EXTCOE,THIKC,TMIN,TMAX
       DIMENSION XIBAR(16),XIDIR(16),XIDIFS(16),XIDIFG(16),
     &   TAU(16),ALPHAC(16),XL2(16),TEMP(16),TSOL(16),E2(16)

       REAL M
       PI=3.1415926
       EPS=1.E-12
C
C  INPUT THE SIZE AND THE ORIENTATION OF THE COLLECTOR
C
       READ(*,*) WIDTH,XLNTH,DEPTH,XLATD,AC,SC
C
C  INPUT PHYSICAL PROPERTIES OF THE COVER PLATES
C
       READ(*,*) N,THIKC,EPSIC,XNR,EXTCOE
C
C  INPUT PHYSICAL PROPERTIES OF THE ABSORBER PLATE
C
       READ(*,*) ALPHAB,EPSIAB
C
C  INPUT DAILY AVERAGE DATA
C
       READ(*,*) NTHDAY,HBAR,GREFL,TMIN,TMAX  ·
C
C  INPUT SIMULATION DATA
C
       READ(*,*) P,F1,ACOL,UL,CAP,UAS,AM2,XIMAS,NO
       READ(*,*) BT,OC,XT
       WRITE(*,10)
   10 FORMAT(15X,'THE COLLECTOR :')
       WRITE(*,20) WIDTH,XLNTH,DEPTH,XLATD,AC,SC
   20 FORMAT(18X,'WIDTH:',F7.4,'M'/18X,'LENGTH:',F7.4,'M'/
     & 18X,'DEPTH :',F7.4,'M'/18X,'LATITUDE:',F7.3,'DEGREES'/
     & 18X,'AZIMUTH:',F7.2, 'DEGREES'/18X,'SLOPE:',F5.2,
     & 'DEGREES'//)
       WRITE(*,25) N,THIKC,EPSIC,XNR,EXTCOE
   25 FORMAT(15X,'MATERIALS USED :'/18X,'COVER :'/21X,
     & 'NO. OF COVERS:',I2/21X,'THICKNESS:',F7.4,'M'/21X,
     & 'EMITTANCE:',F6.3/21X,'INDEX OF REFRACTION:',F6.3/
     & 21X,'EXTINCTION COEFFICIENT:',F6.3//18X,'ABSORBER :')
       WRITE(*,30) ALPHAB,EPSIAB
   30 FORMAT(21X,'ABSORPTANCE:',F6.3/21X,'EMITTANCE:',F6.3)
       WRITE(*,35)
   35 FORMAT(/15X,'SIMULATION DATA :')
       WRITE(*,40)P,XIMAS,OC,BT,UL,F1,UAS,CAP,ACOL
   40 FORMAT(18X,'GENERATION PRESSURE =',F7.3,'BARS'/18X,
     & 'INITIAL SOLUTION MASS =',F7.3,'KG'/18X,
     & 'INITIAL SOLUTION CONC. =',F5.3,'KG/KG'/18X,
```

```
     & 'BUBBLE POINT OF SOLUTION =',F7.3,'DEG.C'/18X,
     & 'TOP LOSS COEFFICIENT =',F7.3,' W/M**2-K'/18X,
     & 'COLLECTOR EFFICIENCY FACTOR =',F6.3/18X,
     & 'STORAGE LOSS COEFFICIENT =',F7.3,' W/K'/18X,
     & 'COLLECTOR HEAT CAPACITY =',E10.4,'J/K'/18X,
     & 'EFFECTIVE COLLECTOR AREA =',F7.3,' M**2')
       WRITE(*,45) NTHDAY,HBAR,GREFL
   45 FORMAT(/18X,'DAY NO.=',I3/18X,'HORIZ. INSOL.=',
     & E14.8,'J/M**2-DAY'/18X,'GROUND REFL.=',F5.2//2X,
     & 'HOUR NO.',4X,'TEMP.',4X,'INSOLATION',4X,
     & 'ABSORBED RADIATION',4X,'EFFICIENCY')
       WRITE(*,50)
   50 FORMAT(14X,'DEG.C',5X,'J/M**2-HR',8X,'J/M**2-HR',
     & 10X,'PERCENT')
       CALL SOLINSO(XLATD,AC,SC,NTHDAY,HBAR,GREFL,SSHD,NHR,
     &              TEMP,XIBAR,XIDIR,XIDIFS,XIDIFG,TAU,ALPHAC)
       D=1.0472
       CALL COVER(N,XNR,EXTCOE,THIKC,D,TAUD,ALPHAD)
       REFLD=1.-TAUD-ALPHAD
C
C  CALCULATE THE EFFECTIVE INCIDENCE ANGLE FOR DIFFUSE
C  GROUND RADIATION
C
       DGEFD=90.-0.5788*SC+0.002693*SC**2
       DGEFR=0.0174532*DGEFD
       CALL COVER(N,XNR,EXTCOE,THIKC,DGEFR,TAUDG,ALPHDG)
C
C  CALCULATE THE EFFECTIVE INCIDENCE ANGLE FOR DIFFUSE
C  SKY RADIATION
C
       DSEFD=59.68-0.1388*SC+0.001497*SC**2
       DSEFR=0.0174532*DSEFD
       CALL COVER(N,XNR,EXTCOE,THIKC,DSEFR,TAUDS,ALPHDS)
       TOTXI=0.0
       TOTE2=0.0
       DO 100 I=1,NHR
       ALPHAE=ALPHAB/(1.-(1.-ALPHAB)*REFLD)
       E2(I)=XIDIR(I)*TAU(I)*ALPHAE+XIDIFS(I)*TAUDS*
     &       ALPHAE+XIDIFG(I)*TAUDG*ALPHAE
       HREFF=100.*E2(I)/XIBAR(I)
       TOTXI=TOTXI+XIBAR(I)
       TOTE2=TOTE2+E2(I)
       WRITE(*,70) I,TEMP(I),XIBAR(I),E2(I),HREFF
   70 FORMAT(I6,8X,F5.2,2X,E14.8,4X,E14.8,9X,F5.2)
  100 CONTINUE
       DAYEFF=100.*TOTE2/TOTXI
       WRITE(*,80) TOTXI,DAYEFF
   80  FORMAT(/5X,'TOTAL SOLAR RADIATION INCIDENT ON',
     & 'THE COLLECTOR = ',E14.8,' J'/5X,'TOTAL DAILY',
     & 'EFFICIENCY = ',F5.2,' PERCENT')
       WRITE(*,85)
   85 FORMAT(//2X,'HOUR NO.',1X,'AMBIENT',1X,'SOLUTION',
     & 2X,'FINAL',3X,'VAP. MASS',2X,'INITIAL',2X,'FINAL'/
```

```fortran
     & 12X,'TEMP.',4X,'TEMP.',3X,'MASS',4X,'CONDENSED',
     & 3X,'CONC.',3X,'CONC.')
       DO 110 I=1,NHR
       IF(TEMP(I).EQ.TEMP(1))THEN
         TSOL(I)=TEMP(I)+E2(I)*(1.-EXP(-UL*3600./CAP))
     &           /(UL*3600.)
       ELSEIF(TEMP(I).NE.TEMP(1).AND.(TSOL(I-1)+XT)
     &         .LT.BT)THEN
           TSOL(I)=TEMP(1)+E2(I)/(3600.*UL)-(E2(I)/
     &             (3600.*UL)-TSOL(I-1)+TEMP(I))*
     &             EXP(-UL*3600./CAP)
         ELSE
           TSOL(I)=TSOL(I-1)+5.*(I)+10.
           FRI=1.-I*.05
           IF(I.EQ.3)THEN
             XL2(I)=OC
           ELSE -
             XL2(I)=X(TSOL(I-1))
           ENDIF
           DO 130 J = 1,50
             TS=TSOL(I)
             IF(TS.GE.100) GOTO 140
             XL3= X(TS)
             SHS= 710.*(XL2(I)+XL3)/2.+4180.
             IF(XL2(1).LT..2.OR.XL2(I).GT..7.OR.XL3.LE..2
     &          .OR.XL3.GT..7) GOTO 150
             CALL INTERXV(P,NO,AM2,XL2(I),XL3,TMVC,TMVG,
     &                    SUM,AM4)
             TS=TSOL(I-1)+(ACOL*FRI*(E2(I)-UL*3600.*
     &          (TSOL(I-1)-TEMP(I)))-UAS*(TSOL(I-1)-
     &          TEMP(I))-SUM)/(AM2*SHS)
             M =-UL*F1*ACOL/(SHS*ALOG(1.-(UL*(TS-TSOL(I-1))
     &          /(E2(I)/3600.-UL*(TSOL(I-1)-TEMP(I))))))
             FR=M*SHS*(1.-EXP(-ACOL*UL*F1/(M*SHS)))/
     &          (ACOL*UL)
             TSOL(I)=TS
             IF((FRI-FR).LE..001)GOTO 120
             FRN=(FRI+FR)/2.
             FRI=FRN
130          CONTINUE
120 AM2=AM4
     ENDIF
     WRITE(*,90)I,TEMP(I),TSOL(I),AM2,TMVC,XL2(I),XL3
 90 FORMAT(I5,7X,F5.2,2X,F6.2,3X,F7.4,2X,F7.4,5X,F5.3,
     &        3X,F5.3)
110 CONTINUE
150 WRITE(*,105)I,XL2(I),XL3
105 FORMAT(/2X,'I =',I3,2X,'XL2 =',F5.3,2X,'XL3 =',F5.3
     &        /2X,'DATA OUTSIDE RANGE')
140 WRITE(*,104)I,TSOL(I),XL2(I),XL3
104 FORMAT(/2X,'I =',I3,2X,'TSOL =',F6.2,2X,'XL2 =',
     &        F5.3,2X,'XL3 =',F5.3/2X,'OUTSIDE RANGE')
     CALL INTERXV(P,NO,XIMAS,XL2(3),XL2(I),TMVC,TMVG,SUM,AM4)
```

```
      WRITE(*,115)XIMAS,TMVG,TMVC,AM4
  115 FORMAT(//2X,'INITIAL SOLUTION MASS =',F7.4/2X,
     & 'MASS OF NH3 VAPOUR GENERATED =',F7.4/2X,
     & 'MASS OF NH3 VAPOR CONDENSED =',F7.4/2X,
     & 'FINAL SOLUTION MASS =',F7.4/)
C
C COEFFICIENT OF THE QUQDRATIC EQUATION ARE GIVEN BY :
C
      A=2.58312E-05
      B=-(2.29649E-03 + AM4/TMVC*7.804E-03)
      C=4.72437E-02 -AM4/TMVC*(5.5847E-01 - XL2(I))
C
C USE OF THE SUBROUTINE QUADEQ
C
      CALL QUADEQ(A,B,C,EPS,R1,R2,INDIC)
      GOTO(12,13,14,15,16)INDIC
      WRITE(*,66)
   66 FORMAT(' THE VALUE OF INDIC DOES NOT LIE BETWEEN
     &        1 AND 5')
      STOP
   12 ROOT1=R1+SIGN(R2,R1)
      ROOT2=C/(A*ROOT1)
      WRITE(*,71)A,B,C,ROOT1,ROOT2
      GOTO 99
   13 WRITE(*,72)A,B,C,R1,R2,R1,R2
      GOTO 16
   14 WRITE(*,73)A,B,C,R1
      GOTO 16
   15 WRITE(*,74)A,B,C
      GOTO 16
   16 STOP
   71 FORMAT('  THE COEFFICIENTS ARE :'/'  A =',E12.6,2X,
     & 'B =',E12.6,2X,'C =',E12.6/'  THE ROOTS OF THE',
     & ' EQUATION ARE :'/'  T5 =',F8.3,' AND ',F8.3)
   72 FORMAT(2X,3(1X,E12.6),4X,F7.3,'+',F7.3,'*I AND'
     &        ,F7.3,'-',F7.3,'*I : COMPLEX ROOTS')
   73 FORMAT(2X,3(1X,E12.6),6X,'INVALID')
   74 FORMAT(2X,3(1X,E12.6),6X,F7.3)
   99 XL5=0.007804*ROOT2+0.55847
      AMFL=AM4*(XL5-XL2(I))/(1.-XL5)
      WRITE(*,75)XL5,AMFL
   75 FORMAT(/2X,'SOLUTION CONC. AT STATE 5 =',F6.4,
     & ' KgNH3/KgSOL'/2X,'MASS OF NH3 FLASHED =',F7.4)
      STOP
      END


      SUBROUTINE SOLINSO(XLATD,AC,SC,NTHDAY,HBAR,GREFL,
     & SSHD,NHR,TEMP,XIBAR,XIDIR,XIDIFS,XIDIFG,TAU,ALPHAC)
C
C  SOLINSO RETURNS HOURLY SOLAR INSOLATION VALUES
C  (TOTAL,DIRECT,AND DIFFUSED) ON A FLAT PLATE COLLECTOR,
C  TRANSMITTANCE AND ABSORPTANCE OF THE GLASS COVERS,AND
```

```
C   AMBIENT TEMPERATURE FOR EACH HOUR DURING THE DAYTIME
C   ON THE NTH DAY OF THE YEAR.
C
C   INPUT----
C   AC: THE AZIMUTH ANGLE OF THE COLLECTOR (THE POINT BEING
C       DUE SOUTH, EAST NEGATIVE, AND WEST POSITIVE),DEGREES.
C   HBAR: DAILY TOTAL TERRESTRIAL RADIATION ON HORIZONTAL
C         SURFACES OF UNIT AREA, J/M**2-DAY.
C   NTHDAY: THE NTH DAY OF THE YEAR, JANUARY 1 BEING THE
C           FIRST DAY.
C   GREFL: THE REFLECTANCE OF THE SURFACE IN FRONT OF
C          THE COLLECTOR.
C   XLATD: LATITUDE (NORTH POSITIVE), DEGREES.
C
C   RETURNED----
C   ALPHAC: AN ARRAY REPRESENTINTING ABSORPTANCE OF THE
C           COVER PLATE AT DIFFERENT HOURS OF THE DAY.
C   SSHD: SUNSET HOUR ANGLE, DEGREES.
C   NHR:  NUMBER OF DAYTIME HOURS, ROUNDED TO THE
C         NEAREST WHOLE NUMBER.
C   TAU: AN ARRAY REPRESENTING SHORTWAVE TRANSMITTANCE
C        OF THE COVER PLATE AT DIFFERENT HOURS OF THE DAY.
C   TEMP: AN ARRAY REPRESENTING TEMPERATURES AT DIFFERENT
C         HOURS OF THE DAY, DEGREE K
C   XIBAR: AN ARRAY REPRESENTING THE HOURLY TOTAL RADIATION
C          RECEIVED BY A TILTED COLLECTOR FOR EACH DAYTIME
C          HOUR, J/M**2-HOUR
C   XIDIFS: AN ARRAY REPRESENTING THE HOURLY DIFFUSE SKY
C           RADIATION RECEIVED BY A TILTED COLLECTOR FOR
C           EACH DAYTIME HOUR, J/M**2-HOUR
C   XIDIFG: AN ARRAY REPRESENTING THE HOURLY DIFFUSE
C           GROUND RADIATION RECEIVED BY A TILTED COLLECTOR
C           FOR EACH DAYTIME HOUR, J/M**2-HOUR
C   XIDIR: AN ARRAY REPRESENTING THE HOURLY DIRECT RADIATION
C          RECEIVED BY A TILTED COLLECTOR FOR EACH DAYTIME
C          HOUR, J/M**2-HOUR
C
      COMMON /CB1/PI,N,XNR,EXTCOE,THIKC,TMIN,TMAX
      DIMENSION XIBAR(16),XIDIR(16),XIDIFS(16),XIDIFG(16),TAU(16),
     &          ALPHAC(16),TEMP(16)
C
C   SOLAR CONSTANT, XISC, IS 1353 W/M**2
C
      XISC=1353.
      DO 5 I=1,16
         XIBAR(I)= 0.
    5 CONTINUE
      ARGM=4.888834+0.0172142*NTHDAY
C
C   CALCULATE THE DECLINATION OF THE SUN IN DEGREES.
C
      DECLN=23.45*SIN(ARGM)
C
```

```fortran
C   CONVERT DEGREES TO RADIANS
C
      ACR=0.0174532*AC
      SCR=0.0174532*SC
      XLATDR=0.0174532*XLATD
      DECLNR=0.0174532*DECLN
C
C   CALCULATE THE SUNSET HOUR ANGLE IN RADIANS.
C
      SSHR=ACOS(-TAN(XLATDR)*TAN(DECLNR))
      SSHD=57.29578*SSHR
C
C   CALCULATE THE DAILY TOTAL EXTRATERRESTRIAL RADIATION
C   INCIDENT UPON A HORIZONTAL SURFACE OF UNIT AREA IN
C   J/M**2-DAY.
C
      HO=(86400.*XISC/PI)*(1.+0.033*COS(0.0172142*NTHDAY))*
     & (COS(XLATDR)*COS(DECLNR)*SIN(SSHR)+SSHR*SIN(XLATDR)*
     & SIN(DECLNR))
      XKT=HBAR/HO
      IF(XKT.LE.0.17)THEN
        XKD=0.99
        ELSEIF(0.17.LT.XKT.AND.XKT.LT.0.75)THEN
          XKD=1.188-2.272*XKT+9.473*XKT**2-21.865*XKT**3
     &        +14.648*XKT**4
          ELSEIF(0.75.LT.XKT.AND.XKT.LT.0.8)THEN
            XKD=-0.54*XKT+0.632
              ELSE
                XKD=0.2
      ENDIF
      HDBAR=XKD*HBAR
      C1=(1.+COS(SCR))*HDBAR/2.
      C2=(1.-COS(SCR))*GREFL*HBAR/2.
      NHR=2.*SSHD/15.+0.5
      ND2=NHR/2.+0.5
      HR1=NHR/2.-0.5
      HR2=NHR/2.+2.
      S=(TMAX-TMIN)/HR2
      DO 18 I=1,NHR
        TIME=1-0.5
        IF(TIME.GE.HR2)GOTO 19
        TEMP(I)=TMIN+S*TIME
        GOTO 18
   19 TEMP(I)=TMAX-S*(TIME-HR2)
   18    CONTINUE
      COSZS1=SIN(DECLNR)*SIN(XLATDR)
      COSZS2=COS(DECLNR)*COS(XLATDR)
      COSSC1=COSZS1*COS(SCR)-SIN(SCR)*COS(ACR)*
     &      SIN(DECLNR)*COS(XLATDR)
      COSSC2=COSZS2*COS(SCR)+SIN(SCR)*COS(DECLNR)*
     &      COS(ACR)*SIN(XLATDR)
      COSSC3=COS(DECLNR)*SIN(SCR)*SIN(ACR)
C
```

```
C     CALCULATE THE XIBAR'S
C
      DO 10 I=1,ND2
         HR=HR1-I+1.
C
C     CALCULATE THE RATIOS OF THE HOURLY TOTAL RADIATION TO
C     THE DAILY RADIATION, RT, AND THE HOURLY DIFFUSE
C     RADIATION TO THE DAILY RADIATION, RD, ON A HORIZONTAL
C     SURFACE:
C
         H=-HR*15.*0.0174532
         A=0.409+0.5016*SIN(SSHR-0.0174532*60.)
         B=0.6609-0.4767*SIN(SSHR-0.0174532*60.)
         RT=PI/24.*(A+B*COS(H))*(COS(H)-COS(SSHR))/
     &       (SIN(SSHR)-SSHR*COS(SSHR))
         RD=PI/24.*(COS(H)-COS(SSHR))/(SIN(SSHR)
     &       -SSHR*COS(SSHR))
         IF(RT.LT.0.) RT=0.
         IF(RD.LT.0.) RD=0.
         COSZS=COSZS1+COSZS2*COS(H)
         IF(COSZS.LE.0.)THEN
            XIBAR(I)=0.
            XIDIR(I)=0.
            XIDIFS(I)=0.
            XIDIFG(I)=0.
            TAU(I)=0.
            ALPHAC(I)=0.
            GOTO 8
         ENDIF
         COSSC=COSSC1+COSSC2*COS(H)+COSSC3*SIN(H)
         AINCDR=ACOS(COSSC)
         CALL COVER(N,XNR,EXTCOE,THIKC,AINCDR,TAU(I),
     &              ALPHAC(I))
         BETA=COSSC/COSZS
         IF(COSSC.LT.0..OR.RT*HBAR.LT.RD*HDBAR) BETA=0.
         IF(RT*HBAR.LT.RD*HDBAR) RD=RT*HBAR/HDBAR
         XIDIR(I)=(RT*HBAR-RD*HDBAR)*BETA
         XIDIFS(I)=C1*RD
         XIDIFG(I)=C2*RT
         XIBAR(I)=XIDIR(I)+XIDIFS(I)+XIDIFG(I)
    8    IF(ABS(HR-0.).LE.0.)GOTO 10
         K=NHR-I+1
         IF(COSZS.LE.0.)GOTO 9
         COSSC=COSSC1+COSSC2*COS(-H)+COSSC3*SIN(-H)
         AINCDR=ACOS(COSSC)
         CALL COVER(N,XNR,EXTCOE,THIKC,AINCDR,TAU(K),
     &              ALPHAC(K))
         BETA=COSSC/COSZS
         IF(COSSC.LT.0..OR.RT*HBAR.LT.RD*HDBAR) BETA=0.
         IF(RT*HBAR.LT.RD*HDBAR) RD=RT*HBAR/HDBAR
         XIDIR(K)=(RT*HBAR-RD*HDBAR)*BETA
         XIDIFS(K)=C1*RD
         XIDIFG(K)=C2*RT
```

```
          XIBAR(K)=XIDIR(K)+XIDIFS(K)+XIDIFG(K)
          GOTO 10
   9      XIBAR(K)=0.
          XIDIR(K)=0.
          XIDIFS(K)=0.
          XIDIFG(K)=0.
          TAU(K)=0.
          ALPHAC(K)=0.
  10  CONTINUE
      RETURN
      END



      SUBROUTINE COVER(N,XNR,EXTCOE,THIKC,AINCDR,TAU,
     &                 ALPHAC)
C
C COVER RETURNS THE SHORTWAVE TRANSMITTANCE AND THE
C ABSORPTANCE OF A SYSTEM OF TWO COVER PLATES.
C VARIABLES ARE USED AS FOLLOWS:
C
C INPUT----
C EXTCOE:   EXTINCTION COEFFICIENT, 1/M
C ANICDR:   ANGLE OF INCIDENCE, RADIANS.
C THIKC:    THE THICKNESS OF THE COVER PLATES, METERS.
C XNR:      INDEX OF REFRACTION
C
C RETURNED----
C ALPHAC:   THE ABSORPTANCE OF THE COVER PLATES, DECIMAL
C TAU:      THE SHORTWAVE TRANSMITTANCE OF THE COVER
C           PLATES, DECIMAL
C
      IF(AINCDR.GE.1.57) GOTO 50
      IF(ABS(AINCDR-0.).GT.0.001) GOTO 10
      THETAR=0.
C
C FRESNEL'S LAW
C
      REFLV=((XNR-1.)/(XNR+1.))**2
      REFLP=REFLV
      GOTO 15
C
C SNELL'S LAW
C
  10  THETAR=ASIN(SIN(AINCDR)/XNR)
C
C FRESNEL'S LAW
C
      REFLV=(SIN(AINCDR-THETAR)/SIN(AINCDR+THETAR))**2
      REFLP=(TAN(AINCDR-THETAR)/TAN(AINCDR+THETAR))**2
  15  XXL=N*THIKC/COS(THETAR)
C
C BOUGER'S LAW
C
```

```fortran
      TAUPRM=EXP(-EXTCOE*XXL)
      TAU1=(1.-REFLV)/(1.+(2.*N-1.)*REFLV)
      TAU2=(1.-REFLP)/(1.+(2.*N-1.)*REFLP)
      TAUM=0.5*(TAU1+TAU2)
      TAU=TAUPRM*TAUM
      REFL=TAUPRM-TAU
      GOTO 60
   50 REFL=1.0
      TAU=0.
   60 ALPHAC=1-REFL-TAU
      RETURN
      END


      SUBROUTINE INTERHV(P,XL,HV)
C
C PROGRAM FOR LINEAR INTERPOLATION OF ENTHALPY-
C CONCENTRATION TABLES FOR AMMONIA-WATER SOLUTION
C
      DIMENSION HVDATA(30,5),PDATA(5),XLDATA(30),XL(0:30),
     &            HV(0:30)
      OPEN(5,FILE='HDATA',STATUS='OLD')
C
C INPUT DATA FROM TABLES.
C
      READ(5,*)NPRESS,NSCONC
      IF(NPRESS.GE.1.AND.NPRESS.LE.5.AND.NSCONC.GE.1.AND.
     &   NSCONC.LE.30) GOTO 1
      WRITE(*,30)NPRESS,NSCONC
   30 FORMAT(2I3,' STOP-DATA EXCEEDS DIMENSIONS')
    1 READ(5,*,ERR=55)(PDATA(J),J=1,NPRESS),(XLDATA(I),
     &               I=1,NSCONC)
   55 READ(5,*,ERR=65)((HVDATA(I,J),I=1,NSCONC),J=1,NPRESS)
      CLOSE(5)
   65 IF(P.GE.PDATA(1).AND.P.LE.PDATA(NPRESS).AND.XL(K)
     &   .GE.XLDATA(1).AND.XL(K).LE.XLDATA(NSCONC))GOTO 4
      WRITE(*,80)P,XL
   80 FORMAT(2F10.4,1X,'OUTSIDE DATA RANGE')
C
C LOCATE POSITION IN TABLE
C
    4 NPM=NPRESS-1
      DO 5 J=1,NPM
      DELP=(P-PDATA(J))/(PDATA(J+1)-PDATA(J))
      IF(DELP.GE.0..AND.DELP.LT.1.) GOTO 6
    5 CONTINUE
      J=NPRESS
    6 NXM=NSCONC-1
      DO 7 I=1,NXM
      DELX=(XL(K)-XLDATA(I))/(XLDATA(I+1)-XLDATA(I))
      IF(DELX.GE.0..AND.DELX.LT.1.) GOTO 8
    7 CONTINUE
      I=NSCONC
```

```
C INTERPOLATE
C
    8 HV(K)=HVDATA(I,J)
      IF(J.NE.NPRESS) HV(K)=HV(K)+DELP*
     &                          (HVDATA(I,J+1)-HVDATA(I,J))
      IF(I.NE.NSCONC) HV(K)=HV(K)+DELX*
     &                          (HVDATA(I+1,J)-HVDATA(I,J))
    9 CONTINUE
      RETURN
      END


      SUBROUTINE INTERXV(P,M,AM2,XL2,XL3,TMVC,TMVG,SUM,AM4)
C
C PROGRAM FOR LINEAR INTERPOLATION OF ENTHALPY-CONCENTRATION
C TABLES FOR AMMONIA-WATER SOLUTION
C
      DIMENSION XVDATA(30,5),PDATA(5),XLDATA(30),XL(0:30),
     &          XV(0:30),HV(0:30),AMVG(30),AMVC(30)
      OPEN(5,FILE='PDATA',STATUS='OLD')
C
C INPUT DATA FROM TABLES.
C
      READ(5,*)NPRESS,NSCONC
      IF(NPRESS.GE.1.AND.NPRESS.LE.5.AND.NSCONC.GE.1.AND.
     &   NSCONC.LE.30)GOTO 1
      WRITE(*,30)NPRESS,NSCONC
   30 FORMAT(2I3,' STOP-DATA EXCEEDS DIMENSIONS')
    1 READ(5,*,ERR=55)(PDATA(J),J=1,NPRESS),(XLDATA(I),
     &                   I=1,NSCONC)
   55 READ(5,*,ERR=65)((XVDATA(I,J),I=1,NSCONC),J=1,NPRESS)
      CLOSE(5)
   65 SUM=0
      TMVG=0
      TMVC=0
      DO 9 K=0,M
      H=(XL2-XL3)/M
      XL(K)=XL2-H*K
      IF(K.EQ.0) GOTO 9
      IF(P.GE.PDATA(1).AND.P.LE.PDATA(NPRESS).AND.XL(K)
     &   .GE.XLDATA(1).AND.XL(K).LE.XLDATA(NSCONC))GOTO 4
      WRITE(*,80)P,XL(K)
   80 FORMAT(2F10.4,1X,'OUTSIDE DATA RANGE')
C
C LOCATE POSITION IN TABLE
C
    4 NPM=NPRESS-1
      DO 5 J=1,NPM
      DELP=(P-PDATA(J))/(PDATA(J+1)-PDATA(J))
      IF(DELP.GE.0..AND.DELP.LT.1.) GOTO 6
    5 CONTINUE
      J=NPRESS
    6 NXM=NSCONC-1
```

```
      DO 7 I=1,NXM
      DELX=(XL(K)-XLDATA(I))/(XLDATA(I+1)-XLDATA(I))
      IF(DELX.GE.0..AND.DELX.LT.1.) GOTO 8
    7 CONTINUE
      I=NSCONC
C
C INTERPOLATE
C
    8 XV(K)=XVDATA(I,J)
      IF(J.NE.NPRESS) XV(K)=XV(K)+DELP*
     &                      (XVDATA(I,J+1)-XVDATA(I,J))
      IF(I.NE.NSCONC) XV(K)=XV(K)+DELX*(
     &                      XVDATA(I+1,J)-XVDATA(I,J))
      AMVC(K)=AM2*(1-XL(0))*(XL(K-1)/(1-XL(K-1))-
     &        XL(K)/(1-XL(K)))
      AMVG(K)=AMVC(K)*(1-XL(K))/(XV(K)-XL(K))
      CALL INTERHV(P,XL(K),HV(K))
      CALL INTERHV(P,XL(K-1),HV(K-1))
      AREA=(HV(K)+HV(K-1))/2.*AMVG(K)
      TMVC=TMVC+AMVC(K)
      TMVG=TMVG+AMVG(K)
      SUM=SUM+AREA
    9 CONTINUE
      AM4=AM2-TMVC
      RETURN
      END


      SUBROUTINE QUADEQ(A,B,C,EPS,R1,R2,INDIC)
C
C SUBROUTINE PROGRAM FOR SOLVING QUADRATIC EQUATIONS
C
      IF(ABS(A).GT.EPS)THEN
C
C GENUINE QUADRATIC EQUATION
C
          DISCR=B**2-4.*A*C
          TWOA=2.*A
          R1=-B/TWOA
          IF(DISCR.GT.0.)THEN
C
C REAL ROOTS
C
              R2=SQRT(DISCR)/TWOA
              INDIC=1
          ELSE
C
C COMPLEX ROOTS
C
              R2=SQRT(-DISCR)/TWOA
              INDIC=2
          ENDIF
      ELSEIF(ABS(B).GT.EPS)THEN
```

```
C
C LINEAR EQUATION WITH ONE ROOT
C
        R1=-C/B
        INDIC=3
      ELSEIF(ABS(C).GT.EPS)THEN
C
C INCONSISTENT LINEAR EQUATION
C
        INDIC=4
      ELSE
C
C ALL COEFFICIENTS ZERO
C
        INDIC=5
      ENDIF
      RETURN
      END


      FUNCTION X(T)
C
C  FUNCTION SUBPROGRAM FOR COMPUTING THE CONCENTRATION, X,
C  AS A FUNCTION OF TEMPERATURE, T.
C
      A=308.36088**2-4.*159.75816*(175.89316-T)
      IF(A.LT.O.) STOP'A IS NEGATIVE'
      X=(308.36088-SQRT(A))/(2.*159.75816)
      RETURN
      END
```

```
THE COLLECTOR :
    WIDTH: 1.0824M
    LENGTH: 1.8000M
    DEPTH : 0.9000M
    LATITUDE: -1.300DEGREES
    AZIMUTH: 180.00DEGREES
    SLOPE: 5.00DEGREES


MATERIALS USED :
    COVER :
        NO. OF COVERS: 2
        THICKNESS: 0.0025M
        EMITTANCE: 0.880
        INDEX OF REFRACTION: 1.526
        EXTINCTION COEFFICIENT:12.000

    ABSORBER :
        ABSORPTANCE: 0.900
        EMITTANCE: 0.900

SIMULATION DATA :
    GENERATION PRESSURE =  9.722BARS
    INITIAL SOLUTION MASS = 12.000KG
    INITIAL SOLUTION CONC. = 0.600KG/KG
    BUBBLE POINT OF SOLUTION = 51.000DEG.C
    TOP LOSS COEFFICIENT =  4.650 W/M**2-K
    COLLECTOR EFFICIENCY FACTOR = 0.970
    STORAGE LOSS COEFFICIENT = ·3.600 W/K
    COLLECTOR HEAT CAPACITY =0.1466E+05J/K
    EFFECTIVE COLLECTOR AREA =   1.463 M**2

    DAY NO.= 47
    HORIZ. INSOL.=0.23902060E+08J/M**2-DAY
    GROUND REFL.= 0.15
```

HOUR NO.	TEMP. DEG.C	INSOLATION J/M**2-HR	ABSORBED RADIATION J/M**2-HR	EFFICIENCY PERCENT
1	17.41	0.27814694E+06	0.11599387E+06	41.70
2	19.04	0.95908881E+06	0.56264025E+06	58.66
3	20.66	0.17104361E+07	0.11513191E+07	67.31
4	22.29	0.24226517E+07	0.16914831E+07	69.82
5	23.91	0.29798405E+07	0.21036135E+07	70.59
6	25.54	0.32856967E+07	0.23273505E+07	70.83
7	27.16	0.32856977E+07	0.23273512E+07	70.83
8	28.79	0.29798427E+07	0.21036152E+07	70.59
9	28.79	0.24226552E+07	0.16914861E+07	69.82
10	27.16	0.17104404E+07	0.11513229E+07	67.31
11	25.54	0.95909287E+06	0.56264400E+06	58.66
12	23.91	0.27815034E+06	0.11599504E+06	41.70

```
TOTAL SOLAR RADIATION INCIDENT ON THE COLLECTOR = 0.23271740E+08 J
TOTAL DAILY EFFICIENCY = 68.34 PERCENT
```

HOUR NO.	AMBIENT TEMP.	SOLUTION TEMP.	FINAL MASS	VAP. MASS CONDENSED	INITIAL CONC.	FINAL CONC.
1	17.41	22.13	12.0000	0.0000	0.000	0.000
2	19.04	42.91	12.0000	0.0000	0.000	0.000
3	20.66	59.21	9.9298	2.0702	0.600	0.517
4	22.29	85.65	7.4920	2.4378	0.517	0.359

I = 5 TSOL =120.65 XL2 =0.360 XL3 =0.359
OUTSIDE RANGE

INITIAL SOLUTION MASS =12.0000
MASS OF NH3 VAPOUR GENERATED = 4.6466
MASS OF NH3 VAPOR CONDENSED = 4.5038
FINAL SOLUTION MASS = 7.4962

THE COEFFICIENTS ARE :
A =0.258312E-04 B =-.152858E-01 C =-.283632E+00
THE ROOTS OF THE EQUATION ARE :
T5 = 609.765 AND -18.007

SOLUTION CONC. AT STATE 5 =0.4179 KgNH3/KgSOL
MASS OF NH3 FLASHED = 0.7503

STATION NAME _____ NAIROBI (D. CORNER).
LATITUDE _01°_ 18'S _____ LONGITUDE _36°_ 45'E

STATION NUMBER _____ 91.36/164
ALTITUDE _5900_ FEET _1798_ METRES

MONTH	ATMOSPHERIC PRESSURE (1955 - 80)		TEMPERATURE (1955 - 80)									RELATIVE HUMIDITY			RAINFALL (1954 - 80)			
			MEANS			EXTREMES		DRY BULB		DEW POINT								
	0600 GMT	1200 GMT	MAX.	MIN.	RANGE	HIGHEST	LOWEST	0600 GMT	1200 GMT	0600 GMT	1200 GMT	0600 GMT	0900 GMT	1200 GMT	MEAN	HIGHEST	LOWEST	MAX 24 HOUR FALL
	mb	mb	°C	°C	°C	°C	°C	°C	°C	°C	°C	%	%	%	mm	mm	mm	mm
January	823.0	819.4	24.5	11.5	13.0	29.7	3.3	17.2	23.7	12.8	11.2	93	76	46	73	253	0	77.0
February	822.5	819.2	25.6	11.6	14.0	29.7	4.7	17.7	24.7	12.8	10.5	91	74	42	60	201	2	104.6
March	822.6	819.3	25.6	13.1	12.5	30.6	6.7	17.4	24.7	14.0	11.3	94	80	44	93	299	15	98.0
April	822.7	819.7	24.1	14.0	10.1	26.8	7.8	17.0	23.0	14.7	13.4	95	86	36	211	499	20	139.1
May	823.9	821.1	22.6	13.2	9.4	27.1	7.2	16.2	21.5	13.9	13.6	96	88	61	195	478	50	97.6
June	824.5	822.1	21.5	11.0	10.5	26.8	4.4	14.6	20.6	12.2	12.1	94	86	59	37	141	2	85.5
July	824.7	822.4	20.6	10.1	10.5	25.8	2.5	13.5	19.6	11.3	11.4	93	87	59	19	85	1	46.7
August	824.5	821.9	21.4	10.2	11.2	27.9	2.9	13.7	20.3	11.3	11.0	93	85	56	25	67	1	53.7
September	824.2	821.1	23.7	10.5	13.2	29.1	3.9	14.8	22.7	11.8	10.5	94	84	47	35	138	2	54.4
October	825.9	820.3	24.7	12.5	12.2	28.3	5.0	16.4	23.7	12.9	10.7	94	80	44	52	196	9	56.3
November	823.3	820.0	23.1	13.1	10.0	27.8	6.7	15.3	22.0	13.9	12.7	94	86	56	157	623	41	83.0
December	822.9	819.7	23.4	12.6	10.8	27.4	5.3	15.9	22.6	13.4	12.2	95	90	53	92	379	8	112.3
Year	823.5	820.5	23.4	11.9	11.5	30.6	2.5	15.9	22.4	12.9	11.7	94	83	50	1049	1632	653	139.1

MONTH	NUMBER OF DAYS OF		DAILY SUNSHINE (1955 - 80)			DAILY RADIATION (1957 - 79) INSTRUMENT 'E'			MONTHLY EVAPORATION (1964 - 80) PAN TYPE 'A'			CLOUD AMOUNT (1955 - 80)				DAILY WIND RUN 1964-80	WIND SPEED 1955-50		CALMS 1966-80		VISIBILITY (1961-80)			
												TOTAL		LOW							FOG		MIST, HAZE	
	RAIN	THUNDER	MEAN	MAX MEAN	MIN MEAN	MEAN	MAX MEAN	MIN MEAN	MEAN	HIGHEST	LOWEST	0600 GMT	1200 GMT	0600 GMT	1200 GMT	1964-80	0600 GMT	1200 GMT	0600 GMT	1200 GMT	0600 GMT	1200 GMT	0600 GMT	1200 GMT
	days	days	hours	hours	hours	langleys	langleys	langleys	mm	mm	mm	octas	octas	octas	octas	miles	knots	knots	days	days	days	days	days	days
January	5	2	9.2	11.0	6.8	548	632	457	187	247	136	4.8	4.4	3.0	3.1	102.1	7	11	2	0	1	0	3	1
February	5	3	9.3	10.5	7.6	572	655	497	178	242	134	4.7	4.6	3.1	3.4	99.0	6	11	2	1	2	1	3	1
March	9	3	8.5	9.7	6.0	541	612	475	191	255	136	6.0	5.1	5.0	3.8	99.0	6	11	3	0	1	0	6	1
April	16	4	7.1	9.4	5.0	458	531	371	149	186	129	6.9	6.0	6.0	4.8	82.4	5	9	4	0	1	1	7	1
May	14	4	6.1	7.9	4.4	402	464	354	124	173	106	6.6	6.0	5.8	5.2	63.3	4	6	7	1	1	1	6	1
June	5	1	5.5	7.5	3.6	367	427	313	98	150	82	6.5	5.8	5.4	5.1	56.3	3	6	9	2	2	0	7	1
July	3	1	4.2	6.2	2.3	318	388	224	89	108	72	6.9	6.5	6.0	5.5	54.5	3	6	9	2	2	0	9	1
August	4	1	4.3	5.9	2.4	345	423	267	100	125	78	6.9	6.3	6.2	5.5	61.5	3	7	7	1	3	1	7	1
September	4	1	6.2	7.6	4.2	451	529	319	138	176	103	6.4	5.3	5.6	4.7	78.9	5	8	6	1	1	1	7	1
October	6	1	7.4	9.0	5.7	484	535	374	167	211	136	6.3	5.3	5.9	4.6	95.1	6	9	2	1	1	0	6	1
November	15	3	7.0	8.5	5.1	460	532	379	140	173	123	6.8	5.4	6.0	4.5	103.2	7	10	2	0	2	0	7	1
December	7	3	8.5	10.2	5.7	516	588	388	160	197	119	5.6	4.8	4.5	3.9	107.9	7	11	2	1	1	1	5	1
Year	93	27	6.9	7.7	6.2	455	477	394	1721	1951	1519	6.2	5.5	5.2	4.5	83.6	5	9	55	10	18	6	73	12

Climatic data for Nairobi. [From Meteorology Department, Nairobi]

APPENDIX E

Ammonia – NH₃ (Refrigerant 717)

t [°C]	p_s [bar]	v_g [m³/kg]	h_f [kJ/kg]	h_g [kJ/kg]	s_f [kJ/kg K]	s_g [kJ/kg K]	h 50 K [kJ/kg]	s 50 K [kJ/kg K]	h 100 K [kJ/kg]	s 100 K [kJ/kg K]
50	0.4089	2.625	−44.4	1373.1	0.194	6.159	1479.8	6.592	1585.9	6.948
45	0.5454	2.005	−22.3	1381.6	0.096	6.057	1489.3	6.486	1596.1	6.839
40	0.7177	1.552	0	1390.0	0	5.962	1498.6	6.387	1606.3	6.736
35	0.9322	1.216	22.3	1397.9	0.095	5.872	1507.9	6.293	1616.3	6.639
30	1.196	0.9633	44.7	1405.6	0.188	5.785	1517.0	6.203	1626.3	6.547
28	1.317	0.8809	53.6	1408.5	0.224	5.751	1520.7	6.169	1630.3	6.512
26	1.447	0.8058	62.6	1411.4	0.261	5.718	1524.3	6.135	1634.2	6.477
24	1.588	0.7389	71.7	1414.3	0.297	5.686	1527.9	6.103	1638.2	6.444
22	1.740	0.6783	80.8	1417.1	0.333	5.655	1531.4	6.071	1642.2	6.411
20	1.902	0.6237	89.8	1420.0	0.368	5.623	1534.8	6.039	1646.0	6.379
18	2.077	0.5743	98.8	1422.7	0.404	5.593	1538.2	6.008	1650.0	6.347
16	2.265	0.5296	107.9	1425.4	0.440	5.563	1541.7	5.978	1653.8	6.316
14	2.465	0.4890	117.0	1427.9	0.475	5.533	1545.1	5.948	1657.7	6.286
12	2.680	0.4521	126.2	1430.5	0.510	5.504	1548.5	5.919	1661.5	6.256
10	2.908	0.4185	135.4	1433.0	0.544	5.475	1551.7	5.891	1665.3	6.227
8	3.153	0.3879	144.5	1435.3	0.579	5.447	1554.9	5.863	1669.0	6.199
6	3.413	0.3599	153.6	1437.6	0.613	5.419	1558.2	5.836	1672.8	6.171
4	3.691	0.3344	162.8	1439.9	0.647	5.392	1561.4	5.808	1676.4	6.144
2	3.983	0.3110	172.0	1442.2	0.681	5.365	1564.6	5.782	1680.1	6.116
0	4.295	0.2895	181.2	1444.4	0.715	5.340	1567.8	5.756	1683.9	6.090
2	4.625	0.2699	190.4	1446.5	0.749	5.314	1570.9	5.731	1687.5	6.065
4	4.975	0.2517	199.7	1448.5	0.782	5.288	1574.0	5.706	1691.2	6.040
6	5.346	0.2351	209.1	1450.6	0.816	5.263	1577.0	5.682	1694.9	6.015
8	5.736	0.2198	218.5	1452.5	0.849	5.238	1580.1	5.658	1698.4	5.991
10	6.149	0.2056	227.8	1454.3	0.881	5.213	1583.1	5.634	1702.2	5.967
12	6.585	0.1926	237.2	1456.1	0.914	5.189	1586.0	5.611	1705.7	5.943
14	7.045	0.1805	246.6	1457.8	0.947	5.165	1588.9	5.588	1709.1	5.920
16	7.529	0.1693	256.0	1459.5	0.979	5.141	1591.7	5.565	1712.5	5.898
18	8.035	0.1590	265.5	1461.1	1.012	5.118	1594.4	5.543	1715.9	5.876
20	8.570	0.1494	275.1	1462.6	1.044	5.095	1597.2	5.521	1719.3	5.854
22	9.134	0.1405	284.6	1463.9	1.076	5.072	1600.0	5.499	1722.8	5.832
24	9.722	0.1322	294.1	1465.2	1.108	5.049	1602.7	5.478	1726.3	5.811
26	10.34	0.1245	303.7	1466.5	1.140	5.027	1605.4	5.458	1729.6	5.790
28	10.99	0.1173	313.4	1467.8	1.172	5.005	1608.0	5.437	1733.2	5.770
30	11.67	0.1106	323.1	1468.9	1.204	4.984	1610.5	5.417	1735.9	5.750
32	12.37	0.1044	332.8	1469.9	1.235	4.962	1613.0	5.397	1739.3	5.731
34	13.11	0.0986	342.5	1470.8	1.267	4.940	1615.4	5.378	1742.6	5.711
36	13.89	0.09.31	352.3	1471.8	1.298	4.919	1617.8	5.358	1745.7	5.692
38	14.70	0.0880	362.1	1472.6	1.329	4.898	1620.1	5.340	1748.7	5.674
40	15.54	0.0833	371.9	1473.1	1.360	4.877	1622.4	5.321	1751.9	5.655
42	16.42	0.0788	381.8	1473.8	1.391	4.856	1624.6	5.302	1755.0	5.637
44	17.34	0.0746	391.8	1474.2	1.422	4.835	1626.8	5.284	1758.0	5.619
46	18.30	0.0706	401.8	1474.5	1.453	4.814	1629.0	5.266	1761.0	5.602
48	19.29	0.0670	411.9	1474.7	1.484	4.793	1631.1	5.248	1764.0	5.584
50	20.33	0.0635	421.9	1474.7	1.515	4.773	1633.1	5.230	1766.8	5.567

Critical point t_c = 132.4 °C, p_c = 113.0 bar.
Molar mass M = 17.030 kg/kmol; further properties of the liquid are given on p. 15.

Properties of liquid and saturated vapour for ammonia. [From Mayhew, Y.R. and Rogers, G.C.F. (1980), Thermodynamic and Transport Properties of Fluid, Basil Blackwell, London]

Enthalpy-Concentration Diagram for Ammonia-Water Solution [From ASHRAE (1980)]

The chart contains the following labeled curves:

SATURATION PRESSURE, KPa

ENTHALPY OF SATURATED VAPOR, KJ/Kg VAPOR

VAPOR COMPOSITION, Kg NH_3/Kg VAPOR

ENTHALPY OF SATURATED LIQUID, KJ/Kg LIQUID

Axis labels:

TEMPERATURE, °C (left)

TEMPERATURE, °C (right)
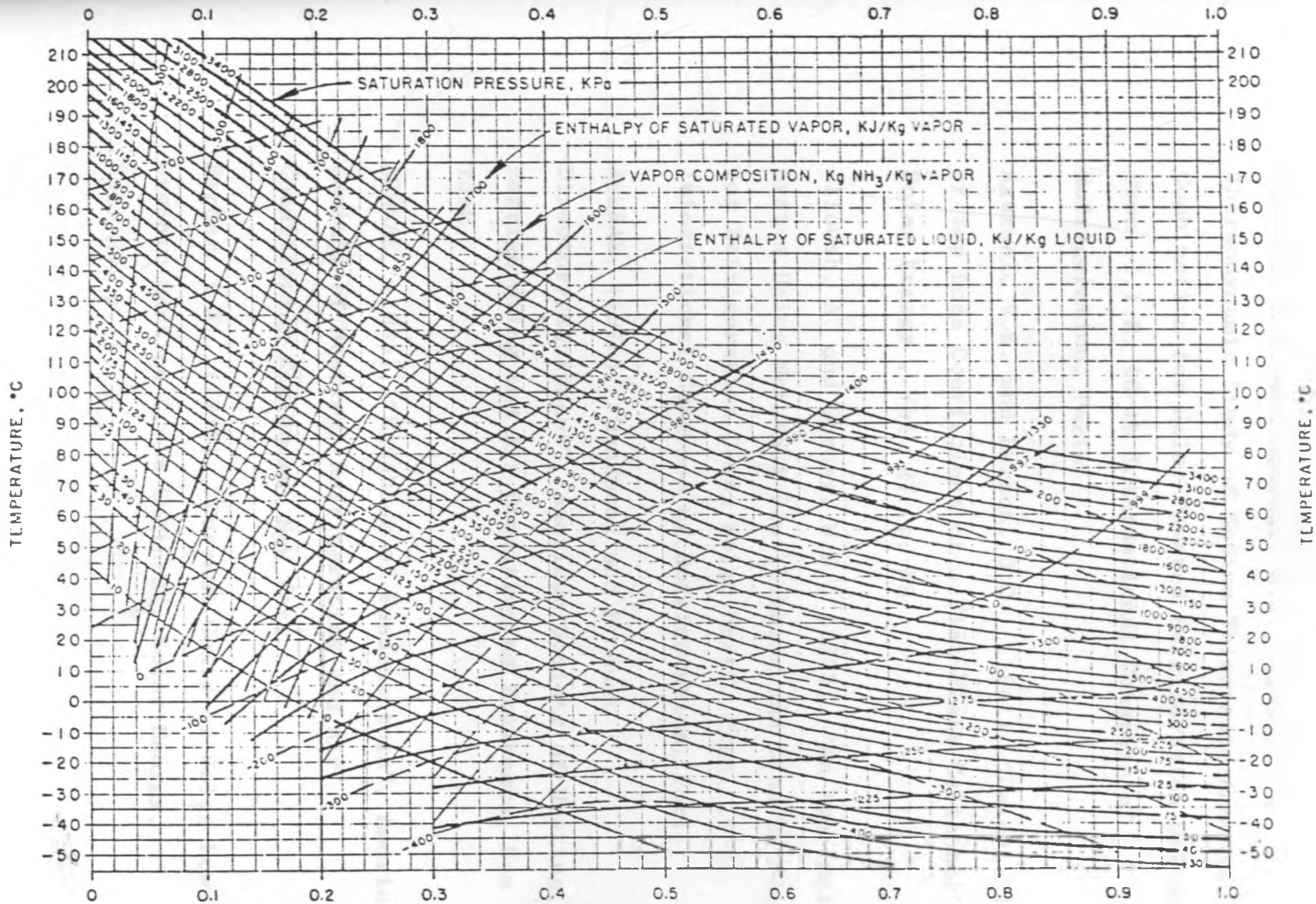
AMMONIA IN SATURATED LIQUID - Kg NH_3/Kg LIQUID

REFERENCES.

Agarwal, R.S. and Agarwal, M.K., (1983), "A Thermodynamic Study of Sodium Thiocynate-Ammonia Combination for Solar-Powered Refrigeration System", **Proc. I.I.R. 16-th International Congress of Refrigeration**, Paris.

Agarwal, V.K. and Larson, D.C., (1981), "Calculation of Top Loss Coefficient of a Flat-Plate Collector", **Solar Energy** , Vol. 27 ,p. 69.

Alloush, A. and Gosney, W.B., (1983), "An Absorption System Using Methanol Plus Lithium and Zinc Bromides for Refrigeration Using Solar Heat", **Proc. 16-th International Congress of Refrigeration**, Paris.

ASHRAE, (1975), "Handbook and Product Directory/Equipment", **American Society of Heating, Refrigerating and Air Conditioning Engineers**, New York.

ASHRAE, (1985), "Handbook of Fundamentals", **American Society of Heating, Refrigerating and Air Conditioning Engineers**, New York.

Barber, R.E., (1977), "Current Costs of Solar Powered Organic Rankine Cycle Engines", **Solar Energy**, Vol. 20, p. 1.

Beekman, D.M., (1975), "The Modeling of a Rankine
Cycle Engine for Use in a Residential Solar Energy
Cooling System", **M. S. Thesis, Mech. Engr.,**
University of Wiscousin-Madison.

Benford, F. and Bock, J.E., (1939), "A Time Analysis
of Sunshine", **Transactions of the American
Illumination Engineering Society,** Vol. 34, p. 200.

Bliss, R.W., (1964), "The Performance of an
Experimental System Using Solar Energy for Heating
and Night Radiation for Cooling a Building",
**Proceedings of the U.N. Conference of New Sources of
Energy,** Vol. 5, p. 148.

Blytas, G.C. and Daniels, F., (1962), "Concentrated
Solutions of NaSCN in Liquid Ammonia", **J. American
Chemical Society,** Vol. **84,** p. 1075.

Bong, T.Y.; Ng, K.G. and Tay, A.O., (1987),
"Performance Study of a Solar-Powered
Air-Conditioning System", **Solar Energy,** Vol. 39,
p. 173.

Brandemuehl, M.J. and Beckman, W.A., (1980),
"Transmission of Diffuse Radiation Through CPC and
Flat-Plate Collector Glazings", **Solar Energy,** Vol. **24**
p. 511.

Buffington, R.M., (1949), "Qualitative Requirements
for Absorbent-Refrigerant Combinations",
Refrigerating Engineering, p. 343.

Brown, C.K. and Gauvin, W.H., (1965), "Combined Free and Forced Convection, Parts I and II", **Can. J. Chem. Eng.**, Vol. **45**, p. 306.

Chinnappa, J.V.C., (1961), "Experimental Study of the Intermittent Vapour Absorption Refrigeration Cycle Employing the Refrigerant-Absorbent System of Ammonia-Water and Ammonia-Lithium Nitrate", **Solar Energy**, Vol. **5**, p. 1.

Chinnappa, J.C.V., (1962), "Performance of an Intermittent Refrigerator Operated by a Flat-Plate Collector", **Solar Energy**, Vol. **6**, p. 143.

Chinnappa, J.V.C., (1974), "Solar Operation of Ammonia-Water Multistage Air Conditioning Cycles in the Tropics", **Solar Energy**, Vol. **16**, p. 165.

Clausen, N.E. and Worsoe-Schmidt, P., (1982), "Analysis of Ammoniated Metal Salt Suspensions for Use in Solar Refrigeration Systems", **Proc. I.I.R. 16-th International Congress of Refrigeration**, Paris.

Clausen N.E. and Worsoe-Schmidt, P., (1983), "Solar Absorption Refrigeration Utilising Suspended Solid Absorbents", **Proc. I.I.R. 16-th International Congress of Refrigeration**, Paris.

Close, D.J., (1962), "The Performance of Solar Water Heaters with Natural Circulation", **Solar Energy**, Vol **6**, p. 33.

Collares-Pereira, M. and Rabl, A., (1979), "The
Average Distribution of Solar Radiation -
Correlations Between Diffuse and Hemispherical and
Between Daily and Hourly Insolation Values", **Solar
Energy**, Vol. 22, p. 155.

Chung, R.; Duffie, J.A. and Löf, G.O.G., (1963),
"A Study of a Solar Air-Conditioner", **Mech. Engng.**,
Vol. 85, p. 31.

Cooper, P.I., (1969), "The Absorption of Solar
Radiation in Solar Stills", **Solar Energy**, Vol. **12**,
p. 3.

Costello, F.A., (1976), "A Hybrid Solar Air
Conditioning System", **Solar Energy**, Vol. **18**, p. 149.

Delgado R., et al., (1982), "Study of the Intermittent
Charcoal-Methanol Cycle for the Realisation of a
Solar-Powered Ice-Maker", **Proc. I.I.R. Session,**
Israel.

Duffie, J.A. and Sheridan, N.R., (1965), "Lithium
Bromide-Water Refrigerators for Solar Operations",
Mechanical and Chemical Engineering Transactions,
Inst. of Engrs., Australia, Vol. **MC1**, p. 79.

Duffie, J.A. and Beckman, W.A., (1980), "**Solar
Engineering of Thermal Processes**", John Wiley and
Sons, New York.

Dupont M., et al., (1982), "Study of Solar-Powered Ice Conservators Using the Day-Night Intermittent Zeolite 13X-Water Cycle in Temperate and Tropical Climates", Proc. I.I.R. Session, Israel.

Eisenstadt, M.M.; Flanigan, F.M. and Farber, E.A., (1959), "Solar Air-Conditioning with Ammonia-Water Absorption Refrigeration System", **American Society of Mechanical Engineers**, paper no. 59-A-276.

El-Shaarawi, M.A.I. and Ramadan, R.A., (1986), "Solar Refrigeration in the Egyptian Climate", **Solar Energy**, Vol. **37**, p. 347.

Farber, E.A., (1970), "Design and Performance of a Compact Solar Refrigeration System", **Engineering Progress at the University of Florida**, Vol. **24**, Part 2.

Freider, F.J. and Kreith, F., (1977), **"Solar Heating and Cooling"**, McGraw-Hill, Washington.

Gallo, N.J.H. and de Souza, M.F., (1982), "Solar Powered Intermittent Absorption Cooler", **Proc. I.I.R. Session**, Israel.

Grosman, E.R., et al., (1983), "Methanol as a Working Medium in Sorption Type Thermal Converters", **Proc. 16-th International Congress of Refrigeration**, Paris.

Gutièrrez, F., (1988), "Behaviour of a Household Absorption-Diffussion Refrigerator Adapted to Auto-nomous Solar Operation", **Solar Energy**, Vol. **40**, p. 17.

Hay, J.R., (1973), "Energy Technology and Solarchitecture", **Mech. Engng.**, Vol. 95(11), p. 18.

Hay, J.R. and Yellot, J.I., (1970), "A Naturally Air-Conditioning Building", **Mech. Engng.**, Vol. 92(1), p. 19.

Hottel, H.C. and Whillier, A., (1958), "Evaluation of Flat-Plate Collector Performance", **Transactions of the Conference on the Use of Solar Energy**, Vol. 2, Part I, p. 74, University of Arizona Press.

Hottel, H.C. and Woertz, B.B., (1942), "Performance of Flat-Plate Solar-Heat Collectors", **Transactions of the American Society of Mechanical Engineers**, Vol. 64, p. 91.

Iedema, P.D. and Machielsen, C.H.M., (1983), "Fundamental Equations for the Free Enthalpy of LiBr and $ZnBr_2$ Solutions in Methanol", **Proc. 16-th International Congress of Refrigeration**, Paris.

Iloeje, O.C., (1986), "Quantitative Comparisons of Treated $CaCl_2$ Absorbent for Solar Refrigeration", **Solar Energy**, Vol. 37, p. 253.

Iloeje, O.C., (1988), "Parametric Effects on the Performance of a Solar Powered Solid Absorption Refrigerator", **Solar Energy**, Vol. 40, p. 191.

Jacob, X.; Albright, L.F. and Tucker, W.H., (1969), "Factors Affecting the Coefficient of Performance for Absorption Air-Conditioning Systems", **ASHRAE Transactions**, Vol. 75, Part I, p. 103.

Jansen, T.J., (1985), **"Solar Engineering Technology"**, Prentice-Hall Inc., Englewood Cliffs, New Jersey, pp. 154-164.

Jordan, R.C. and Priester, G.B., (1948), **"Refrigeration and Air-Conditioning"**, Prentice-Hall, New York, pp. 253-256.

Klein, S.A., (1977), "Calculation of Monthly Average Insolation on Tilted Surfaces", **Solar Energy** , Vol. 7, p. 79.

Linge, K.Z., (1929), ges. kalte Ind., Vol. **36**, p. 149.

Liu, B.Y.H. and Jordan, R.C., (1960), "The Inter-relationship and Characteristic Distribution of Direct, Diffuse and Total Solar Radiation", **Solar Energy**, Vol. **4**, p. 3.

Liu, B.Y.H. and Jordan, R.C., (1962), "Daily Insolation on Surfaces Tilted toward the Equator", **ASHRAE Journal**, Vol. 3(10), p. 53.

Liu, B.Y.H. and Jordan, R.C., (1963), "The Long-Term Average Performance of Flat-Plate Collectors", **Solar Energy**, Vol. 7, p. 53.

Liu, B.Y.H. and Jordan, R.C., (1977), "Availability of Solar Energy for Flat-Plate Solar Energy for Heating and Cooling of Buildings, ASHRAE, New York.

Lunde, P.J., (1980), "Solar Thermal Engineering: Space Heating and Hot Water Systems", John Wiley and Sons, New York.

McAdams, W.H., (1954), "Heat Transmission", 3rd ed., McGraw-Hill, New York.

Macriss, R.A., (1968), "Physical Properties of Modified Lithium Bromide Solution", A.G.A. Symposium on Absorption Air-Conditioning Systems.

Metais, B. and Eckert, E.R.G., (1964), "Forced, Mixed and Free Convection regimes", J. Heat Transfer, Trans. ASME, Vol. 86, p. 295.

Murungi, D., (1982), "The Design, Construction and Testing of a Solar Operated Refrigeration Unit", M.Sc. Thesis, Mech. Engr.,University of Nairobi.

Norton, B.; Probert, S.D. and Uppal, A.H., (1986), "Thermal Solar Refrigeration for Vaccine Storage-A Viable Alternative to Photovoltaic Units in Remote Locations", Private Communication to Frank Sebbowa.

Olson, T.J., (1977), "Solar Source Rankine Cycle Engines for Use in Residential Cooling", M.S. Thesis, University of Wiscosin-Madison.

Oonk, R.L.; Beckman, W.A. and Duffie, J.A., (1975), "Modeling of the CSU Heating/Cooling System", **Solar Energy**, Vol. 17, p. 21.

Page, J.K., (1961), "The Estimation of Monthly Mean Values of Daily Total Short-Wave Radiation on Vertical and Inclined Surfaces from Sunshine Records for Latitudes $40°N$ to $40°S$", **Proc. U.N. Conference on New Sources of Energy**, Vol. **4**, p. 378.

Perry, E.H., (1975), "Theoretical Performance of the Lithium Bromide-Water Intermittent Absorption Refrigeration Cycle", **Solar Energy**, Vol. 17, p. 321.

Perry, R.H. and Green, D., (1984), **"Perry's Chemical Engineers' Handbook"**, Sixth Edition, McGraw-Hill Book Company, pp. 3-264-3-284.

Prausnitz, J.M.; Lichtenthaler, R.N. and Azevede, E.G., (1986), **"Molecular Thermodynamics of Fluid-Phase Equilibria"**, Second Edition, Prentice-Hall Inc., Englewood Cliffs, New Jersey, p. 383.

Prigmore, D.R., and Barber, R.E., (1974), "A Prototype Solar Powered Rankine Cycle System Providing Residential Air Conditioning and Electricity", 9th I.E.C.E.C. Conference.

Sargent, S.L., and Beckman, W.A., (1968), "Theoretical Performance of an Ammomia-Sodium Thiocyanate Intermittent Absorption Refrigeration Cycle, **Solar Energy**, Vol. 12, p. 137.

Sheridan, N.R., (1970), "Performance of the brisbane Solar House", **In International Solar Energy Society Conference**, Melbourne.

Sherwin, K., (1983), "Study of Solar-Powered Refrigerator with Thermally Powered Vapour Compression System", Proc. 16-th **International Congress of Refrigeration**, Paris.

Swartman, R.K. and Ha, V., (1972), "Performance of a Solar Refrigeration System Using Ammonia-Sodium Thiocyanate", **American Society of Mechanical Engineers**, paper 72-WA/Sol-3.

Swartman, R.K.; Ha, V., and Newton, J.A., (1973), "Survey of Solar Powered Refrigeration", **American Society of Mechanical Engineers**, paper 73-WA/Sol-6.

Swartman, R.K.; Ha, V. and Swaminathan, C., (1975), "Comparison of Ammonia-Water and Ammonia-Sodium Thiocyanate as the Refrigerant-Absorbent in Solar Refrigeration System", **Solar Energy**, Vol. **17**, p. 123.

Swartman, R.K. and Swaminathan, C., (1970), "Further Studies on Solar Powered Intermittent Absorption Refrigeration", **In International Solar Energy Society Conference**, No. 6/114.

Tarbor, H., (1958), "Radiation, Convection and Conduction Coefficients on Solar Collectors", **Bulletin of the Research Council of Israel**, Vol. **6C**, p. 155.

Teagen, W.P. and Sargent, S.L., (1973), "A Solar Powered Combined Heating/Cooling System with the Air Conditioning Unit Driven by an Organic Rankine CycleEngine", **I.S.E.S. Paris Conference**, paper EH-94-1.

Threlkeld, J.L., (1970), **"Thermal Environmental Engineering"**, Prentice-Hall Inc., Englewood, CA, 2nd ed.

Trombe, F and Foex, M., (1957), "The Production of Cold by Means of Solar Radiation", **J. Solar Energy Science and Engineering**, Vol. 1, p. 51.

Velatine de Sa, (1964), "Experiments with Solar Energy Utilization at Dacca", **Solar Energy**, Vol. 8, p. 83.

Vella, G.J.; Harris, L.B. and Goldsmid, H.J., (1976), "A Solar Thermoelectric Refrigerator", **Solar Energy**, Vol. 18, p. 355.

Venkatesh, A. and Gupta, M.C., (1978), "Analysis of Ammonia-Water Intermittent Solar Refrigerator Operating with a Flat-Plate Collector", **In Solar Energy International Progress Proceedings of the International Symposium-Workshop on Solar Energy, Cairo, Egypt.**

Ward, D.S. and Löf, G.O.G., (1975), "Design and Construction of a Residential Solar Heating and Cooling System", **Solar Energy**, Vol. 17, p. 3.

Weil, S.A., (1968), "Correlation of the LiSCN-liBr-H$_2$O Thermodynamic Properties", **A.G.A. Symposium on Absorption Air-Conditioning Systems.**

Wilbur, P.J., and Mancini, T.R., (1976), "A Comparison of Solar Absorption Air Conditioning Systems", **Solar Energy**, Vol. 18, p. 569.

Wilbur, P.J. and Mitchell, C.E., (1975), "Solar Absorption Air Conditioning Alternatives", **Solar Energy**, Vol. 17, p. 193.

Whillier, A., (1956), "The Determination of Hourly Values of Total Radiation from Daily Summations", **Arch. Met. Geoph. Biokl. Series B**, Vol. 7, p. 197.

Whillier, A., (1965), "Prediction of Performance of Solar Collectors", **Application Solar Energy for Heating and Cooling of Buildings, ASHRAE**, New York.

Whillier, A. and Saluja, G., (1965), "Effects of Materials and of Construction Details on the Thermal Performance of Solar Water Heaters", **Solar Energy**, Vol. 9, p. 21.

Williams, D.A.; Chung, R.; Löf, G.O.G.; Fester, D.A.; and Duffie, J. A., (1975), "Intermittent Absorption Cooling Systems with Solar Regeneration", **American Society of Mechanical Engineers**, paper 57-A-260.

Williams, D.A.; Chung, R.; Löf, G.O.G., Fester, D.A.; and Duffie, J. A., (1958), "Cooling Systems Based on Solar Regeneration", **Refrigeration Engineering**, Vol. **66**, p. 66.

Yanagimachi, M., (1958), "How to Combine : Solar Energy, Nocturnal Radiation Cooling, Radiant Panel System of Heating and Cooling, and Heat Pump to Make a Complete Year-Round Air Conditioning System", **Transactions of the Conference on Use of Solar Energy**, Vol. 3, p. 22, University of Arizona Press, Tucson.

Yanagimachi, M, (1964), "Report on Two and a Half Years' Experimental Living on Yanagimachi Solar House II", **Proc. U.N. Conference on New Sources of Energy**, Vol. 5, p. 233.